May 2015

# Topics in Supersymmetry: Implications for Cosmology and Non-Perturbative Studies on a Spacetime Lattice

Richard Anthony Galvez
*Syracuse University*

# Topics in Supersymmetry: Implications for Cosmology and Non-Perturbative Studies on a Spacetime Lattice

by

Richard Anthony Galvez

## Abstract

Moduli fields, scalar fields which parametrize different vacuum states of a given theory, are commonly predicted to exist within compactifications of UV complete theories, and in particular those theories exhibiting supersymmetry. But if such theories' dynamics are present during the inflationary phase of the universe and thereafter, what are the implications for cosmology and the evolution of the universe? In this thesis a review is presented on generic consequences of the presence of these scalar fields during inflation and the post-inflationary era of the universe. An unexpected consequence arises in the study of dark matter production, where a deviation from the usual thermal production mechanism is shown to be required.

In addition to studies in cosmology, the dynamics of a twisted construction of supersymmetric lattice quantum field theory is explored. An analysis of the fermionic sign problem is presented and it is shown to be absent in the studied formulation. A first study of the phase structure of supersymmetric $\mathcal{N} = 4$ supersymmetric gauge theory is also presented.

Thesis Supervisor: Scott Watson
Title: Assistant Professor

# Topics in Supersymmetry: Implications for Cosmology and Non-Perturbative Studies on a Spacetime Lattice

by

## Richard Anthony Galvez

B.S., Florida International University 2007
M.S., Florida International University 2009

Dissertation
Submitted to the Department of Physics
in partial fulfillment of the requirements for the degree of

Doctor of Philosophy in Physics

at

SYRACUSE UNIVERSITY

May 2015

# Acknowledgments

This thesis would certainly have not been possible without the substantial support I received from my family, friends and colleagues. Particularly I am most thankful for my parents' support who were there for me throughout each and every step of the way, though the PhD process was completely alien to them. Thank you!

This thesis would have of course also not been possible without the guidance of my thesis advisor Scott Watson. He gave me many opportunities in which to explore my interests in particle cosmology and this thesis is ultimately the result of that study. Professor Simon Catterall's guidance was also priceless as it allowed me to research the non-perturbative states of quantum field theories possibly present at energy scales accessible by particle accelerators today.

Kuver Sinha's deep knowledge of supersymmetric particle phenomenology and string theory helped out tremendously towards the final portions of this dissertation dealing with inflation in the context of superstring theory. His help, guidance and assistance could not be understated. During my research on Supersymmetric lattice quantum field theories the advice and guidance of Anosh Joseph and Dagash Mehta was always there, and always needed. I would also like to thank A. P. Balachandran and Kameshar Wali for useful discussions during my studies in string theory.

Beyond this I would like to thank Jayanth Neelekanta and Ogan Özsoy for being the best and funniest officemates anyone could ever ask for. We spent so many late nights in the office together and it just made the years fly by. Thanks guys!

Last and not least, I would like to thank my mentors Gina Lee-Glauser and Patricia Stith for always being there for me and always giving me the best advice in my development towards becoming a scientist. My life and personality, without their advice and conversations would lack much depth and dimension.

# Contents

# List of Figures

# Chapter 1

# Introduction

For the first time in the history of science precise experimental observations are encountering theoretical predictions from what may have occurred during the first $10^{-36}$ seconds after the Big Bang. In particular, it is the theory of cosmic inflation that proposes a burst of exponential expansion during these early times which provides the best candidate theory for this era.

The predictions of inflation include explanations for the observed smooth, large and nearly isotropic universe as well as the large-scale structure formation we observe today. Predictions from this theory are tested by experimental observations of the relic Cosmic Microwave Background Radiation (CMB), a snapshot of the state of the universe when it was 380,000 years old. In March of 2013, the state-of-the-art results from the European Space Agency's Planck satellite were published, reporting the highest precision measurements of the CMB to date.

In parallel, the Large Hadron Collider at CERN (LHC) has probed energies of 14 TeV, or equivalently $10^{-14}$ seconds after the Big Bang. This experiment has verified the Standard Model of particle physics, the fundamental theory of the universe up to energies of 10 TeV and finally discovered the much anticipated Higgs Boson. The theory of inflation and the standard model tell very precise stories, but unfortunately of two disjoint eras of the early universe. An understanding of the fundamental physics between these two eras, is required to link together the experimental observations from both Planck and the LHC.
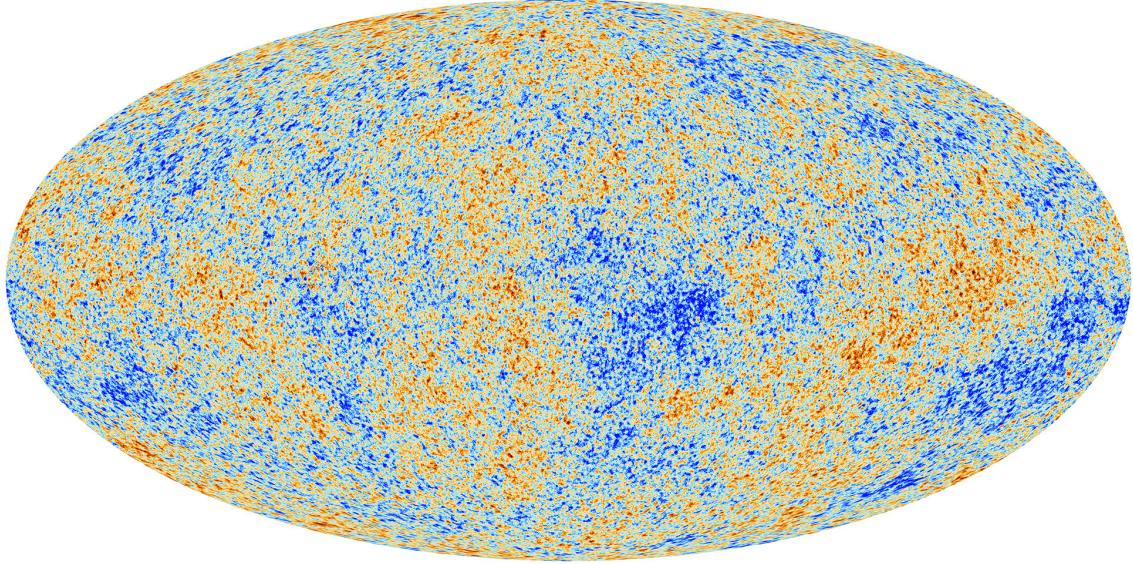
Figure 1-1: An all-sky scan of the Cosmic Microwave Background (CMB) radiation after the subtraction of background noise (Courtesy of the Planck collaboration). In this image only the overall *difference from the mean temperature* is plotted, with the cooler regions at -230 $\mu K$ away from the mean depicted in blue and the warmer regions at $+188$ $\mu K$ away from the mean depicted in red.

## 1.1  Inflation and the uncertainties in its observables

Inflation provides a mechanism for large scale structure formation in the universe [1,2]. Quantum effects result in very small fluctuations around a perfectly homogenous density distribution in the infant universe. These small differences would be inflated to much larger scales through the exponential expansion, thus "freezing" these quantum effects that seed the large scale structure we see today in galactic superclusters and beyond.

This mechanism results in the CMB possessing regions of over and under densities, with exceedingly small but finite temperature differences from the overall mean temperature. This prediction is verified by a careful analysis of the CMB, revealing small differences of $\pm 3 \times 10^{-4}$K from the mean temperature of $2.7260 \pm 0.0013$ K.

The information for structure formation is encoded in these small temperature fluctuations and is derived from a fundamental theory via two parameters, $n_s$ and $r$, which have unique theoretical signatures depending on the model. $n_s$ and $r$ are
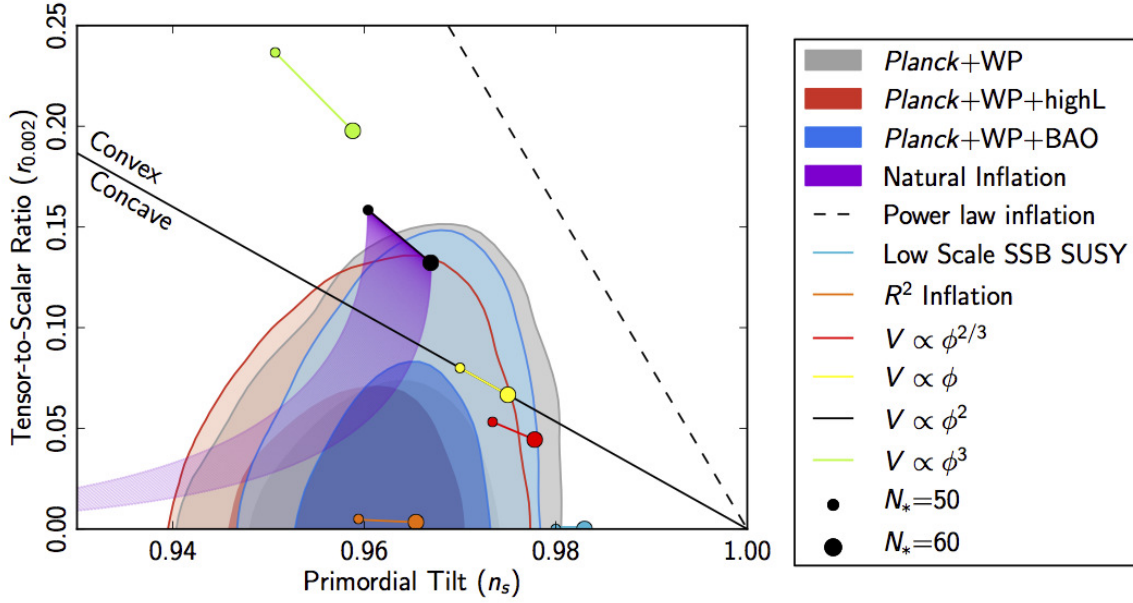
Figure 1-2: The $n_s$ vs $r$ confidence contours of the Planck CMB measurements combined with data from WMAP9 and BAO measurements (Courtesy of the Planck collaboration). In this plot we see the 95% (lighter) and 68% (darker) confidence contours for the combined experimental measurements while the locations of various included and excluded inflationary models are listed.

also directly measurable by the Planck satellite, and one may use this as a probe to determine which inflationary model is in agreement with experimental measurements.

The Planck collaboration successfully placed stringent constraints on the $n_s$ and $r$ parameters restricting the possible set of inflationary models greatly. In figure 1-2, the 95% (lighter) and 68% (darker) confidence contours are shown for the data measured by the Planck experiment and further supplemented by various other experiments. In addition to the experimental contours, the Planck team also included where well studied inflationary potentials fall on this plot.

The mapping from the inflationary model to the observables $n_s$ and $r$ is however inherently imprecise due to our lack of understanding of the post-inflationary history [3]. A way to establish the post-inflationary history is through its effects on the evolution of the primordial density perturbations initially provided by inflation [2]. The expansion history during this time can alter both the predictions for the growth of large-scale structure and the anisotropies of the CMB. The uncertainty in the expansion history in turn leads to an uncertainty in the inflationary parameters and

thus can be used to develop constraints on the post-inflationary history of the universe.

The standard assumption about the cosmological history from post-inflation until the TeV era is that it was dominated by a radiation bath. This prototypical history is referred to as a *thermal* history while any deviation from it is described as *non-thermal*. For example, one possibility of such a deviation is depicted in figure 1-3 In this scenario a scalar field from the low-energy limit of a hypothetical quantum gravity theory modifies the thermal history giving rise to an alternative non-thermal matter dominated phase as this scalar decays to dark-matter candidate particles.

There are a number of other motivations from fundamental theory for expecting departures from a strictly thermal history after inflation ends (at a GUT scale). In fact, the requirement of adequate reheating to realizing a hot big bang consistent with observations already requires departures from a purely thermal scenario [4]. Additionally, theories beyond the Standard Model of particle physics generically predict the existence of additional scalar fields - examples include the sizes and shapes of extra dimensions, or Supersymmetry (SUSY) flat directions in the moduli space of the scalars. In the very early universe the vacuum expectation values of these fields are generically displaced [5] and energy can become stored in the form of coherent oscillations, forming a scalar condensate.

The cosmological scaling of the condensate depends on the symmetries of the theory and which term in the scalar potential is dominant. When the dominant term in the potential scales as $V \to \phi^\gamma$ the pressure of the condensate depends on the energy density as

$$p = \left(\frac{2\gamma}{2+\gamma} - 1\right)\rho, \tag{1.1}$$

where $\rho$ scales as

$$\rho = \rho_0 a^{-6\gamma/(2+\gamma)}, \tag{1.2}$$

and $a(t)$ is the cosmological scale factor. Two examples are a massive scalar field with negligible interactions, for which $\gamma = 2$ and the condensate scales as pressureless matter $p = 0$, whereas if physics at the high scale is dominant - in the form of non-renormalizable operators - then $\gamma \geq 4$ and the condensate evolves as a stiff fluid

4
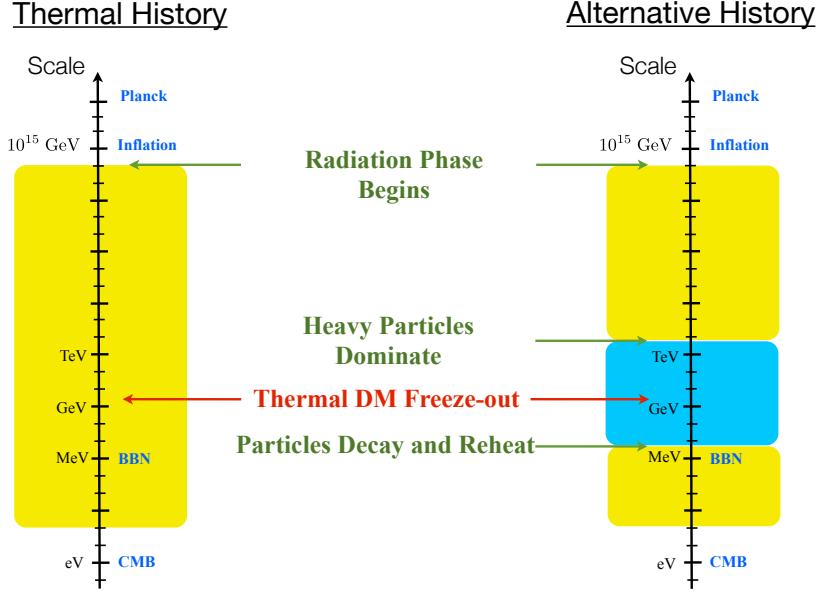
Figure 1-3: One possible variation from a thermal history. On the left side the usual thermal evolution is depicted and on the right hand side one possible deviation from it. This modification is phenomenologically interesting since it proposes an extra matter dominated phase which gives rise to an alternative non-thermal origin to dark matter.

$p \gtrsim \rho$ for large $\gamma$.

In addition to the presence of condensates, there are many other phenomenologically motivated reasons to consider a modified expansion history including symmetry breaking phase transitions, prolonged reheating, curvatons [6], Q-balls [7], kination models [8], frustrated cosmic string networks [9], or a short period of thermal inflation [10].

Regardless of the consideration however, in many scenarios the post-inflationary history will depart from a strictly thermal history and the evolution during this time can be parametrized through an equation of state parameter $w(t) = p/\rho$. In fact, one may consider a direct mapping of the exotic scenarios listed above to a particular value of $w$. The investigation of the consequences of a departure from a standard post-inflationary history (being the radiation dominated universe $w = 1/3$) can thus be reduced to studying the effects of $w$ on the evolution of cosmological perturbations through the post-inflationary phase.

Deviations of $w$ from the strictly thermal case ($w = 1/3$) may lead to observable

imprints on the CMB spectrum. For example, situations where $w < 1/3$ can lead to an enrichment of substructure (seeded by cosmological perturbations) depending on the properties and interactions of the particles and fields at this time. If dark matter primarily originates as a decay product - as in some non-thermal histories - it can undergo enhanced clumping to form a larger number of sub-halos [11]. If equilibrium is never reached during the alternative post-inflationary history, CMB measurements restrict the level of isocurvature modes to be less than around ten percent, thus providing a constraint on histories that rely on out-of-equilibrium particle decays [12].

We therefore reach the conclusion that **the establishment of the post-inflationary history and its connection to the growth of small and large-scale structure we can constrain classes of non-thermal histories purely based on CMB observations.** This is the main motivation of the work presented in this thesis and the focus of chapter 3.

We can now be more concrete about how changes in the post-inflationary expansion history can alter the way in which predictions of fundamental theories of inflation are linked to cosmological observables. Particularly, we may focus on the effect of the change in the history to predictions on how long inflation took place measured by a quantity called *e-folds*– how many orders of exponential expansion occurred during inflation. In this analysis we will not be concerned with the total number of e-folds of inflation, but rather the number of e-folds, denoted by $N$, that elapsed from the moment the CMB scale mode left the Hubble horizon to the end of inflation.

The correlation between the post-inflationary thermal history and *inflationary observables* is usually expressed via the *matching equation*, as surveyed in [13–15]. However, changes in the equation of state parameter $\tilde{w}$ following inflation can alter this matching, since the expansion controls how rapidly perturbations re-enter the Hubble horizon.

For slow-roll inflation, the number of e-foldings between horizon exit and re-entry

is given by

$$N(k) = 56.12 - \log(\frac{k}{k_*}) + \frac{1}{3(1+\tilde{w})}\log(\frac{2}{3}) + \log(\frac{V_k^{\frac{1}{4}}}{V_{end}^{\frac{1}{4}}}) \tag{1.3}$$

$$+ \frac{1-3w}{3(1+\tilde{w})}\log\big(\frac{\rho_{reh}^{\frac{1}{4}}}{V_{end}^{\frac{1}{4}}}\big) + \log\big(\frac{V_k^{\frac{1}{4}}}{10^{16}GeV}\big), \tag{1.4}$$

where $k_* = 0.05 Mpc^{-1}$ is chosen as the pivot scale[1], $\rho_r^{1/4} \sim T_r$ is the temperature at which the thermalization took place, $V_{end}$ is the value of the slow-roll potential at the end of inflation and $V_k$ the value of the potential when the $k$-th mode exists the horizon, and

$$\tilde{w} = \frac{1}{\Delta \log a}\int w(a)d\log(a) \tag{1.5}$$

is the averaged equation of state parameter. For smaller values of $\tilde{w}$ the value of $N$ at which the pivot leaves the horizon will be decreased. Therefore, changes to the equation of state lead to a theoretical uncertainty in the number of e-foldings $\Delta N$, which is found to shift the momentum scale of modes as $k_* \to k_* e^{\Delta N}$.

For simple models of high scale inflation, where reheating is not immediate but followed by a short period of matter domination, there is an uncertainty in the number of e-foldings $\Delta N \simeq 10$, when thermalization occurs at the TeV scale [16]. This introduces an error into the tilt of the power spectrum $\Delta n_s \simeq 0.005$ - comparable to the statistical errors of Planck. These uncertainties, and additional ones for the tensor to scalar ratio, result from the correlation between the running of the spectrum $\alpha_s \equiv dn_s/d\log k$ and the post-inflationary history - e.g. for a scalar tilt $\Delta n_s \sim \alpha_s \Delta N$. We therefore carefully consider the implications of the inflationary uncertainties and use them to constraint inflationary parameters.

In the next section we introduce a lattice formulation of $N = 2, 4$ Supersymmetric quantum field theories in two and four dimensions for the purpose of exploring non-perturbative dynamics of supersymmetric quantum field theories.

---

[1]The specific value of this constant is chosen based on the dataset being considered.

## 1.2 Supersymmetric quantum field theories, a lattice description

Though highly successful at describing the universe at the TeV scale, it is clear that the Standard Model of Particle Physics is an incomplete description of the fundamental interactions [17]. An extension of the Standard Model to one that exhibits supersymmetry may enlighten our understanding of nature further and ultimately lead us one step closer to finding a field theory that encompasses all natural processes.

In essence, supersymmetry (SUSY) is the extension of space time symmetries, such as Poincaré symmetry, by fermionic generators [18]. This new symmetry then serves as the theoretical scheme that unifies fermions and bosons, giving each known particle a superparticle partner through a supersymmetric transformation.

Whether or not supersymmetry is a symmetry exhibited by nature, it is interesting to study it for purely theoretical reasons. Supersymmetric field theories possess chiral symmetry breaking, confinement, conformal behavior, a mass gap and more [19]. Thus even if supersymmetry was discredited, the understanding found in studying confining supersymmetric models for example may lead to new understandings one of the presently confounding problems of quantum chromodynamics.

Also, many breakthroughs have been made using supersymmetry in fields such as Topology and String Theory [19]. In String Theory, connections between Large $N$ supersymmetric field theories and Quantum Gravity have been conjectured [20] and even extended to condensed matter systems.

With the success of lattice methods in quantum chromodynamics and non-abelian gauge fields in general, it is quite reasonable to seek a lattice formulation of supersymmetric field theories on a discretized space-time lattice. Until recently, methods for formulating supersymmetric field theories on the lattice have been difficult to formulate [19]. The reason for the difficulty is that supersymmetry extends the Poincaré symmetry which breaks upon discretization, since a generator of infinitesimal translations does not exist on the lattice. Recent advancements in understanding of the so called orbifolding/deconstruction and the topological twisting procedure have made

it possible to construct exact rigorous supersymmetric theories on the lattice [19]. In this thesis the focus is on the twisted field theory approach.

## 1.2.1 Global Supersymmetry

As stated previously, supersymmetry is an extension of Poincarè symmetry by adding fermionic generators. One must be careful as to what is allowed in this extension of the Poincarè algebra as Coleman and Mandula proved that for any theory with a mass-gap, the only conserved quantity other than the generators of the Poincarè algebra must trivially be Lorentz scalars [21]. It was later shown that supersymmetry was an exception to this theorem since the generators of supersymmetry (the super charges) are spinors. This result is due to Haag, Lopuszanski and Sohnius [22].

Poincaré symmetry consists of translations in spacetime generated by $P_\mu$ and Lorentz boosts generated by $\Sigma_{\mu\nu} = -\Sigma_{\nu\mu}$ . Disregarding structure constants, the Poincaré algebra has the structure [19]

$$[P, P] = 0 \quad , \qquad [P, \Sigma] \backsim P \quad , \qquad [\Sigma, \Sigma] \backsim \Sigma .$$

The first term means that each translation $P_\mu$ commutes with eachother, the second that translations transform with the Lorentz group as four vectors $(P)$, and the last term means that Lorentz boosts transform under the Lorentz symmetry to something proportional to another Lorentz boost (at least an antisymmetric tensor).

The supersymmetry algebra is an extension of the Poincaré algebra with the following transformation properties

$$\{Q, Q\} = 0 \quad , \qquad [P, Q] = 0 \quad , \qquad \{Q, \Sigma\} \backsim Q \quad , \qquad [Q, \bar{Q}] \backsim P$$

Where $Q_\alpha$ and $\bar{Q}_{\dot\alpha}$ are the generators of the supersymmetry. The first term tells us that Q anticommutes with itself or that it is Grassmann; the second term that translations commute with $Q$; the third that $Q$ transforms under Lorentz transformations as a 2-component Weyl spinner; and finally the last term tells us that two successive

supersymmetric transformations gives something proportional to a translation. The last point implies that the generator $Q$ is in a sense the square root of a transformation and hence related to the square root of the Hamiltonian. The $\alpha$ index of $Q_\alpha$ counts how many generators there are in the given theory ranging from $1 \ldots \mathcal{N} \in \mathbb{Z}_n$. Since the number of supercharges changes for a given $\mathcal{N}$ changes with $d$, it becomes convenient to categorize a theory by how many real super charges $\mathcal{Q}$ in a given $d$. For example, in $\mathcal{N} = 1$ and $d = 4$ we have $\mathcal{Q} = 4$ since there is one $Q$ and $\bar{Q}$ each being a two component spinor.

It is quite common for supersymmetric theories to possess global chiral symmetries (called "R-Symmetries" due to historical reasons). These symmetries do not commute with $Q$, meaning that members of the supermultiplets transform as different multiplets under R-symmetry transformations. These symmetries play a crucial role building supersymmetric lattice field theories with scalars, as is discussed in section 1.2.3.

## 1.2.2 Accidental symmetries

An "accidental symmetry" is a symmetry that emerges as one takes the continuum limit of a lattice field theory that was not present on the lattice due to symmetry breaking operator terms [19]. Essentially building such a theory on the lattice means to build an action naively and then see which terms violate the symmetry. These symmetry breaking terms then may be fine tuned so that they disappear in the continuum limit rendering a symmetric continuum action.

In principle, one may construct a lattice field theory in such a way that any desired symmetry appear as an accidental symmetry in the continuum limit. This would require careful work with fine-tuning, and may lead one through a process, not only unnecessary, but also excessively difficult and prone to errors– it might even be impossible. Such an undertaking may be used for supersymmetry, to gain all symmetries as accidental symmetries, however this is not required. A more viable approach is to impose as many symmetries on the lattice as possible and then aim to regain the remaining symmetries in the continuum limit.

The process of constructing such an emergent symmetry is to consider the symmetry breaking operators on the lattice. If such operators are irrelevant operators (tending towards zero in the continuum limit[2]), then the symmetry is restored in the continuum, if not, one may also fine-tune certain parameters in order to restore this symmetry. For the case of supersymmetry, it is shown in [19] that $\mathcal{N} = 1$ in $d = 4$ without scalars recovers supersymmetry as an accidental symmetry by setting a gaugino mass term to zero. This however is not the case for supersymmetry with scalars.

$\mathcal{N} = 1$ in $d = 4$ supersymmetric field theory with scalars poses a problem when one tries to have supersymmetry emerge as an accidental symmetry. One of the symmetry violating terms emerges as a relevant operator responsible for scalar masses. Following the process for supersymmetry with no scalar terms, we would like to find a symmetry that can be implemented on the lattice exactly which is broken by a scalar mass term. Unfortunately the only symmetry that one can use in this case is supersymmetry itself and hence unusable for this purpose.

It is then reasonable to consider the possibility that if only a subalgebra of the full extended supersymmetric algebra is realized on the lattice, the rest may be recovered in the continuum limit. The full extended supersymmetric algebra is given by the relations

$$\{Q^i_\alpha, Q^j_\beta\} = 0 \ , \qquad \{\bar{Q}^i_{\dot\alpha}, \bar{Q}^j_{\dot\beta}\} = 0 \ , \qquad \{Q^i_\alpha, \bar{Q}^j_{\dot\beta}\} = 2P_m\sigma^m_{\alpha\dot\beta}\delta^j_i \ ,$$

where $i$, $j$ range from $1 \ldots \mathcal{N}$.

Immediately one realizes a number of issues that need to be considered. How can one select the correct subalgebra to implement on the lattice given that $P_m$, the generator of infinitesimal translations does not exist on the lattice? Secondly, is it possible to isolate a sector of the subalgebra that will not destroy the hypercubic lattice symmetry leaving the Poincaré symmetry intact? Another concern is how one would go about placing the bosons, fermions and scalars on the lattice, considering

---

[2]This is of course assuming that such irrelevant operators remain finite as one takes the continuum limit

that their superpartner particles, seemingly, have to be placed in the same locations[3]. And finally, since supersymmetric theories possess global chiral symmetries, it is not entirely clear how the boson superpartners of the chiral fermions will be placed on the lattice.

These issues seem to rule out the construction of supersymmetric lattice field theories, however the key to circumvent these issues is to first consider that $Q^i$ and $\bar{Q}^i$ are independent. Then one may consider a subset of the supercharges $\{q^j\}$ that remains nilpotent. This resolves the issue of not having infinitesimal $P_m$ generators on the lattice, however it does not address the issue of Lorentz invariance since the supercharges on the lattice belong to an incomplete representation of the full Lorentz group[4]. A workaround of other issues plaguing supersymmetric formulations on the lattice is resolved by considering Dirac-Kähler fermions where the discrete point symmetry of the lattice is not embedded in the full Lorentz group, but in the product of the Lorentz × Flavor group. Under the point lattice symmetry, fermions in this representation transform as $n$-index antisymmetric tensors which naturally allows for scalars to be embedded in the tensors. Then, if one selects the correct supercharges to maintain on the lattice, the ones that contain the scalars, it is possible that Lorentz symmetry may be emergent in the continuum theory.

The Dirac-Kähler representation of fermions on the lattice seems to provide a method for realizing supersymmetry on the lattice, but the exact details are unclear on how to do this. As is presented in the next section, the deus ex machina appears to be considering a twisted field theory with the Dirac-Kähler fermions and then discretizing that continuum theory onto the lattice, preserving only a particular subset of the supercharges. Orbifolding provides another mean for a lattice construction, yet this leads to the identical supersymmetric lattice theory.

---

[3]That is, if fermions are placed on the vertices, then the bosonic superpartners of the fermions must also lie on the vertices.

[4]Euclidean time is assumed throughout unless otherwise noted.

### 1.2.3 Twisted supersymmetry

The $R$-symmetry discussed previously plays a pivotal role in the twisted construction [23]. The bosonic and fermionic fields described in the Dirac-Kähler context along with the supercharges provide a representation of the relevant $R$-symmetry[5] and the $SO(d)$ Lorentz symmetry. The $R$-symmetry possess a Lorentz subgroup $SO(d)_R \in G_R$ where $G_R$ is the full global R-symmetry. We may thus find a subgroup of the full global symmetry group $SO(d) \times SO(d)_R \subset SO(d) \times G_R$. To construct the twisted theory, we first identify the diagonal subgroup of $SO(d) \times SO(d)_R$

$$SO(d)' = SO(d) \times SO(d)_R$$

as the new Lorentz symmetry of the theory, obtaining a new effective supersymmetric theory. When we discretize this theory, the point group symmetry of the lattice will be a discrete subgroup of the $SO(d)'$ symmetry, not of the original $SO(d)$. Thus the twisting procedure is a way of "twisting together" the $R$-symmetry and the original $SO(d)$ symmetry in such a way that the new symmetry of the theory will respect the lattice point group symmetry upon discretization.

In most cases of practical importance, fermionic fields transform as spinor representations under both $SO(d)$ and $SO(d)_R$. All fermionic degrees of freedom will be in integer spin representations in $SO(d)'$ manifesting themselves as general $p$-form tensors (direct products of scalars and vectors included). Let us label each $p$-form fermion as $\psi^{(p)}$, then

$$\text{fermions} \rightarrow \frac{\mathcal{F}}{2^d}(\psi^{(0)} \oplus \psi^{(1)} \oplus \dots \psi^{(p)})$$

where $\frac{\mathcal{F}}{2^d}$ may either be one, two, four or eight and $\mathcal{F}$ is the total number of fermions in the theory [19]. Supercharges decompose in a similar fashion allowing themselves to be represented as $p$-forms also while bosonic degrees of freedom will manifest themselves as 1-forms. This means that we may write all of the supersymmetric algebra in terms

---

[5]Recall that different $d$ and $\mathcal{N}$ theories possess different $R$-symmetries.

of $p$-forms with respect to $SO(d)'$, disregarding spin indices. Since both fermionic and bosonic degrees of freedom are now in terms of $p$-forms under $SO(d)'$, we are much better suited to place the theory on a lattice. This is the advantage that is gained by twisting the theory.

As an aside on orbifold lattices, it is of interest to note that from this point one may either construct a supersymmetric lattice field theory of an orbifold lattice. A $p$-form continuum field (in this case a boson or fermion) may naturally be associated with a $p$-cell on a hypercubic lattice. The approach taken with the orbifold lattice method is to map the $p$-form continuum field onto the $p$-cell on a hypercubic lattice.

One can then see that the problems with placing supersymmetry on the lattice previously are avoided by a few ideas. First, by focusing on a subset of the nilpotent supercharge, the association between Poincaré invariance and infinitesimal transla- tions is sidestepped. Secondly, if considers the twisted subgroup $SO(d)'$, it is noted that the lattice point symmetry is a discrete subgroup of $SO(d)'$ and implementing the supercharges as $SO(d)'$ $p = 0$ scalars, one may recover full Poincaré invariance in the continuum limit. Lastly we find that with fermions and bosons both being represented by $p$-form tensors, it is natural to imagine that they can coexist as a similar entity on the lattice.

$R$-symmetry is the only issue not addressed in this twisting method, however, it is noted that $R$-symmetry emerges as an accidental symmetry in the continuum limit along with Poincaré invariance and full supersymmetry. In order to exemplify this general discussion on supersymmetric lattices from twisting, let us consider the example of two dimensional $\mathcal{N} = (2, 2)$ supersymmetric Yang-Mills (SYM), and then on to four dimensional $\mathcal{N} = 4$ SYM.

## 1.2.4 Two dimensional $\mathcal{N} = (2, 2)$ supersymmetric Yang-Mills

The Dirac-Käler fermions discussed previously may be expressed in matrix form as $\Psi = (\frac{1}{2}\eta, \psi_\mu, \chi_{12})$ encompassing the scalars, vectors and $p$-forms of the theory. $\Psi$ may

be written in the basis of gamma matrices $(I, \gamma_\mu, \gamma_1 \gamma_2)$ as

$$\Psi = \frac{\eta}{2} I + \psi_\mu \gamma_\mu + \chi_{12} \gamma_1 \gamma_2.$$

It is known [19] that the fermionic kinetic term may be written in matrix form as

$$S_F = \int d^2 x \, \mathrm{Tr} \, \Psi^\dagger \gamma . \mathrm{D} \Psi \tag{1.6}$$

where the dot operator means to that all corresponding tensor components are multiplied and then integrated over all space and $D$ is the covariant derivative operator. The action given in equation 1.6 is invariant under

$$\Psi \to \Psi \Gamma^i \tag{1.7}$$

where $i = 1 \ldots 4$ and $\Gamma^i$ corresponds to one of the members of the $(I, \gamma_\mu, \gamma_1 \gamma_2)$ basis.

For the case of $\Psi \to \Psi \gamma_1 \gamma_2$, we find that

$$\frac{\eta}{2} \to -\chi_{12}$$
$$\chi_{12} \to \frac{\eta}{2}$$
$$\psi_\mu \to -\epsilon_{\mu\nu} \psi_\nu.$$

This transformation leaves the entire continuum action invariant and is thus a symmetry of the theory. By combing this transformation with the action of the original supercharge $Q$, one may construct an additional supersymmetry in the theory, one that corresponds to the twister supercharge $Q_{12}$. The supersymmetric algebra of the theory is now extended to include

$$\{Q_{12}, Q_{12}\} = \delta_\phi$$
$$\{Q, Q_{12}\} = 0.$$

In a similar fashion one may also analyze a new supersymmetry produced by con-

sidering a transformation of the type in equation 1.7 but for the other basis elements. With the same procedure as before, one finds other supercharges $Q_1$ and $Q_2$. The complex combination of these supercharges produces yet another supersymmetry of the theory. Eventually it is found that

$$\hat{Q}_\pm = Q \pm i Q_{12}$$
$$\bar{Q}_\pm = Q_1 \pm i Q_2$$

which are the total pair of complexified nilpotent supercharges of the theory.

### 1.2.5   Self-dual twist

Defining $\mathcal{Q} \equiv \hat{Q}_-$, we arrive at the result that

$$\mathcal{Q}\mathcal{A} = 2(\psi_1 + i\psi_2)$$
$$\mathcal{Q}(\psi_1 + i\psi_2) = 0$$
$$\mathcal{Q}\bar{\mathcal{A}} = 0.$$

where $\mathcal{A} \equiv A_1 + iA_2$ and $\bar{\mathcal{A}} = A_1 - iA_2$. This new supercharge is associated with an alternative twist referred to as the "self-dual twist." $\mathcal{Q}$ adds a new set of transformations to the twisted variables of the theory along with the ones given by $Q$.

From , the actions of the supercharge $Q$ are

$$QA_\mu = \psi_m u$$
$$Q\psi_m u = -D_\mu \phi$$
$$Q\bar{\phi} = \eta$$
$$Q\eta = [\phi, \bar{\phi}]$$
$$QB_{12} = [\phi, \chi 12]$$
$$Q\chi_{12} = B_{12}$$
$$Q\phi = 0.$$

16

While the actions of the new supercharge $\mathcal{Q}$ are

$$\mathcal{Q}\mathcal{A}_\mu = \psi_m u$$

$$\mathcal{Q}\psi_m u = 0$$

$$\mathcal{Q}\bar{\mathcal{A}}_\mu = 0$$

$$\mathcal{Q}\chi_{\mu\nu} = -\bar{\mathcal{F}}_{\mu\nu}$$

$$\mathcal{Q}\eta = d$$

$$\mathcal{Q}d = 0$$

with $\mathcal{A}_\mu = A_\mu + iB_\mu$. The twisted action may be written in $\mathcal{Q}$-exact form. That is, that it can be written in the form of $S = \beta\mathcal{Q}\Lambda$[6]. In this case, $\Lambda$ is given by

$$\Lambda = \int \mathrm{Tr}\left(\chi_{\mu\nu}\mathcal{F}_{\mu\nu} + \nu[\bar{\mathcal{D}}_\mu, \mathcal{D}_\mu - \frac{1}{2}\eta d]\right) \tag{1.8}$$

where

$$\mathcal{D}_\mu \equiv \partial_\mu + \mathcal{A}_\mu$$

$$\bar{\mathcal{D}}_\mu \equiv \partial_\mu + \bar{\mathcal{A}}_\mu.$$

Carrying out the $\mathcal{Q}$ operation on each term in the action and integrating out the $d$ field, one finds the action

$$S = \int \mathrm{Tr}\left(-\bar{\mathcal{F}}_{\mu\nu}\mathcal{F}_{\mu\nu} + \frac{1}{2}[\bar{\mathcal{D}}_\mu, \mathcal{D}_\mu]^2 - \mathcal{D}_{[\mu}\psi_{\nu]} - \eta\bar{\mathcal{D}}_\mu\psi_\mu\right). \tag{1.9}$$

We will now move on to discretize this twisted self-dual theory.

## 1.2.6   Lattice theory for (2,2) SYM

We employ a geometric discretization scheme proposed in [24]. In order to map the continuum theory onto the lattice, we essentially place each $p$-form with indices

---

[6]These actions are of pinnacle interest for topological field theories.

$\mu_1 \dots \mu_p$ on the link connecting $x$ with $(x + \mu_1 \dots \mu_p)$. Each link has two possible orientations and hence an orientation must also be specified for a given field.

On the lattice, continuum derivative operators transform to difference operators acting on these link fields. Covariant derivative operators appearing in wedge like operations and acting on positively oriented fields are replaced by forward difference operators, whose actions on vectors and scalars are given by

$$\mathcal{D}_\mu^+ f(x) = \mathcal{U}_\mu(x) f(x + \hat{\mu}) - f(x) \mathcal{U}_\mu(x)$$
$$\mathcal{D}_\mu^+ f_\mu(x) = \mathcal{U}_\mu(x) f_\nu(x + \hat{\mu}) - f_\nu(x) \mathcal{U}_\mu(x + \hat{\nu}).$$

Note that $\mathcal{U}_\mu = e^{i\mathcal{A}_\mu}$, in the usual way and that $\hat{\mu} = (1, 0)$ and $\hat{\nu} = (0, 1)$ since we are in two dimensions. The backwards difference operator $\bar{\mathcal{D}}_\mu^-$ replaces the divergence like operators of the continuum and it's action on positively oriented lattice vector fields is simply the adjoint of the forward operator, or

$$\mathcal{D}_\mu^- f_\mu(x) = f_\mu(x) \bar{\mathcal{U}}_\nu(x) - \bar{\mathcal{U}}_\mu(x - \hat{\mu}) f_\nu(x - \hat{\nu}). \tag{1.10}$$

We adapt only a subagebra of the full supersymmetry as was discussed earlier. It suffices to include the nilpotent complexified supercharge from the self-dual twist, and it acts on the lattice fields as

$$\mathcal{Q}\mathcal{U}_\mu = \psi_m u \tag{1.11}$$

$$\mathcal{Q}\psi_\mu = 0 \tag{1.12}$$

$$\mathcal{Q}\bar{\mathcal{U}}_\mu = 0 \tag{1.13}$$

$$\mathcal{Q}\chi_{\mu\nu} = \mathcal{F}_{\mu\nu}^{L\dagger} \tag{1.14}$$

$$\mathcal{Q}\eta = d \tag{1.15}$$

$$\mathcal{Q}d = 0 \tag{1.16}$$

18

where the lattice field strength tensor is written as

$$\mathcal{F}_{\mu\nu}^L = \mathcal{D}_\mu^+ \mathcal{U}_\mu(x) = \mathcal{U}_\mu(x)\mathcal{U}_\nu(x+\hat{\mu}) - \mathcal{U}_\nu(x)\mathcal{U}_\mu(x+\hat{\nu}) \qquad (1.17)$$

Notice that $\mathcal{F}_{\mu\nu}^L = -\mathcal{F}_{\nu\mu}^L$ and hence the continuum limit will also be antisymmetric.

Equation 1.14 implies that $\chi_{\mu\nu}$ must have the same orientation as $\mathcal{F}_{\mu\nu}^{L\dagger}$ and thus must be assigned to the negatively oriented link running from $(x+\hat{\mu}+\hat{\nu})$ to $x$. This lattice construction admits the following gauge symmetries

$$\eta(x) \to G(x)\eta(x)G^\dagger(x)$$

$$\psi_\mu(x) \to G(x)\psi_\mu(x)G^\dagger(x+\hat{\mu})$$

$$\chi_{\mu\nu}(x) \to G(x+\hat{\mu}+\hat{\nu})\chi_{\mu\nu}(x)G^\dagger(x)$$

$$\mathcal{U}(x) \to G(x)\mathcal{U}(x)G^\dagger(x).$$

Since the continuum action was $\mathcal{Q}$-exact, the lattice action will be $\mathcal{Q}$-exact also with

$$\Lambda = \sum_x \text{Tr}\left(\chi_{\mu\nu}\mathcal{D}_\mu^+\mathcal{U}_\nu + \eta\bar{\mathcal{D}}_\mu^- - \frac{1}{2}\eta\text{d}\right). \qquad (1.18)$$

Again, integrating out the $d$ field and applying the $\mathcal{Q}$ variation on $\Lambda$ yields

$$S = \sum_x \text{Tr}\left(\mathcal{F}_{\mu\nu}^{L\dagger}\mathcal{F}_{\mu\nu}^L + \frac{1}{2}\left(\bar{\mathcal{D}}_\mu^-\mathcal{U}_\mu\right)^2 - \chi_{\mu\nu}\mathcal{D}_{[\mu}^+\psi_{\nu]} - \eta\bar{\mathcal{D}}_\mu^-\psi_\mu\right). \qquad (1.19)$$

This is action is also obtained via the orbifold lattice method in [19] showing the duality between both procedures.

Now we will move on to the four dimensional SYM theory with $\mathcal{N} = 4$. The construction of this theory is very similar to the two dimensional case with some differences, but is most relevant to possible phenomenological theory describing TeV scale physics.

## 1.2.7 Four dimensional $\mathcal{N} = 4$ supersymmetric Yang-Mills

Four dimensional $\mathcal{N} = 4$ SYM is potentially one of the most interesting applications of exact lattice supersymmetry. A lattice theory may be constructed from only one supercharge that is exact on the lattice, yet the complete supersymmetry is restored in the continuum limit. One potential application that makes this model so attractive is that it is hypothesized to be dual to a type IIB string theory in $AdS^5 \times S^5$ space. in the 't Hooft limit[7], $d = 4$, $\mathcal{N} = 4$ SYM is conjectured to describe the supergravity limit of that string theory.

This theory possess a global Euclidean Lorentz symmetry $SO(4)_L$ and a $R$-symmetry of $SO(6)$ [25]. The $R$-symmetry contains a subgroup $SO(4)_R \times U(1)$. We declare the new twisted subgroup $SO(4)' = $ diagonal $(SO(4)_L \times SO(4)_R)$ and leave the remaining $U(1)$ intact which remains a global chiral symmetry of the twisted theory.

In this twisted diagonal subgroup, we have two vector boson fields that may be represented by $V_\mu$ and four scalars $S_\mu$. Under this diagonal subgroup, decomposed into it's $SU(2)$ representation, both $V_\mu$ and $S_\mu$ transform as 2-forms. The resulting theory is compactly written using a complex vector field as

$$ z^\mu = \frac{1}{\sqrt{(2)}}(S^\mu + iV^\mu), \quad \bar{z}_\mu = \frac{1}{\sqrt{(2)}}(S_\mu - iV_\mu) \quad \mu = 1\ldots 4. \quad (1.20) $$

We now construct this theory as a $\mathcal{N} = 4$ five dimensional reduced theory to four dimensions. First, the complexified gauge fields may be joined by a fifth component as:

$$ \left( \frac{1}{\sqrt{(2)}}(S_\mu + iV_\mu) , \; \frac{1}{\sqrt{(2)}}(S_5 + iS_6) \right) = z^m , \quad m = 1,\ldots 5. \quad (1.21) $$

Now we may express the fermionic degrees of freedom as five dimensional antisymmetric tensor fields as $\Psi = (\lambda, \psi^m, \xi_{mn})$. A nilpotent supersymmetry relates the

---

[7]The 't Hooft limit is when one takes the large $N$ limit of a gauge theory in such a way that $g^2 N$ remains finite. $g$ is the gauge field coupling.

components of these fields as

$$\mathcal{Q}z^m = \sqrt{2}\psi^m$$

$$\mathcal{Q}\psi^m = 0$$

$$\mathcal{Q}\bar{z}_m = 0$$

$$\mathcal{Q}\xi_{mn} = -i\bar{\mathcal{F}}_{mn}$$

$$\mathcal{Q}\lambda = id$$

$$\mathcal{Q}\,id = 0$$

where

$$\mathcal{D}^\mu\cdot = \partial^\mu\cdot + \sqrt{2}[z^\mu,\cdot], \quad \bar{\mathcal{D}}_\mu\cdot = -\partial^\mu\cdot + \sqrt{2}[\bar{z}^\mu,\cdot], \tag{1.22}$$

and the field strength tensor given by

$$\mathcal{F}^{\mu\nu} = -i[\mathcal{D}^\mu,\mathcal{D}^\nu] = F_{\mu\nu} - i[S_\mu,S_\nu] - iD_{[\mu}S_{\nu]}$$

$$\bar{\mathcal{F}}_{\mu\nu} = -i[\bar{\mathcal{D}}_\mu,\bar{\mathcal{D}}_\nu] = F_{\mu\nu} + i[S_\mu,S_\nu] + iD_{[\mu}S_{\nu]}$$

with d being an auxiliary field as was the case in two dimensions.

We may now extract the Marcus theory directly from a $\mathcal{Q}$ exact form as was done also for the two dimensional case in the previous section. We find that $S = \beta\mathcal{Q}\Lambda$ with

$$\Lambda = \int \mathrm{Tr}\left(\lambda\left(\frac{1}{2}id + \frac{1}{2}[\bar{\mathcal{D}}_m,\mathcal{D}^m]\right) + \frac{i}{4}\xi_{mn}\mathcal{F}^{mn}\right) \tag{1.23}$$

Carrying through the $\mathcal{Q}$ variation on the action and integrating out the auxiliary field d, one arrives at the action

$$S = \int \mathrm{Tr}\left(\frac{1}{4}\bar{\mathcal{F}}_{mn}\mathcal{F}^{mn} + \frac{1}{8}\left([\bar{\mathcal{D}}_m,\mathcal{D}^m]\right)^2 + \lambda\bar{\mathcal{D}}_m\psi^m + \xi_{mn}\mathcal{D}^m\psi^n\right). \tag{1.24}$$

This is the dimensionally reduced representation of the action from a five dimensional effective theory to a four dimensional "target" theory.

21

In order to discretize this theory, we employ exactly the same tactic as was used in the previous section for the two dimensional theory. We first must recognize that we complexified the gauge fields and hence the $\mathcal{U}_\mu$ will change to

$$\mathcal{U}^\mu = \frac{1}{\sqrt{2}} e^{(S_{\mu,n} + iV_{\mu,n})}, \qquad \mathcal{U}^5 = \frac{1}{\sqrt{2}} e^{(S_{5,n} + iS_{6,n})} \tag{1.25}$$

The exact $\mathcal{Q}$ supercharge is implemented on that lattice and its actions on the fields are

$$\mathcal{Q}\mathcal{U}^m = \sqrt{2}\psi^m$$
$$\mathcal{Q}\psi_m = 0$$
$$\mathcal{Q}\bar{\mathcal{U}}_m = 0$$
$$\mathcal{Q}\chi_{mn} = -2\mathcal{F}^{L\dagger}_{mn}$$
$$\mathcal{Q}\lambda = id$$
$$\mathcal{Q}d = 0$$

and the field strength tensor is the same as in section 1.17.

As was cautioned in the two dimensional case, one must also be careful about the orientation of the lattice fields. Consider a lattice scheme based on a hypercubic lattice. The link matrices $\mathcal{U}^\mu$ should be placed on the links in the directions from $x \to x + \hat{\mu}$. By inspecting the field strength equation, this operation traverses from $x \to x + \hat{\mu} + \hat{\nu}$ and due to supersymmetry $\chi_{\mu\nu}$ runs oppositely.

In terms of the lattice gauge transformations, we have

$$\lambda(x) \to G(x)\lambda(x)G^\dagger(x)$$
$$\psi^m(x) \to G(x)\psi^m(x)G^\dagger(x + \hat{\mu}_m)$$
$$\xi_{mn}(x) \to G(x + \hat{\mu}_m + \hat{\mu}_n)\xi_{\mu\nu}(x)G^\dagger(x)$$
$$\mathcal{U}^m(x) \to G(x)\mathcal{U}^m(x)G^\dagger(x + \hat{\mu}).$$
$$\bar{\mathcal{U}}_m(x) \to G(x + \mu_m)\bar{\mathcal{U}}_m(x)G^\dagger(x).$$

In the same process as was shown for the two dimensional case, we can thus arrive at a $\mathcal{Q}$-exact action, conduct the $\mathcal{Q}$ variation on a the fields and arrive at

$$S = \sum_x \left( \mathcal{F}_{mn}^{L\dagger} \mathcal{F}_{mn}^L + \frac{1}{2} \left( \bar{\mathcal{D}}_m^- \mathcal{U}_m \right)^2 - \sqrt{2} \left( \lambda \bar{\mathcal{D}}_m^- \psi_m + \xi_{mn} \mathcal{D}_{[m}^+ \psi_{n]} \right) \right). \qquad (1.26)$$

This is the same action that is found using the orbifolding procedure.

### 1.2.8 Summary

It was shown that lattice supersymmetry is not out of reach as it may have seem with such insurmountable issues (such as the lack of infinitesimal translation generators on the lattice). Through a twisting approach, that is, combining a subgroup of the Lorentz symmetry of the original space with a subgroup of the chiral supersymmetry symmetry ($R$-symmetry), one may avoid many of the issues seen in constructing supersymmetric lattice field theories. A review of accidental symmetries was also presented, and the importance of preserving one exact supercharge on the lattice was emphasized. All of these points are key ingredients in the construction of supersymmetric lattice field theories.

Lastly, two examples were given, one on two dimensional $\mathcal{N} = (2,2)$ SYM and the other in four dimensional $\mathcal{N} = 4$ SYM.

## 1.3 Outline of the thesis

The focus of this dissertation is twofold. First the implications of supersymmetry on the inflationary and post-inflationary eras of the universe will be discussed laying an overarching theoretical foundation over the unknown evolutionary eras. Secondly, nonperturbative studies on the presented lattice formulation will be discussed.

In chapter 2 we begin by considering the consequences of requiring supersymmetry during the inflationary phase of the universe. Inflation being driving by Kähler moduli arising in Type IIB String Theory compactified on O3/O7 orientifolds is presented

as an example. In chapter 3 the implications for the post-inflationary era of the universe until LHC energy scales are explored with an emphasis on the effects on CMB observables and unexpected implications for dark matter production.

The final two chapters conclude by investigating the fermionic sign problem and then a discussion of the phase structure in maximally extended supersymmetric quantum field theories on the lattice.

# Chapter 2

# Kähler Moduli Inflation in Type IIB String Theory: Insights from the Holomorphic Curvature

An important question that has guided string phenomenology for over a decade is whether string theory can make predictive contact with the inflationary paradigm. The large number of scalar moduli fields that appear in generic string compactifications provide many candidate fields to drive inflation [26].

The possibility of inflation driven by moduli fields is addressed in the $N = 1, D = 4$ low-energy effective supergravity theory descending from a UV complete theory of quantum gravity. The scalar part of the Lagrangian density is given by

$$\mathcal{L} = \frac{1}{2}R - g_{i\bar{j}}\partial\Phi^i\partial\overline{\Phi}^{\bar{j}} - V(\Phi^i, \overline{\Phi}^{\bar{j}}) \tag{2.1}$$

where $g_{i\bar{j}}$ is the metric of moduli space spanned by the scalars $\Phi$. Given a full string theoretic construction with stabilized moduli, the potential of the moduli fields $V$ should in principle be determined to enough accuracy to address an inflationary scenario that is consistent with cosmological observations. Of course, such a situation is notoriously difficult to obtain, given the complexity of such compactifications and the difficulty of fully incorporating quantum corrections [27].

The purpose of this chapter is to explore slow roll inflation in the context of the moduli space geometries descending from supersymmetric gravity, taking one crucial ingredient: the fact that the finite vacuum energy during inflation breaks supersymmetry.

The connection between supersymmetry breaking and inflation leads to a particularly simple order parameter for slow roll inflation: the *holomorphic sectional curvature* along the Goldstino direction [28, 29]. This order parameter has to be larger than a value that depends on the relative values of the Hubble scale and the Gravitino mass during inflation, with an absolute lower bound[1] of

$$\mathbb{H}[\Psi] > -\frac{2}{3}, \tag{2.2}$$

where

$$\mathbb{H}[\Psi] \equiv -\frac{R_{\Psi\overline{\Psi}\Psi\overline{\Psi}}}{g_{\Psi\overline{\Psi}}g_{\Psi\overline{\Psi}}}. \tag{2.3}$$

This condition is *necessary* (but *not* sufficient) for slow roll inflation and depends solely on the details of the Kähler geometry of the moduli space and not on the superpotential.

This allows one in principle to restrict geometries where the necessary condition is satisfied, before embarking on the task of constructing a full model including a realistic superpotential. Secondly, it reduces the problem to one of identifying and studying the Goldstino direction, which is somewhat simpler than studying the full scalar potential of inflation.

Several mathematical features of the holomorphic sectional curvature make this analysis particularly robust: (*i*) the shape and peak structure of the distribution over many geometries and field values are largely independent of the number of moduli and range of field values. Secondly, (*ii*) incorporating quantum corrections does not change the distribution structure to any appreciable degree in the geometric limit.

As an example in this chapter we consider the case of Calabi-Yau compactifica-

---

[1] This is in the case of low scale inflation where $m_{3/2}^2 >> H^2$.

tions of the heterotic string which are dual to type IIB compactifications on O3/O7 orientifolds. The main result found is that the vast majority of Calabi-Yau compactifications do not satisfy the inflationary bound. The addition of $\alpha'$ corrections does not alter this conclusion. We note, therefore, that the majority of compactifications inspected have a supergravity $\eta$ problem even at tree level.

## 2.1 The Holomorphic Curvature and Slow-Roll Inflation

For the purpose of exploring how to make use of this technology, we present a study of inflation within the context of superstring theory, considering the effective $D = 4, N = 1$ supergravity theory arising in the low-energy limit of the compactified superstring theory. Considering chiral multiplets $\Phi_I \equiv (\Phi_i, \Phi_{\bar{i}})$[2], the scalar potential depends on the Kähler potential $K$ and the superpotential $W$, and their derivatives with respect to $\Phi_i$ and $\overline{\Phi}_{\bar{j}}$. We take $\{\Psi_I\} \subset \{\Phi_I\}$ as the field that acquires non-zero $F-$terms during inflation.

The scalar fields $(\Phi_i, \overline{\Phi}_{\bar{i}})$ span a Kähler manifold which yields a scalar potential given by[3]

$$V = e^K(g^{i\bar{j}}F_i F_{\bar{j}} - 3|W^2|) \ , \tag{2.4}$$

where

$$
\begin{aligned}
F_i &= D_i W = \partial_i W + \partial_i K W \\
m_{3/2}^2 &= e^K |W|^2.
\end{aligned}
\tag{2.5}
$$

While equation 2.1 describes a generic gravity theory coupled to scalars, the above potential is the unique potential generated by a supergravity theory. The metric,

---

[2]We use the same notation for a superfield and its scalar component.

[3]We work in units where the Planck Mass $M^2 = 1$

connection, and curvature tensor of the Kähler manifold is given by

$$
\begin{aligned}
g_{i\bar{j}} &= \partial_i \partial_{\bar{j}} K, \\
\Gamma_{ij}^k &= g^{\bar{l}k} \partial_i g_{j\bar{l}}, \\
R_{\bar{k}\bar{l}ij} &= \partial_{\bar{i}} \partial_j \partial_l \partial_{\bar{k}} K - g^{\bar{n}m}(\partial_{\bar{i}}\partial_{\bar{k}}\partial_m K)(\partial_j \partial_l \partial_{\bar{n}} K).
\end{aligned}
\tag{2.6}
$$

The other geometric quantity of interest is the the holomorphic sectional curvature of a plane $(\Psi, \overline{\Psi})$ defined in the tangent space at a given point in the manifold as [28]

$$
\mathbb{H}[\Psi] = -\frac{R_{\Psi\overline{\Psi}\Psi\overline{\Psi}}}{g_{\Psi\overline{\Psi}} g_{\Psi\overline{\Psi}}}.
\tag{2.7}
$$

For a general theory of Kähler moduli inflation, the holomorphic sectional curvature $\mathbb{H}[\Psi]$ becomes intrinsically tied to the slow-roll condition [29]. To see this, we first consider the multifield potential slow-roll parameters given by [30] as

$$
\begin{aligned}
\epsilon &= \frac{\nabla^i V \nabla_i V}{V^2} \\
\eta &= \min \; \text{eigenvalue} \, \{N\} \,,
\end{aligned}
\tag{2.8}
$$

where

$$
N = \frac{1}{V}
\begin{pmatrix}
\nabla^i \nabla_j V & \nabla^i \nabla_{\bar{j}} V \\
\nabla^{\bar{i}} \nabla_j V & \nabla^{\bar{i}} \nabla_{\bar{j}} V
\end{pmatrix}.
\tag{2.9}
$$

The covariant derivative on the Kähler manifold is defined as

$$
\nabla_i f^k \equiv \partial_i f^k + \Gamma_{ij}^k f^j
\tag{2.10}
$$

for any vector $f^k$ on $\mathcal{M}$. In the above, $I = (i, \bar{i})$ and $J = (j, \bar{j})$ and $\nabla_i$ is a covariant derivative with respect to the metric $g_{i\bar{j}}$. For any given unit vector $u^I = (u^i, u^{\bar{i}})$ one has $\eta \leq u_I N_J^I u^J$. Choosing $u^I = (F^\Psi, F^{\overline{\Psi}})/(\sqrt{2}|F|)$ and evaluating the relevant covariant derivatives, one finds that

$$
\eta \leq \eta_{\max} \equiv \frac{2}{3\gamma} + \frac{1+\gamma}{\gamma} \mathbb{H}[\Psi] + \mathcal{O}(\sqrt{\epsilon}) \,,
\tag{2.11}
$$

29

where $\gamma = \frac{1}{3}\frac{V}{m_{3/2}^2} \sim \frac{H^2}{m_{3/2}^2}$. We drop all terms involving $\epsilon$, since $\sqrt{\epsilon} < \mathcal{O}(10^{-3})$. The spectral index is given by $n_s = 1+2\eta \Rightarrow \eta_{\text{observed}} \sim -0.01$. Therefore, $\eta_{\text{max}} \geq -0.01$.

This yields the following necessary bound on the holomorphic sectional curvature along the SUSY breaking direction

$$\mathbb{H}[\Psi] \geq -\frac{2}{3}\frac{1}{1+\gamma} \ . \tag{2.12}$$

While this bound depends on the ratio of the inflationary scale and the value of $m_{3/2}$, the hard bound is given by Eq. 2.2 [29]. This is a *necessary* but not a *sufficient* condition for slow-roll inflation. We may therefore consider the case in which once we found a suitable Kähler function that satisfies relation 2.12, we can attempt to pair it with a superpotential $W$ which could then possibly result in a rich phenomenological model.

## 2.2 Heterotic Calabi-Yau Compactifications

With the geometric bound of the holomorphic sectional curvature defined, we may now consider Kähler functions of a specific type. In this section we consider the case of heterotic string models with Calabi-Yau compactifications since they are physically dual to Type IIB compactified on O3/O7 orientifolds. The moduli space manifold of these geometries have Hodge numbers $(h^{1,1}, h^{2,1})$ with a basis of divisors $S_i$, $i = 1, ..., h^{1,1}$ [31]. The Kähler moduli $t^i$ are defined from the Kahler form $J = t^i S_i$. In the case of a Calabi-Yau 3-fold the volume of the moduli space is given by

$$V_{\text{CY}} = \frac{1}{6}d_{ijk}(t_i - \bar{t}_i)(t_j - \bar{t}_j)(t_k - \bar{t}_k), \tag{2.13}$$

with the $d_{ijk}$ being the triple intersection numbers in the integral basis of the toric divisors[4]. The Kähler potential for the moduli $t^i$ is given by

$$K = -3 \ln V_{\text{CY}}, \tag{2.14}$$

in the absence of $\alpha'$ and $g_s$ corrections.

As an example of these constructions, consider the case where $h^{1,1} = 1$. The moduli space volume then takes the form

$$K = -3 \ln \left( \frac{1}{6}(t_1 - \bar{t}_1)^3 \right), \tag{2.15}$$

and it is simple to check that $\mathbb{H}[t_1] = -2/9$ and hence the bound is satisfied for low-scale inflation but not high-scale.

The situation changes slightly when the Kähler potential takes the form

$$K = -n \log(t_1 - \bar{t}_1 + X\overline{X}) \ \forall n , \tag{2.16}$$

which defines maximally symmetric coset spaces. for which $\mathbb{H}(t_1) = \mathbb{H}(X) = -2/n$. This implies that inflationary scenarios based on these stringy supergravity geometries in which $n = 3$ and supersymmetry breaking is dominated by the modulus $t_1$ or the field $X$ face the $\eta$ problem [32].

### 2.2.1 Randomized Supergravity

Given a suitable potential that satisfies the slow roll conditions, it is of course possible to embed such a potential in supergravity - see for example [33]. The embedding will satisfy the constraint on the sectional curvature, and typically locate the supersymmetry breaking field to a flat, decoupled sector.

Conversely, it is interesting to ask what happens in the case of supergravity potentials one obtains from string theory. As outlined in the introduction, this is the

---

[4]Because the metric of the moduli space is uniquely determined by the Kähler function, the set of $d_{ijk}$ determines the overall topology of the Calabi-Yau manifold.

goal of the present work. We will consider Kähler geometries of the form Eq. 2.14, with supersymmetry breaking during inflation dominated by a modulus. Moreover, we will consider Kähler potentials of the sequestered form

$$K = -3\log(V + X\overline{X}) . \tag{2.17}$$

We first note from Eq. 2.14 that the Kähler function can be seen as a log of a cubic polynomial, where the precise form of the cubic polynomial is given when the intersection numbers $d_{ijk}$ are specified.

For example, consider the form of the volume for the case of two moduli

$$V = a_1 s_1^3 + a_2 s_1^2 s_2 + a_3 s_1 s_2^2 + a_4 s_2^3 \tag{2.18}$$

where the $a_i$'s take the obvious definition and $t_i - \bar{t}_i = s_i$.

With random cubic functions of this general form we can make general statements about the holomorphic sectional curvature. First consider the simplified case when

$$K = -n \ln V \tag{2.19}$$

$$V \propto (t_1 - \bar{t}_1)^p \tag{2.20}$$

which corresponds to the case when a single term of the volume dominates. In this case, by a simple computation similar to Eq. 2.15, one obtains $\mathbb{H}[t_1] = -\frac{2}{np}$. This leads to an understanding of the expected peak structure of a randomized distribution in the two moduli case based on Eq. 2.14: the peaks of the distribution will lie at values given by

$$\text{peak values of } \mathbb{H}[t_1] = -\frac{2}{np} \quad \text{with } p = \{1, 2, 3\}. \tag{2.21}$$

This result is immediately extended to the logs of random polynomials of degree m as

$$\text{peak values of } \mathbb{H}[t_1] = -\frac{2}{np} \quad \text{with } p = \{1, 2, \ldots, m\} \tag{2.22}$$

allowing one to analyze more generic geometries[56]. We also expect that the expectation value over all fields will yield

$$< \mathbb{H}[t_1] > \quad = \quad < \mathbb{H}[t_2] > \quad = \quad \ldots < \mathbb{H}[t_N] > \tag{2.23}$$

where $N$ is the dimension of the moduli space.

Moreover, three important facts are clear:

$(i)$ the peak structure in Eq. 2.22 is independent of the dimensionality of the moduli space.

This is because the structure only depends on the fact that the volume is a generic polynomial of degreee $m$, regardless of the number of variables. This makes it clear that this generic polynomial procedure is orthogonal to random matrix theory methods which rely crucially on large numbers of moduli.

$(ii)$ the peak structure is independent of the range of the variables $x_i$, as long as the range is democratic in moduli space.

This is due to the fact that the Kähler potential is a log of a homogeneous polynomial, and the sectional curvature only depends on derivatives of the Kahler potential.

$(iii)$ the peak structure is independent of the range of the intersection numbers, as long as the range is democratic, for the same reason as above.

These three features make the study of a distribution over geometries exceptionally general, a fact that will be apparent when we study candidate Calabi-Yau geometries. A statistical scan is performed over a representative range of intersection numbers and

---

[5] Though this may be physically unnecessary since we need only consider CY 3 folds for our given universe.

[6] This result has use beyond inflation in string models as one can right-away consider if the holomorphic bound is satisfied by analyzing the exponents in Kähler functions.

field values (with values at least $\mathcal{O}(1)$ in string units to suppress $\alpha'$ corrections) and intersection numbers $d_{ijk}$.

This study is orthogonal to a study performed in [34] where methods in computational algebraic geometry [35] were utilized to arrive at similar (negative results).

### 2.2.2 The basis of the complexified volumes of divisors

The holomorphic coordinates that appear in Type IIB compactifications on O3/O7 orientifolds [34] are not the $t^i$ moduli, but the complexified volumes of divisors

$$\tau_i = \int_{S_i} \frac{1}{2} J \wedge J - iC_4. \tag{2.24}$$

The volume and hence the Kahler potential can be written implicitly in terms of the $\tau_i$, by using the relations

$$\tau_i = \frac{\partial V}{\partial t_i} = \frac{1}{2} S_i J^2 = \frac{1}{2} d_{ijk} t^j t^k . \tag{2.25}$$

In Type IIB, the natural supersymmetry breaking variables are the $\tau_i$ hence the phenomenologically correct distribution to study is the distribution of $\mathbb{H}(\tau_i)$ for this case[7].

The Legendre transformation in Eq. 2.25 is in general non-trivial, and obtaining an analytical expression for the Kähler potential and hence $\mathbb{H}(\tau_i)$, given the intersection numbers $d_{ijk}$ may also be non-trivial. However, within the method of generic polynomials described above, the volume may simply be regarded as a homogeneous function of power 3/2 with random coefficients

$$V = a_1 s_1^{3/2} + a_2 s_1 s_2^{1/2} + a_3 s_1^{1/2} s_2 + a_4 s_2^{3/2} \tag{2.26}$$

---

[7]The reader may notice that in the heterotic case, the distributions turn out to be identical. This is because there exist dualities between Type IIB and the heterotic string such that the inflationary observables are exactly the same in both cases, as they should be.
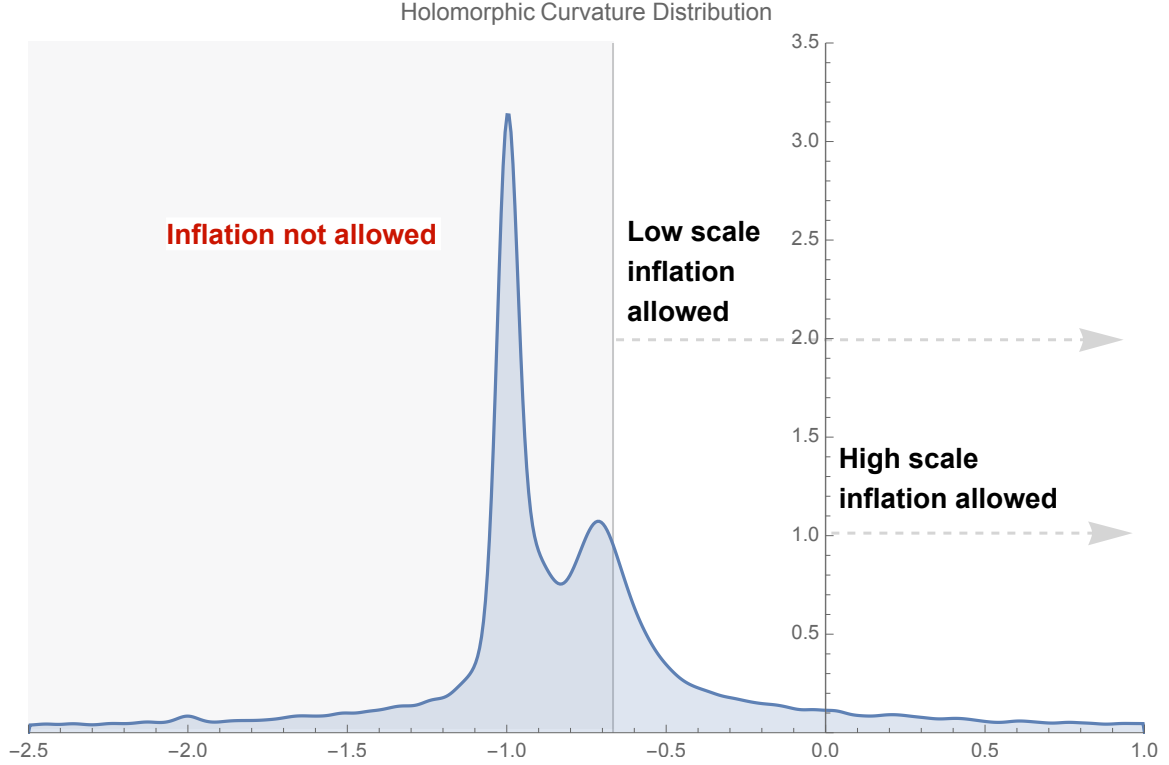
Figure 2-1: The distribution of $\mathbb{H}[t_1]$ sampled over moduli values between $[1,12]$ and intersection numbers ranging between $[-8,8]$. The peak values are as expected, though the -1.0 and -2/3 peak dominates the distribution possibly for deeper symmetry reasons.

where the Kähler potential in the case of Type IIB is given by

$$K = -2\ln V. \tag{2.27}$$

The corresponding peak distribution for the holomorphic sectional curvature would therefore be given by peak values of

$$\mathbb{H}[t_1] = \{-2, \ -1, \ -\frac{2}{3}\}. \tag{2.28}$$

We verified this claim by investigating the distribution of $\mathbb{H}[t_1]$ by sampling over moduli values between $[1,12]$ and intersection number range between $[-8,8]$. The distribution is presented in figure 2-1 and verifies our claim. The only exception is that the peak at -2 is no where nearly as pronounced as the peaks at -1 and -2/3. We

hypothesize deeper symmetry reasons within the functional form of $\mathbb{H}[t_1]$. Never the less, the conclusion remains that the majority of holomorphic curvature values lies in the forbidden inflation region.

We thus conclude that while in general, the Legendre transformation in Eq. 2.25 is difficult to solve explicitly, the generic polynomial method shows that the peaks for the holomorphic sectional curvature lead to the conclusion that *low-scale inflation is unlikely in Type IIB compactifications and hence, due to dualities between Type IIB and the heterotic string, also unlikely in Calabi-Yau compactifications.*

Since quantum corrections to the Kähler potential are proportional to the Euler character of the Calabi-Yau 3-fold [36], this result does not affect the holomorphic sectional curvature calculation and are therefore inconsequential[8]. Hence modular inflation in type IIB and heterotic models lead to a severe eta problem.

## 2.3 Conclusions

In this chapter we discussed the implications of considering supersymmetry to be present during the inflationary phase of the universe. We considered in more detail the example of Calabi-Yau compactications in the heterotic string and then type IIB O3/O7 orientifold compactifications. We showed that in these examples inflation driven by moduli fields is unlikely from a statistical analysis.

Though these results are negative, we only considered the case where moduli fields could drive inflation and break supersymmetry. Since the full form of the quantum gravity potential that explains the dynamics of the universe during the inflationary era (supposing there was indeed an inflationary era) is unknown, it is entirely possible that other fields are present during this time. For example if there was a Kähler potential of the form

$$K = -2\ln V + X\bar{X} \tag{2.29}$$

the holomorphic sectional bound would be trivially satisfied for all scenarios since $\mathbb{H}[X] = 0$.

# Chapter 3

# Supersymmetry, Nonthermal Dark Matter and Precision Cosmology

Within the Minimal Supersymmetric Standard Model (MSSM), LHC bounds suggest that scalar superpartner masses are far above the electroweak scale. Given a high superpartner mass, nonthermal dark matter is a viable alternative to WIMP dark matter generated via freezeout. In the presence of moduli fields nonthermal dark matter production is associated with a long matter dominated phase, modifying the spectral index and primordial tensor amplitude relative to those in a thermalized primordial universe. Nonthermal dark matter can have a higher self-interaction cross-section than its thermal counterpart, enhancing astrophysical bounds on its annihilation signals. The contributions to the neutralino mass from the bino, wino and higgsino are constrained using existing astrophysical bounds and direct detection experiments for models with nonthermal neutralino dark matter. Using these constraints we quantify the expected change to inflationary observables resulting from a nonthermal phase.

## 3.1   Introduction

Cosmological observations allow us to determine the geometry, composition and age of the universe with great accuracy, and to tightly constrain the primordial pertur-

bation spectrum. Big Bang Nucleosynthesis (BBN) and the recently revealed cosmological neutrino background imply that the universe was thermalized at MeV scales. Further, the correlation between temperature and E-mode polarization anisotropies in the Cosmic Microwave Background (CMB) gives strong evidence that primordial perturbations were laid down before recombination.

Standard Model physics cannot generate the primordial perturbations, drive baryogenesis or supply the dark matter content of the universe. Consequently, key processes occur at very high energies during the *primordial dark age* in which the universe is dominated by physics beyond the Standard Model. This period is weakly constrained, given our ignorance of the underlying physics. Crucially, while the neutrino background and BBN require that the universe was thermalized at MeV scales, it need not be thermalized at higher energies. The equation of state during the primordial dark age determines the expansion rate, and thus the rate at which modes (re)enter the horizon, modifying the observed power spectrum if the spectral index, $n_s$, is not strictly scale-invariant [13, 16, 37–43]. This issue has primarily been discussed in the context of inflation, but it arises in any mechanism generating perturbations well beyond Standard Model scales.

If the primordial universe is thermalized, massive long-lived particles may *freeze-out* with a final abundance determined primarily by their mass and annihilation cross-section [44]. This is the basis of thermal WIMP[1] dark matter, which assumes a weak-scale cross-section, $\sigma$ and $\langle \sigma v \rangle_{th} \simeq 10^{-26}$ cm$^3$/s, where $v$ is the typical velocity. Alternatively, *nonthermal* dark matter is produced via the decay of heavier particles into a long-lived final state and does not require thermal equilibrium [45–49] (for a review see [50], and for recent related work [51–53]). Dark matter models are constrained by both direct detection experiments and searches for astrophysical signals generated by their annihilation products. Nonthermal dark matter can have a higher self interaction cross-section than thermal dark matter so astrophysical signals are potentially stronger for these scenarios, particularly in indirect experiments such as FERMI and AMS-2 [54–59].

---

[1]Weakly Interacting Massive Particles

Simple supersymmetric (SUSY) versions of the Standard Model face considerable pressure from LHC data, but SUSY remains a candidate symmetry of high energy physics and SUSY models provide a wide range of dark matter candidates. In the Minimal SUSY Standard Model (MSSM), LHC data requires large scalar superpartner masses of 10 TeV or more [60] while the dark matter species can be lighter. This a situation that naturally leads to nonthermal dark matter production (e.g. [61, 62]) and a similar argument applies to anomaly mediated SUSY breaking [63]. Further, a primordial nonthermal phase may be generic in SUSY models with a high energy completion in the presence of gravity [50,64]. This was seen explicitly in the *G2-MSSM* [65], and later generalized to models with *strong* moduli stabilization [66,67]. In many cases nonthermal dark matter production is naturally favored in these scenarios.

Given LHC bounds on the SUSY spectrum in the MSSM, cosmological constraints – while indirect – are key to explorations of the SUSY parameter space at higher energies. In this paper we explore nonthermal dark matter production in the MSSM, quantifying the extent to which the nonthermal phase changes expectations for inflationary observables. For nonthermal production, the cross-sections are often larger than typical for thermal dark matter, increasing the sensitivity of astrophysical searches for dark matter decay products. In particular, we discuss constraints on the mass of neutralino dark matter and the allowed contributions to the neutralino mass from the bino, wino and higgsino.

The paper is organized as follows. In Section 2 we review uncertainties in inflationary observables derived from the unknown post-inflationary equation of state. In Section 3, we summarize nonthermal dark matter phenomenology and the associated expansion history. In Section 4, we explore the post-inflationary expansion history of the universe in an MSSM model with SUSY breaking above the TeV scale, and show how this is constrained by existing and future constraints from dark matter experiments. In the final section we conclude.

## 3.2 CMB Uncertainties from the Post-Inflationary Expansion

To determine the predictions of a specific inflationary model[2] the comoving wavenumber $k$ is matched to the instant it exits the Hubble horizon [13, 16, 37–43]. This occurs when $k = a_k H_k$ where $H$ and $a$ denote the Hubble parameter and scale factor respectively, and a subscript $k$ labels values at horizon crossing. $N$ is defined as the number of e-efolds before the end of inflation,

$$e^{N(k)} \equiv \frac{a_{end}}{a_k},$$ (3.1)

where $a_{end}$ denotes the scale factor at the end of inflation and rewrite $N(k)$ as

$$N(k) = \ln\left(\frac{H_k}{H_{end}}\right) - \ln\left(\frac{k}{a_0 H_0}\right) + \ln\left(\frac{a_{end} H_{end}}{a_0 H_0}\right),$$ (3.2)

where $(a_0 H_0)^{-1}$ is the value of the co-moving Hubble radius today [16]. The first term in equation (3.2) can be determined for any specific model, while the final term depends on the post-inflationary expansion history of the universe. We assume single-field slow-roll inflation for the purposes of illustration and characterize the post-inflationary expansion by an effective equation of state $w$. One finds the matching equation [13]

$$N(k, w) \simeq 71.21 - \ln\left(\frac{k}{a_0 H_0}\right) + \frac{1}{4}\ln\left(\frac{V_k}{m_p^4}\right) + \frac{1}{4}\ln\left(\frac{V_k}{\rho_{end}}\right) + \frac{1 - 3w}{12(1 + w)}\ln\left(\frac{\rho_r}{\rho_{end}}\right)$$ (3.3)

where $\rho_{end}$ is the value of the energy density at the end of inflation, $V_k$ is the inflaton potential as the $k$th mode leaves the horizon, and $\rho_r$ is the energy density at which the universe is assumed to become thermalized. The first two terms in (3.3) are model independent. For GUT scale inflation the third term is roughly $-10$. The fourth term is typically order unity given that the value of the inflaton potential necessarily

---

[2]We focus on inflation, but our arguments apply to any mechanism which generates perturbations on super-Hubble scales with a power spectrum whose spectral index in not strictly scale-invariant.

evolves slowly as inflation proceeds. Finally, if the universe thermalizes promptly the last term is negligible, and we recover the familiar result that $50 \lesssim N \lesssim 60$ for modes contributing to the CMB.

If $\rho_{end}^{1/4} \gg \rho_r^{1/4}$ and $w \neq 1/3$ then $N$ differs from its benchmark value[3] by

$$\Delta N = \frac{1 - 3w}{12(1 + w)} \ln \left( \frac{\rho_r}{\rho_{end}} \right), \tag{3.4}$$

where $\rho_{\text{end}} = 3V_{\text{end}}/2$ for a given potential. If $w < 1/3$, $\Delta N$ is negative, since $\rho_r < \rho_{end}$.

The equation of state during the primordial dark age induces uncertainties in inflationary predictions for the scalar tilt and tensor-to-scalar ratio $n_s$ and $r$. The uncertainty in $n_s$ is clearly associated with the running $\alpha_s = dn_s/d\ln k$ and to lowest order in slow roll [68–70]

$$\begin{aligned} \Delta n_s &= (n_s - 1) \left[ -\frac{5}{16}r - \frac{3}{64}\frac{r^2}{n_s - 1} \right] \bigg| \Delta N, \\ \Delta r &= r \left[ (n_s - 1) + \frac{r}{8} \right] \bigg| \Delta N. \end{aligned} \tag{3.5}$$

The resulting fractional uncertainties $\Delta r/r$, $\Delta n_s/|n_s - 1|$ in these observables can be substantial [16,40]. In particular, the theoretical uncertainty in $n_s$ can be comparable to the precision with which it is measured by Planck [71]. Our primary focus is the implications for $w$ and $\rho_r$ of MSSM scenarios with nonthermal dark matter, which will lead to tighter predictions for the primordial spectrum of specific inflation models.

## 3.3   Thermal and Nonthermal Dark Matter

In the early universe, the density in WIMPs relative to the critical density at freeze-out is [72]

$$\Omega_{dm}h^2 \simeq 8.63 \times 10^{-11} \left( \frac{m_X}{g_*^{1/2}\langle\sigma v\rangle T} \right) \text{GeV}^{-2}. \tag{3.6}$$

---

[3]In models that make an explicit prediction for $\rho_r$ we can insert this value into equation (3.3). If the post-inflationary thermal history is unknown $\rho_r^{1/4}$ is the energy scale by which thermalization is required to have occurred [38].
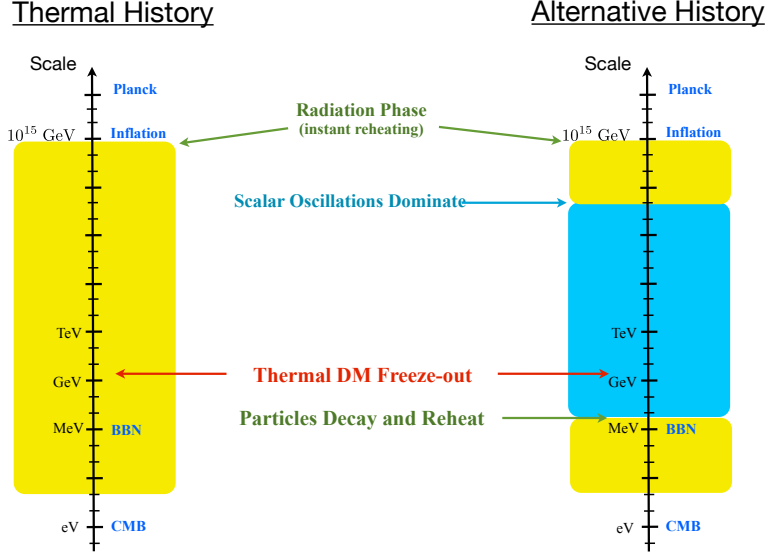
Figure 3-1: The lefthand timeline represents the thermal history of the early universe when dark matter is populated in the thermal bath that emerges shortly after after inflation. The right timeline represents a possible nonthermal history where dark matter production occurs directly from scalar decay.

where $m_X$ is the dark matter particle's mass, $\langle \sigma v \rangle$ is the *total* thermally averaged cross-section, $g_*$ and $T$ are the number of relativistic degrees of freedom and temperature at freeze-out and $h$ is the present Hubble parameter in units of 100 km/s/Mpc. If the universe is thermalized, freeze-out occurs at $T_f \simeq m_X/20$ and $g_* \sim 100$, assuming the effective number of degrees of freedom is similar to that of the Standard Model [73]. The abundance simplifies to

$$\Omega_{dm}^{therm} h^2 \simeq 0.12 \left( \frac{1.63 \times 10^{-26} \text{cm}^3/\text{s}}{\langle \sigma v \rangle} \right) . \tag{3.7}$$

where we have used $\text{GeV}^{-2} \cdot c \simeq 1.17 \times 10^{-17}$ cm$^3$/s. WIMPs with typical speeds ($v \simeq 0.3c$) and electroweak cross-sections ($\approx 1$ pb) yield $\Omega_{dm}^{therm} h^2 \simeq 0.12$ in agreement with the data, a coincidence often called the *WIMP miracle*.

Simple SUSY models with thermal WIMPs are in growing conflict with collider data and direct detection experiments [74]. By contrast, nonthermal models posit that dark matter production occurs at temperatures below standard thermal freeze-

out[4] leading to dark matter with novel and unexpected experimental signatures. For example, if a heavy relic comes to dominate the energy density following inflation and the dark matter particle is one its decay products, the resulting relic density is still given by (3.6) but with $T = T_r$ and $g_* = g_*(T_r)$, the value at the time of reheating

$$
\begin{aligned}
\Omega_{dm}^{NT} h^2 &\simeq 8.60 \times 10^{-11} \left( \frac{m_X}{g_*(T_r)^{1/2} \langle \sigma v \rangle T_r} \right), \\
&\simeq 0.10 \left( \frac{m_X}{100 \text{ GeV}} \right) \left( \frac{10.75}{g_*} \right)^{1/2} \left( \frac{3 \times 10^{-23} \text{ cm}^3/\text{s}}{\langle \sigma v \rangle} \right) \left( \frac{10 \text{ MeV}}{T_r} \right). (3.8)
\end{aligned}
$$

The similarity to the thermal freezeout result (3.6) arises because when the WIMPs are produced from scalar decay they will rapidly annihilate until their number density reduces to the point where annihilations can no longer occur. This process is essentially instantaneous (on cosmological time scales) and so this second "freeze-out" occurs at the reheat temperature $T_r$ (see [50] for a review). Any thermally produced dark matter is diluted by the increase in entropy during the decay by a factor of $(T_r/T_f)^3$. Equation (3.8) demonstrates both the benefits and disadvantages of nonthermal dark matter. There is no longer a robust relationship between $m_X$ and and freeze-out temperature but there is more flexibility to satisfy the observational constraint $\Omega_{dm} h^2 = 0.12$, and the possibility of larger annihilation rates. The extreme case of MeV scale reheating enhances the annihilation rate by three orders of magnitude, relative to the thermal WIMP case. This would yield larger fluxes in indirect detection experiments, and modifies design strategies for direct detection and collider probes. This has led to new model building possibilities for SUSY neutralino dark matter, many of which are already tightly constrained by PAMELA and FERMI [55–59].

There have been several phenomenological studies of nonthermal dark matter over the years. This option became more attractive when it was realized that in SUSY based solutions to the hierarchy problem – where gravity is important – the reheat temperature is not a free parameter, but is fixed by the high energy behavior of the

---

[4]If the particles were produced above their freeze-out threshold, they could thermalize via their mutual interactions.

theory [64,65]. In combination with tightening collider and dark matter detection constraints on thermal dark matter there is thus considerable motivation for considering nonthermal dark matter.

A comparison of the thermal history of the universe for representative thermal and nonthermal scenarios appears in Figure 1. There are many possible alternatives to a strictly thermal history, which are generally associated with dark matter production that occurs at a temperature below that of thermal production, or out of equilibrium. These can include cosmic histories where there is a second phase of low-scale inflation (thermal inflation [10]), or if the decay of heavy particles leads to a significant source of dark matter and entropy production prior to BBN.

### 3.3.1 Nonthermal Dark Matter: A Realization Through Scalar Decay

Many Beyond the Standard Model (BSM) proposals contain scalar degrees of freedom beyond the minimal higgs. This is the case in supergravity and string theoretic approaches to BSM, where the vacuum expectation values of scalar fields determine the couplings of the low energy theory. However, these fields also lead to the cosmological moduli problem [75–77] – the fields are displaced from the low-energy minima in the early universe and undergo coherent oscillations, mimicking a matter dominated epoch[5] prior to BBN. The fields typically decay through gravitational strength couplings, and the universe reheats via the production of relativistic Standard Model and BSM particles – the lightest of which, if stable, may provide a WIMP candidate.

For scalars of mass $m_\sigma$ the decay rate typically scales as $\Gamma \sim m_\sigma^3/m_p^2$ and the corresponding reheat temperature is

$$T_r \simeq \left(\frac{m_\sigma}{10 \text{ TeV}}\right)^{3/2} \text{ MeV}. \tag{3.9}$$

If this temperature is below the thermal freeze-out scale $T_f \simeq m_X/20$ and the

---

[5]This is strictly true only if the mass term in the potential gives the dominant contribution, otherwise the cosmological scaling of the energy density is determined by the dominant term in the potential [78].

field dominates the energy density at the time of decay we have a nonthermal dark matter scenario. Successful BBN and observations of neutrino decoupling require $T_r \gtrsim 3$ MeV [79–82]. For dark matter with a mass not too far above the electroweak scale, fixing $T_r < T_f \sim m_x/20$ provides an upper bound

$$20 \text{ TeV} \lesssim m_\sigma \lesssim 10^4 \text{ TeV}. \tag{3.10}$$

To give a specific example[6], consider a supersymmetric model with a singlet scalar field $\sigma$ with a shift symmetry $\sigma \to \sigma + c$ where $c$ is a constant, so the potential is independent of the field, or $V(\sigma) = 0$. If this remains a good symmetry until SUSY breaking and SUSY breaking is mediated by gravitational interactions the resulting mass is comparable that of the gravitino $m_{3/2}$. If SUSY addresses the electroweak hierarchy problem

$$m_{3/2} = \frac{\Lambda^2}{m_p} \simeq 0.1 - 10^3 \text{ TeV}, \tag{3.11}$$

where $\Lambda$ is the SUSY breaking scale, the electroweak hierarchy implies $\Lambda \simeq 10^{11} - 10^{12}$ GeV. Thus, SUSY theories can easily lead to masses in the range given by equation (3.10). The lower bound of 0.1 TeV is the origin of the term *cosmological moduli problem*, as it leads to scalar decay and a reheat temperature in conflict with the bounds set by BBN and neutrino decoupling. Within the MSSM, such low scales are already disfavored by LHC data since squarks in this mass range have not been detected, pushing up the mass scale of the gravitino.

A shift-symmetric scalar in a fundamental theory – such as supergravity or string theory – typically has additional geometric factors that lift its mass to larger values. For Type-IIB flux compactifications the mass is of order $m_\sigma \sim \log(m_p/m_{3/2})m_{3/2}$ [83] if the model accounts for both the electroweak hierarchy and the present-day vacuum energy. The authors of [64] argued that in supergravity and string frameworks the mass of a scalar which is stabilized and which meets the above requirements is typically within the range of equation (3.10), implying a nonthermal history.

---

[6]The arguments that follow will not rely strongly on the presence of SUSY, and it would seem that the main ingredients in our argument – the existence of scalars and symmetry breaking associated with the electroweak scale – could be realized in other approaches to BSM physics.

In the early universe and during inflation, the shift symmetry is broken by both the finite energy density of the universe and quantum gravity effects, contributing a Hubble scale mass and a tower of non-renormalizable operators to the effective potential,

$$\Delta V(\sigma) = -c_1 H_{inf}^2 \sigma^2 + \frac{c_2}{m_p^2}\sigma^6 + \dots , \tag{3.12}$$

where we expect the couplings $c_1, c_2 \simeq \mathcal{O}(1)$. During high scale inflation $H > m_\sigma$ and $\langle\sigma\rangle \simeq m_p$, as opposed to the low-energy minimum $\langle\sigma\rangle \simeq 0$ resulting from SUSY breaking. The displacement from the low energy minima provides the initial amplitude for the coherently oscillating field $\sigma$. The energy density of the coherent field is

$$\rho_{osc}^\sigma(t) = \frac{1}{2}m_\sigma^2 \Delta\sigma^2 \left(\frac{a(t_{osc})}{a(t)}\right)^3 . \tag{3.13}$$

Coherent oscillations begin as the expansion rate reaches $H \simeq m_\sigma$, corresponding to a temperature

$$T_{osc} = \left(\frac{\pi^2 g_*(T_{osc})}{90}\right)^{-1/4} (m_\sigma m_p)^{1/2} \simeq 2.25 \times 10^{11} \left(\frac{g_*(T_{osc})}{200}\right)^{-1/4} \left(\frac{m_\sigma}{100\,TeV}\right)^{1/2} \text{GeV.} \tag{3.14}$$

The Universe remains effectively matter dominated until the field decays into Standard Model and SUSY particles when $\Gamma_\sigma \simeq H$. For a gravity mediated process, the decay rate is

$$\Gamma_\sigma = c_3 \frac{m_\sigma^3}{m_p^2}, \tag{3.15}$$

where $c_3 = 1/(4\pi)$ is a typical value. At the time of decay the transfer of energy from the scalar field to Standard Model and SUSY particles will be instantaneous compared to the expansion rate and, because the scalar dominates the energy density, we expect a large yield of dark matter and radiation[7]. The radiation represents the relativistic Standard Model particles, whereas the dark matter results from rapid decays of SUSY particles down to the Lightest SUSY Particle (LSP). Due to the large production of LSPs, some annihilations take place, and these particles will achieve

---

[7]If the decay to SUSY particles was for some reason further suppressed compared to the Standard Model, amount of dark matter would be set by the corresponding branching ratio and the initial amount of scalar field condensate. Such a situation is difficult to arrange in practice.

kinetic equilibrium quickly by scattering off the relativistic bath of Standard Model particles.

The reheat temperature of the universe is

$$T_r = \left(\frac{\pi^2 g_*}{90}\right)^{-1/4} (\Gamma_\sigma m_p)^{1/2} \simeq 20 \; c_3^{1/2} \left(\frac{g_*}{10.75}\right)^{-1/4} \left(\frac{m_\sigma}{100 \text{ TeV}}\right)^{3/2} \text{ MeV}. \quad (3.16)$$

and $g_* \equiv g_*(T_r) = 10.75$ if $T_r$ is low. Using this expression and (3.8), we estimate the relic density in nonthermal dark matter,

$$\begin{aligned}
\Omega_{dm}^{NT} h^2 &\simeq 8.60 \times 10^{-11} \left(\frac{m_X}{g_*^{1/2} \langle \sigma v \rangle T_r}\right), \\
&\simeq 0.08 \left(\frac{m_X}{g_*^{1/4} \langle \sigma v \rangle m_\sigma^{3/2}}\right),
\end{aligned} \quad (3.17)$$

which now depends only on the properties of the dark matter (mass and annihilation rate) and the mass of the decaying scalar resulting from SUSY breaking. As discussed above, in most models the scalar mass is not a free parameter, but similar to the gravitino mass $m_{3/2}$, which is related to the scale of SUSY breaking as $\Lambda_{susy}^2 = m_{3/2} m_p$. Thus, the mass of the scalar (and so the relic density of dark matter) is controlled by the need for SUSY to generate a hierarchy between the electroweak and Planck scale (i.e. $\Lambda_{EW} \sim m_{3/2} \ll m_p$). With a typical SUSY breaking scale of $\Lambda = 10^{11}$ GeV, corresponding to a gravitino mass of around 4 TeV the resulting relic density is

$$\Omega_{dm}^{NT} h^2 \simeq 0.11 \left(\frac{m_X}{100 \text{ GeV}}\right) \left(\frac{10.75}{g_*}\right)^{1/4} \left(\frac{3 \times 10^{-23} \text{ cm}^3/\text{s}}{\langle \sigma v \rangle}\right) \left(\frac{4 \text{ TeV}}{m_{3/2}}\right)^{3/2} \left(\frac{34}{k}\right)^{3/2} (3.18)$$

where we have set $c_3 = 1/(4\pi)$, and the ratio between the scalar and gravitino mass as $k = m_\sigma/m_{3/2} \simeq \log(m_p/m_{3/2})$ – which is only logarithmically sensitive to changes in the hierarchy. This constant is model dependent and typically between $\mathcal{O}(1-100)$. We have chosen a fiducial value for the annihilation rate that yields roughly the right amount of dark matter for the hierarchy set by the choice of low-scale SUSY breaking $\Lambda = 10^{11}$ GeV. The cross-section is three orders of magnitude higher than expected

with a thermal history with important experimental consequences, as discussed in Section 4.

The reheat temperature in this framework is not a free parameter, but a consequence of the hierarchy between the electroweak and Planck scale (determined by $\Lambda^2_{susy} = m_{3/2}m_p$), which also helps determine the SUSY breaking masses of other sparticles in the theory. In both supergravity and string motivated approaches, the key lesson is that the reheat temperature is intimately connected to other aspects of the theory and not a free and tunable parameter. Given that gravitationally coupled scalars are generic in high energy completions of the Standard Model and in no sense exotic, we see that nonthermal histories are a feasible and robust possibility.

### 3.3.2 Nonthermal Histories and CMB Observables

For simplicity we assume inflationary (p)reheating was instantaneous (on gravitational time scales) and focus on the oscillations of the scalars, which come to dominate the energy density, as specified by equation (3.14). Following [13, 16, 40], we make the substitution $\rho_{end} \to \rho^\sigma_{osc}$, using $\rho^\sigma_r = (\pi^2/30)g_*(T^\sigma_r)(T^\sigma_r)^4$. At the onset of oscillations $\rho^\sigma_{osc}(t_{osc}) = \frac{1}{2}m^2_\sigma \Delta\sigma^2$ and

$$
\begin{aligned}
\Delta N &= -0.04 + \frac{1}{12}\ln\left(\frac{g_*(T^\sigma_r)T^4_r}{m^2_\sigma \Delta\sigma^2}\right), \\
&= -10.75 + \frac{1}{12}\ln\left[\left(\frac{g_*(T^\sigma_r)}{10.75}\right)\left(\frac{T_r}{3\text{ MeV}}\right)^4\left(\frac{100\text{ TeV}}{m_\sigma}\right)^2\left(\frac{m_p}{\Delta\sigma}\right)^2\right], (3.19)
\end{aligned}
$$

where we used $w = 0$, and the second line expresses the parameters relative to fiducial values. If scalar decay proceeds via a gravitational strength coupling, equation (3.15) eliminates the mass dependence in (3.19). With $c_3 = 1/(4\pi)$ we find

$$
\Delta N = -10.68 + \frac{1}{18}\ln\left[\left(\frac{g_*(T^\sigma_r)}{10.75}\right)\left(\frac{T_r}{3\text{ MeV}}\right)^4\left(\frac{m_p}{\Delta\sigma}\right)^3\right]. \tag{3.20}
$$

This shift and its effect on physical modes is described qualitatively in Figure 3-2. We see that $\Delta N$ is logarithmically sensitive to changes in parameters, including
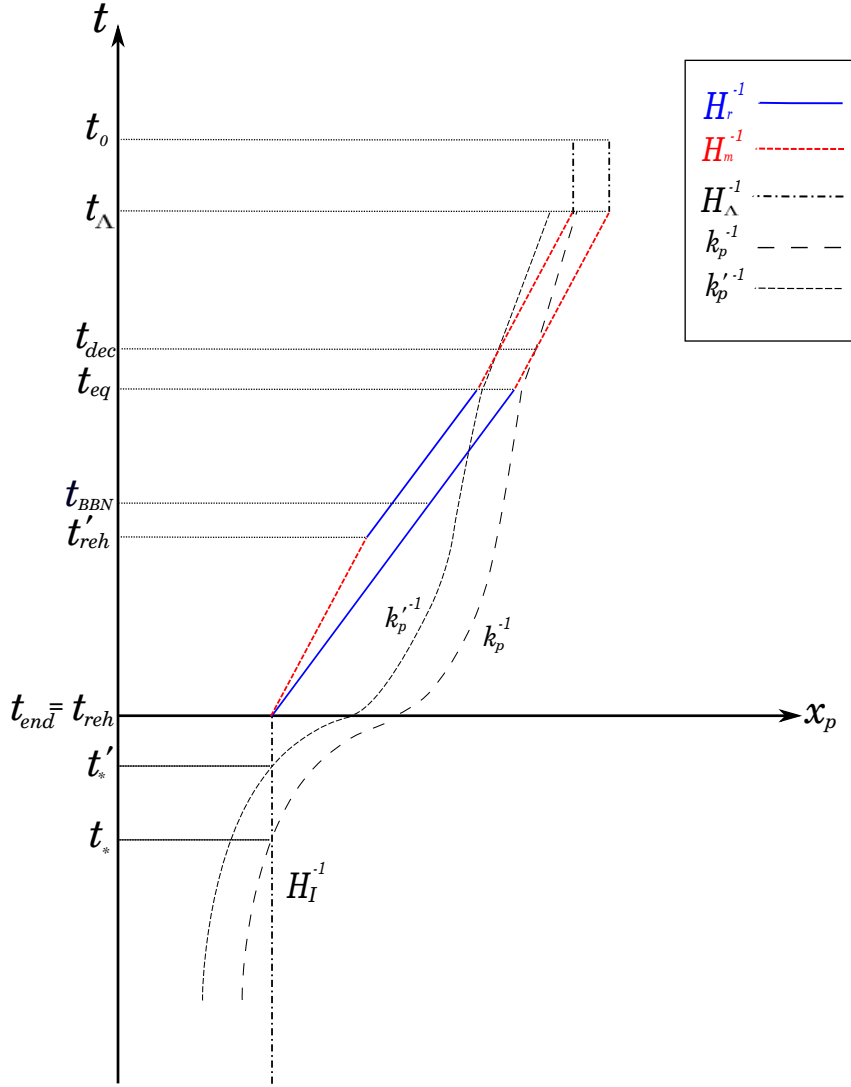
Figure 3-2: Evolution of physical wavelengths as labelled by their inverse wavenumber $k_p^{-1}$ during inflation (below the x-axis) and during the post-inflationary epoch (above the x-axis). The solid (blue) line represents the Hubble radius, $H_r^{-1}$ in a Universe dominated by a radiation fluid $w = 1/3$, the dashed (red) line is the Hubble radius, $H_m^{-1}$ in a post-inflationary era dominated by a pressure-less fluid, $w = 0$. We compare the evolution of a physical mode $k_*$ that re-enters at CMB decoupling in the standard scenario (Radiation $\rightarrow$ Matter $\rightarrow$ Dark energy) with a mode $k'_*$ that re-enters at CMB decoupling in the nonthermal scenario (Matter$\rightarrow$ Radiation$\rightarrow$ Matter$\rightarrow$ Dark Energy). These modes exit the Hubble radius at different times during inflation, $t_*$ and $t'_*$, which translates into a shift in the number of e-folds $\Delta N = H\Delta t$. The corresponding shift in the pivot scale or any co-moving mode is given by $k'_* = k_* e^{-\Delta N}$.

51

the reheat temperature. To generate nonthermal dark matter, the reheat temperature must typically be below about $T_r \simeq 10$ GeV, but above the BBN and neutrino bounds of about $T_r \simeq 3$ MeV. The range of possible temperatures is more than four orders of magnitude, but (3.20) the corresponding shift in $\Delta N$ is $-10.68 \lesssim \Delta N \lesssim -8.51$. Thus, for the scenarios considered here we have a relatively robust $|\Delta N| \simeq 10$. Physically, a more massive field decays earlier while a lighter field decays later, but oscillations and the corresponding matter dominated phase also begin later as well (as seen from (3.14)), leading to similar values of $\Delta N$.

The change in inflationary observables is estimated by recalling that for most simple models of inflation, the running of the spectral index $\alpha_s \equiv dn_s/d\log k$ is typically $-10^{-4} \gtrsim \alpha \gtrsim -10^{-3}$ [16], so $\Delta n_s$ is between $-10^{-3}$ and $-10^{-2}$, relative to the value seen with instant reheating. The remaining uncertainty in the $n_s$ and $r$ is significantly reduced, since these models predict that the universe is matter dominated through most of the primordial dark age.

## 3.4   Constraining Nonthermal Dark Matter

We focus on SUSY neutralinos as the WIMPs, but we expect our conclusions to be easily extended to other non-SUSY dark matter candidates. The neutralino is an electrically charge neutral state and linear combination of the superpartners of the Standard Model $B$, $W^3$, and higgses[8]

$$\chi^0 = N_{10}\tilde{B} + N_{20}\tilde{W}^3 + N_{30}\tilde{H}_1^0 + N_{40}\tilde{H}_2^0, \tag{3.21}$$

where $\tilde{B}$ and $\tilde{W}^3$ are the bino and wino, and $\tilde{H}_{1,2}$ are higgsinos. The $N_{i0}$'s denote the amount each component contributes to the neutralino. The neutralino or WIMP mass is determined by[9] diagonalizing a matrix which depends on the masses of the bino, wino, and higgsino ($M_1$, $M_2$, and $\mu$, respectively), the Weinberg angle $\theta_W$, and $\tan(\beta)$ which is the ratio of the vacuum expectation values of the higgs vevs.

---

[8]The MSSM extension of the Standard Model higgs sector requires two higgs doublets.
[9]We refer the reader to [84] for more details.

When dark matter is composed of thermally produced neutralinos, the neutralino must be bino-dominated, which causes neutralinos to annihilate less efficiently, generating the correct relic density of dark matter [84]. However, if the reheat temperature following scalar decay is below thermal freeze-out, larger annihilation cross-sections are required. Likewise, because the decaying scalar gets a mass from SUSY breaking there is a natural relationship between the reheat temperature and the scale of SUSY breaking, which addresses the hierarchy problem and sets other sparticle masses. The hierarchy problem requires $m_\sigma \sim m_{3/2} \sim$ TeV, which results in reheat temperatures below neutralinio freeze-out temperature ($T_f \simeq m_X/20$), favoring a nonthermal history. The resulting dark matter density is given by (3.8) as

$$\Omega_{dm}^{NT}h^2 \simeq 0.10 \left(\frac{m_X}{100 \text{ GeV}}\right) \left(\frac{10.75}{g_*}\right)^{1/2} \left(\frac{3 \times 10^{-23} \text{ cm}^3/\text{s}}{\langle \sigma v \rangle}\right) \left(\frac{10 \text{ MeV}}{T_r}\right) \tag{3.22}$$

requiring a larger annihilation cross-section. For neutralinos, the larger cross-section requires a more significant contribution from wino and higgsinos, changing expectations for colliders, and for direct and indirect detection experiments.

Existing data from these experiments place a lower bound on the reheat temperature. From (3.22), with Planck's central value $\Omega_{dm}h^2 \simeq 0.12$ and constraints from indirect detection on $\sigma v$ and solving for the reheat temperature we arrive at a minimum value which is typically above the hard lower bound of 3 MeV, further constraining the equation of state in the primordial dark ages.

### 3.4.1 Nonthermal Wino-like Neutralinos

The thermally averaged cross-section for the dominantly wino-like neutralino is given by [63]

$$\langle \sigma v \rangle = \frac{g_2^4}{2\pi M_2^2} \left(\frac{(1 - x_W)^{3/2}}{(2 - x_W)^2}\right) \tag{3.23}$$

where $x_W \equiv m_W^2/M_2^2$ ($m_W$ is the mass of the W-boson), $g_2 \simeq 0.66$ is the $SU_L(2)$ electro-weak gauge coupling (at the weak scale) in the MSSM, $M_2$ is the wino mass, and we note that the result is independent of the velocity (s-wave channel). From

Figure 3-3: The thermally average annihilation rate $\langle \sigma v \rangle$ for a dominantly wino neutralino to annihilate to a pair of $W$-bosons, as a function of mass. The Fermi constraint comes from two years of data from 10 Dwarf spheroidal galaxies [85]. These results have been obtained using DarkSUSY [86], but the general shape of the curve is in good agreement with the analytic expression (3.23). For this scan we took the MSSM parameters to vary over: $M_2 = 100$ GeV to 2 TeV, $\mu = 100$ GeV to 2 TeV, and $\tan \beta = 5$ to 50. We applied all LEP2 constraints and color charged particles were taken to decouple by setting their masses to be above 2 TeV, allowing agreement with LHC constraints.

(3.23), a wino of mass $M_2 = 100$ GeV, the annihilation rate will be around $\langle \sigma v \rangle = 4.06 \times 10^{-24}$ cm$^3$/s, exceeding the cross-section expected for thermal WIMPs by about two orders of magnitude. The cosmological constraint (3.22) then requires a reheat temperature of around 67 MeV. From (3.23) we see that as the wino mass increases, the corresponding annihilation rate decreases, requiring larger reheat temperatures via (3.22). At this point it seems that the reheat temperature is a free and tunable parameter. However, additional experimental constraints can be placed on the wino cross-section through the indirect detection of dark matter.

The wino annihilation rate is s-wave[10] so the annihilation rate above remains relevant for winos in the galaxy today, which are non-relativistic with $v \simeq 10^{-3}c$. Annihilation is dominantly into W-boson pairs, providing a source of anti-protons, positrons, and gamma rays. Indirect detection measurements constrain the cross-section, but suffer from a number of astrophysical complications, which includes uncertainties in the halo profile and propagation models [89]). Therefore, the best constraints on the wino arguably come from gamma rays as opposed to charged anti-matter, and we will use bounds from FERMI's two year data from observations of 10 Dwarf Spheroidal galaxies [85], showing our results for the cross-section in Figure 3-3. For masses less than roughly 375 GeV the wino annihilation rate is too large, giving $\langle \sigma v \rangle \lesssim 6.13 \times 10^{-25}$ cm$^3$/s. Using this in the cosmological constraint (3.22) we find $T_r \gtrsim 696$ MeV (where $g_* = 61.75$). Finally, the corresponding change in the number of e-folds from (3.20) is $\Delta N = -9.37$.

### 3.4.2  Neutralino WIMPs: The General Case

Neutralinos can also contain bino and higgsinos in their composition as indicated in (3.21). We now consider more general neutralinos within the nonthermal framework. For a large bino contribution to (3.21) the annihilation rate is too small to allow a nonthermal history. Thus, we restrict the bino fraction to be less than 10% to ensure that a nonthermal history is realized[11]. On the other hard, a neutralino with a large higgsino component is compatible with a nonthermal history. In Figure 3-4 we present the FERMI constraints on annihilations to W-bosons allowing for this possibility. We scan the MSSM parameter space using DarkSUSY [86] and present results for around $100,000$ models. We restrict the bino-fraction to be less than 10%, and we take $\mu$ and the wino mass ($M_2$) to range from 100 GeV up to 2 TeV, and $\tan \beta$ between $10 - 50$.

---

[10]We note that annihilations with other light MSSM states (coannihilations) can be crucial when calculating the relic density [87], and for high mass winos ($m_X >>$ TeV) Sommerfield enhancement may also play an important role [88]. However, for the range of masses and temperatures we will consider (in order to establish a *lower bound* on the reheat temperature) these effects are negligible.

[11]We refer the reader to [90] for a recent account of the phenomenology of bino-mixed neutralinos as thermal dark matter and their observational consequences.
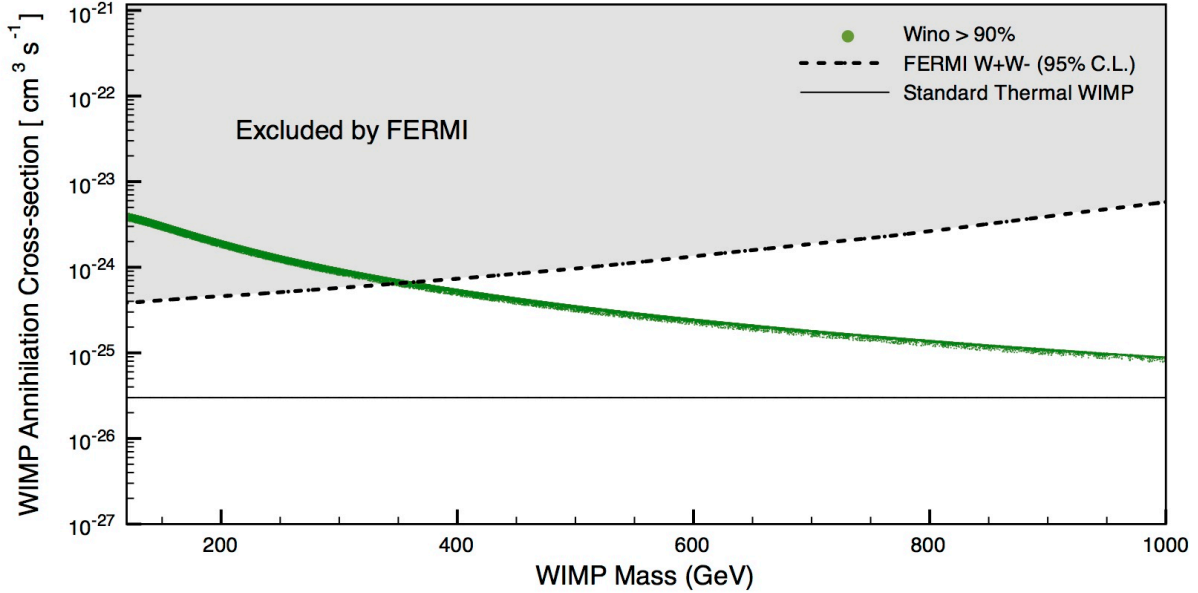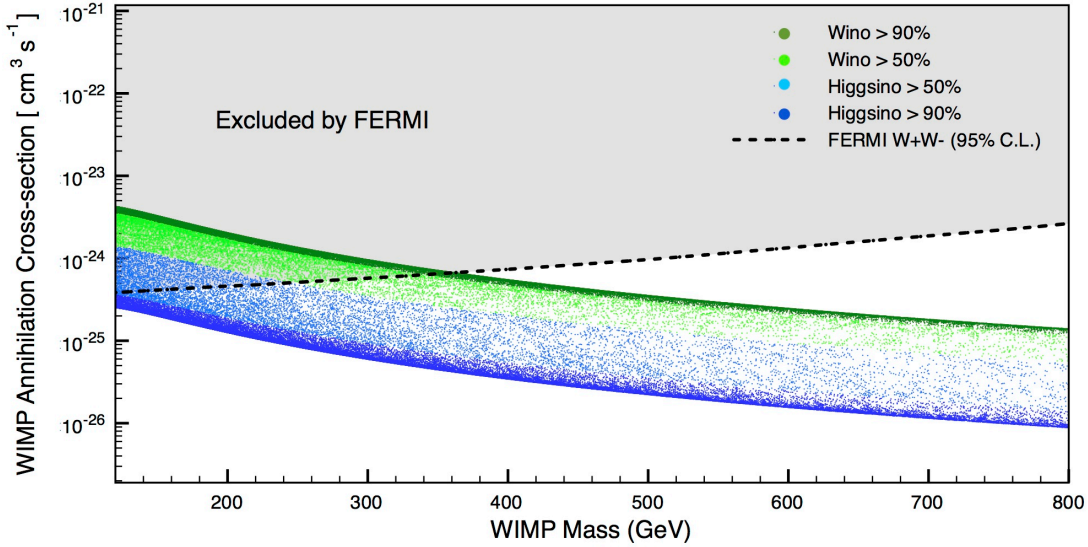
Figure 3-4: The thermally average annihilation rate $\langle\sigma v\rangle$ for a general neutralino to annihilate to a pair of $W$-bosons, with a bino fraction of less than 10%, to realize a nonthermal history. The constraint from Fermi comes from two years of data from 10 Dwarf spheroidal galaxies [85]. These results have been obtained using DarkSUSY [86], however the general shape of the upper curve is in good agreement with the analytic expression (3.23) and the shape of the lower, higgsino curve agrees with the expectation that $\langle\sigma v\rangle \sim 1/\mu^2$. Other parameter choices match those in Figure 3-3.

We reject models that are incompatible with collider data, but properties of neutralino WIMPs are primarily determined by the gaugino masses ($M_1$ and $M_2$), $\mu$ and $\tan\beta$ – see e.g. the recent discussion in [91]. Thus, it is easy to obtain models consistent with LHC constraints on color charged super-partners. We also require a 126 GeV higgs[12]. From Figure 3-4, we see that our numeric results agree well with the analytic expectation that a pure wino annihilation rate should scale as $1/M_2^2$ (top curve in Figure 3-4), whereas a pure higgsino would scale as $1/\mu^2$ (bottom curve in Figure 3-4). Allowing for a higgsino contribution relaxes the bound on the reheat temperature provided by FERMI – with a pure higgsino being completely unconstrained.

We have restricted attention to the $W$-boson annihilation channel, which is typ-

---

[12]There are constraints from LHC on light neutralinos, but because we are considering masses larger than around 100 GeV these constraints are not important here [92, 93].
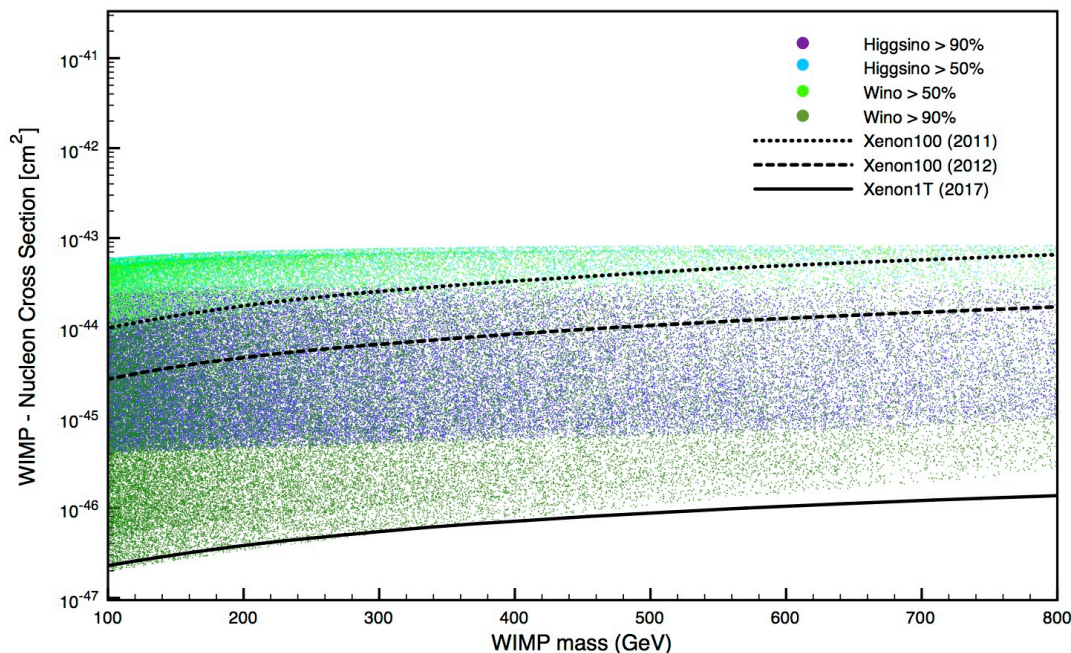
Figure 3-5: The WIMP-nucleon (proton) scattering cross-section as a function of WIMP mass. For wino-higgsino mixtures we find that most models are excluded by the Xenon 2011 / 2012 data. For purified WIMPs (dominantly wino or higgsino) many models escape existing constraints and for models with wino fractions 90% we must wait until Xenon1T for meaningful constraints to be established. However, for the dominantly higgsino models many are already disfavored. For this scan we took the MSSM parameters to vary over: $M_2 = 100$ GeV to 2 TeV, $\mu = 100$ GeV to 2 TeV, and $\tan \beta = 5$ to 50. We have applied all LEP2 constraints and color charged particles were taken to decouple by setting their masses to be above 2 TeV – allowing agreement with LHC constraints.

ically dominant for well-mixed neutralinos, but we find similar constraints for annihilations to other common channels such as bottom quarks. Our key observation is that indirect detection alone does not put a useful bound on the reheat temperature when more general neutralinos are considered. However, bounds from direct searches partially remedy this situation. Recall that a pure wino-like neutralino gives little direct detection signal, as the WIMP-nucleon interaction is loop suppressed [91] but for more general neutralinos the situation changes and direct detection experiments

provide meaningful constraints.

Consider the spin independent constraints provided by Xenon100 [94], as well as future constraints expected from Xenon1T [95]. In Figure 3-5 we use the Xenon 2011 and 2012 null results to constrain the nonthermal neutralino models considered above. Although higgsino mixing relaxed the constraint on the reheat temperature coming from FERMI, many of these models are then ruled out by Xenon100. As seen in Figure 3-5, unless the neutralino is purely wino or higgsino, it is typically in tension with the Xenon100 data. Xenon1T will constrain these models even further, and would potentially bringing the pure wino into tension if it yields a null result. Thus, for generically mixed neutralinos, the nonthermal history is in tension with direct detection data, and for the pure wino the lower bound on the reheat temperature is 696 MeV. The only exception is the pure higgsino, which in the low mass range is somewhat constrained by direct detection but does allow in some cases for a lower reheat temperature.

## 3.5    Conclusion

Current LHC constraints on scalar super-partner masses suggest a new mass scale $m_{3/2} = \Lambda^2/m_p$ around the $10 - 100$ TeV range. When the MSSM is accompanied by additional singlets which receive SUSY breaking masses near this scale, this implies a nonthermal history for the early universe. It has been shown that a nonthermal history modifies the predictions of inflationary models relative to those seen with a thermal history, and that these changes are comparable to the precision of parameter estimates made with Planck data.

A caveat to this analysis is provided by the recent work in [91] (see also [87, 96]), showing that there are certain regions of the neutralino parameter space 'hidden' to direct detection experiments. Although one may expect such points to be atypical, it has been argued for some time that special relations between parameters (e.g. in the case of well-tempered neutralinos [87]) may be the only way for SUSY based WIMPs to survive, given existing collider constraints. We leave a more detailed analysis –

including these subtleties and constraints from spin-dependent interactions – to future work. In addition, perturbations grow in a matter dominated universe, so density inhomogeneities with an initial amplitude of $\delta\rho/\rho \sim 10^{-5}$ grow to be of order unity during the matter dominated phase, a phenomenon also seen in inflationary models with inefficient reheating [97]. Consequently, there will be large, short wavelength inhomogeneities in the moduli fields before thermalization, and the impact of this on their dynamics has not yet been properly explored.

More generally, these preliminary results show that within a complete theory of particle physics (in this case SUSY), understanding the origin of the present-day dark matter abundance can constrain the expansion history of the universe during the primordial dark age, and lead to more precise predictions for the primordial power spectrum.

While this thesis was being prepared, word was received about a draft from the authors of [98]. In their paper they perform a comprehensive study of the non-thermal wino, performing a careful analysis which takes into account astrophysical uncertainties associated with indirect detection and additional data from HESS [99]. In some instances they are able to arrive at more stringent constraints on the wino self-annihilation cross-section. This should lead to an improvement in the theoretical priors used for our analysis here and so stronger constraints on inflationary model building.

For the remainder of the thesis physics in the energy scales of 10-100 TeV will be considered in lattice constructions of supersymmetric gauge theories.

# Chapter 4

# On the sign problem in 2D lattice super Yang–Mills

In recent years a new class of supersymmetric lattice theories have been proposed which retain one or more exact supersymmetries for non-zero lattice spacing. Recently there has been some controversy in the literature concerning whether these theories suffer from a sign problem. In this chapter this issue is addressed by conducting simulations of the $\mathcal{N} = (2,2)$ and $\mathcal{N} = (8,8)$ supersymmetric Yang–Mills theories in two dimensions for the $U(N)$ theories with $N = 2, 3, 4$, using the new twisted lattice formulations. The results presented here provide evidence that these theories do *not* suffer from a sign problem in the continuum limit. These results thus boost confidence that the new lattice formulations can be used successfully to explore non-perturbative aspects of four-dimensional $\mathcal{N} = 4$ supersymmetric Yang–Mills theory.

## 4.1   Introduction

Supersymmetric Yang-Mills (SYM) theories are interesting from a variety of perspectives; as toy models for understanding theories such as QCD, as potential theories of Beyond the Standard Model (BSM) physics and via the AdS/CFT correspondence because of a possible connection to quantum gravity. Many features of these theories, for example, dynamical supersymmetry breaking, are inherently non-perturbative in

61

nature and this serves as motivation to study such theories on the lattice.

Unfortunately, historically it has proven difficult to discretize supersymmetric theories using traditional methods. This stems from the fact that the supersymmetry algebra is an extension of the usual Poincaré algebra and hence is broken completely by naïve discretization on a space-time lattice. However, recently the development of a series of new theoretical tools have enabled us to construct certain supersymmetric theories on the lattice while preserving a subset of the continuum supersymmetries - see the reviews [19, 100–102] and references therein. Other recent complementary approaches to the problem of exact lattice supersymmetry can be found in [103–111].

One way to understand the new constructions is to realize that they correspond to discretizations of topologically twisted forms of the target continuum theories. Currently, lattice constructions exist for a set of SYM theories, including the four-dimensional $\mathcal{N} = 4$ SYM theory.

Lattice theories constructed this way are free of doublers, respect gauge-invariance, preserve a subset of the original supersymmetries and target the usual continuum theories in the naïve continuum limit. These constructions are possible only if the continuum SYM theories possess sufficient extended supersymmetry; the precise requirement is that the number of supercharges must be an integer multiple of $2^D$ where $D$ is the space-time dimension. This includes the $\mathcal{N} = (2, 2)$ SYM theory in two dimensions and $\mathcal{N} = 4$ SYM in four dimensions. In this paper we study both theories in two dimensions -the $\mathcal{N} = 4$ model yielding the $\mathcal{N} = (8, 8)$ theory after dimensional reduction from four to two dimensions.

However, even when a supersymmetric lattice construction exists, it is still possible to encounter an additional difficulty that renders the use of numerical simulation problematic – the fermionic sign problem. To understand the nature of this problem consider a generic lattice theory with a set of bosonic $\phi$ and fermionic $\psi$ degrees of freedom. The partition function of the theory is

$$
\begin{aligned}
Z &= \int [d\phi][d\psi] \exp\left(-S_B[\phi] - \psi^T M[\phi]\psi\right), \\
&= \int [d\phi] \, \mathrm{Pf}(M) \, \exp\left(-S_B[\phi]\right),
\end{aligned}
\tag{4.1}
$$

where $M$ is antisymmetric fermion matrix and $\mathrm{Pf}(M)$ the corresponding Pfaffian. For a $2n \times 2n$ matrix $M$, the Pfaffian is explicitly given as $\mathrm{Pf}(M)^2 = \mathrm{Det}\, M$. In the supersymmetric lattice constructions we will consider in this paper, $M$ at non zero lattice spacing is a complex operator and one might worry that the resulting Pfaffian could exhibit a fluctuating phase depending on the background boson fields $\phi$. Since Monte Carlo simulations must be performed with a positive definite measure, the only way to incorporate this phase is through a reweighting procedure, which folds this phase in with the observables of the theory. Expectation values of observables derived from such simulations can then suffer drastic statistical errors which overwhelm the signal – the famous fermionic *sign problem*. Thus, if such a complex phase is present, the Monte Carlo technique is rendered effectively useless. Lattice theories such as QCD with finite chemical potential are known to suffer from a severe sign problem, which makes it very difficult to extract physical observables from simulations using conventional methods. The lattice sign problem exists not only in relativistic field theories but also in a variety of condensed matter systems [112].

In the construction of supersymmetric lattice gauge theories, there has been an ongoing debate on the existence of a sign problem in the two-dimensional $\mathcal{N} = (2,2)$ supercharge lattice theory [113–115]. The resolution of this sign problem is crucial as the extraction of continuum physics from the lattice model depends very much on whether the results from phase quenched simulations can be trusted. Moreover, if a sign problem were to be found in this model it makes it more likely that the four-dimensional $\mathcal{N} = 4$ theory also suffers from a sign problem which would render practical simulation of this theory impossible. In [113], it was shown that there is a potential sign problem in the two-dimensional $\mathcal{N} = (2,2)$ SYM lattice theory. Furthermore, in [115] numerical evidence was presented of a sign problem in a phase quenched dynamical simulation of the theory at non-zero lattice spacing. More recently Hanada et al. [114] have argued that there is no sign problem for this theory in the continuum limit. However, the models studied by these various groups differed in detail; Catterall et al. studied an $SU(2)$ model obtained by truncating the supersymmetric $U(2)$ theory and utilized bosonic link fields valued in the group $SL(2,C)$,

while Hanada et al. used a $U(2)$ model where the complexified bosonic variables take their values in the algebra of $U(2)$ together with the inclusion of supplementary mass terms to control scalar field fluctuations.

In this paper, we present results from simulations of the two dimensional $\mathcal{N} = (2,2)$ $U(N)$ SYM theory (which we will refer to from now on as the $\mathcal{Q} = 4$ theory, with $\mathcal{Q}$ the number of supercharges) and the maximally supersymmetric $\mathcal{N} = (8,8)$ $U(N)$ SYM theory (we refer to this theory as the $\mathcal{Q} = 16$ theory). Our results provide strong evidence that there is no sign problem in the supersymmetric continuum limit for these theories. In the next four sections we summarize the details of the lattice constructions of both theories including a discussion of the possible parameterizations of the bosonic link fields. We then present our numerical results for $\mathcal{Q} = 4$ and $\mathcal{Q} = 16$ lattice SYM theories in two dimensions.

## 4.2 Supersymmetric Yang–Mills theories on the lattice

As discussed in the introduction it is possible to discretize a class of continuum SYM theories using ideas based on topological twisting[1]. Though the basic idea of twisting goes back to Witten in his seminal paper on topological field theory [23], it actually had been anticipated in earlier work on staggered fermions [119]. In our context, the idea of twisting is to decompose the fields of the Euclidean SYM theory in $D$ space-time dimensions in representations not in terms of the original (Euclidean) rotational symmetry $SO_{\mathrm{rot}}(D)$, but a twisted rotational symmetry, which is the diagonal subgroup of this symmetry and an $SO_{\mathrm{R}}(D)$ subgroup of the R-symmetry of the theory, that is,

$$SO(D)' = \mathrm{diag}(SO_{\mathrm{Lorentz}}(D) \times SO_{\mathrm{R}}(D)) \ . \tag{4.2}$$

As an example, let us consider the case where the total number of supersymmetries is $Q = 2^D$. In this case we can treat the supercharges of the twisted theory as a

---

[1]Note that the lattice actions constructed using orbifold and twisted methods are equivalent [116–118].

$2^{D/2} \times 2^{D/2}$ matrix $q$. This matrix can be expanded on the Dirac–Kähler basis as

$$q = \mathcal{Q}I + \mathcal{Q}_a\gamma_a + \mathcal{Q}_{ab}\gamma_a\gamma_b + \ldots \tag{4.3}$$

The $2^D$ antisymmetric tensor components that arise in this basis are the twisted supercharges that satisfy the corresponding supersymmetry algebra inherited from the original algebra

$$\mathcal{Q}^2 = 0 \tag{4.4}$$

$$\{\mathcal{Q}, \mathcal{Q}_a\} = p_a \tag{4.5}$$

$$\vdots \tag{4.6}$$

The presence of the nilpotent scalar supercharge $\mathcal{Q}$ is most important; it is the algebra of this charge that is compatible with discretization. The second piece of the algebra expresses the fact that the momentum is the $\mathcal{Q}$-variation of something which makes the statement plausible that the energy-momentum tensor and hence the entire action can be written in a $\mathcal{Q}$-exact form[2]. Notice that an action written in such a $\mathcal{Q}$-exact form is trivially invariant under the scalar supersymmetry $\mathcal{Q}$ provided the latter remains nilpotent under discretization.

The recasting of the supercharges in terms of twisted variables can be repeated for the fermions of the theory and yields a set of antisymmetric tensors $(\eta, \psi_a, \chi_{ab}, \ldots)$, which for the case of $Q = 2^D$ matches the number of components of a real Kähler–Dirac field. This repackaging of the fermions of the theory into a Kähler–Dirac field is at the heart of how the discrete theory avoids fermion doubling as was shown by Becher, Joos and Rabin in the early days of lattice gauge theory [120, 121]. It is important to recognize that the transformation to twisted variables corresponds to a simple change of variables in flat space – one more suitable for discretization.

---

[2]In the case of four-dimensional $\mathcal{N} = 4$ SYM there is an additional $\mathcal{Q}$-closed term in the action.

### 4.2.1  Two-dimensional $\mathcal{Q} = 4$ SYM on the lattice

The two-dimensional $\mathcal{Q} = 4$ SYM theory is the simplest example of a gauge theory that permits topological twisting and thus satisfies our requirements for supersymmetric lattice constructions. Its R-symmetry possesses an $SO(2)$ subgroup corresponding to rotations of the its two degenerate Majorana fermions into each other. After twisting the fields and supersymmetries of the target theory, the action takes the following form in the continuum

$$S = \frac{1}{g^2}\mathcal{Q}\int \mathrm{Tr}\, \left(\chi_{ab}\mathcal{F}_{ab} + \eta[\overline{\mathcal{D}}_a, \mathcal{D}_b] - \frac{1}{2}\eta d\right)\ ,\tag{4.7}$$

where $g$ is the coupling parameter. We use an anti-hermitian basis for the generators of the gauge group with $\mathrm{Tr}(T^a T^b) = -\delta^{ab}$.

The degrees of freedom appearing in the above action are just the twisted fermions $(\eta, \psi_a, \chi_{ab})$ and a complexified gauge field $\mathcal{A}_a$. The latter is built from the usual gauge field $A_a$ and the two scalars $B_a$ present in the untwisted theory: $\mathcal{A}_a = A_a + iB_a$. The twisted theory is naturally written in terms of the complexified covariant derivatives

$$\mathcal{D}_a = \partial_a + \mathcal{A}_a,\quad \overline{\mathcal{D}}_a = \partial_a + \overline{\mathcal{A}}_a\ ,\tag{4.8}$$

and complexified field strengths

$$\mathcal{F}_{ab} = [\mathcal{D}_a, \mathcal{D}_b],\quad \overline{\mathcal{F}}_{ab} = [\overline{\mathcal{D}}_a, \overline{\mathcal{D}}_b]\ .\tag{4.9}$$

Notice that the original scalar fields transform as vectors under the original R-symmetry and hence become vectors under the twisted rotation group while the gauge fields are singlets under the R-symmetry and so remain vectors under twisted rotations. This structure makes the appearance of a complex gauge field in the twisted theory possible. This action is invariant under the original $U(N)$ gauge symmetry from the untwisted theory.

The nilpotent transformations associated with the scalar supersymmetry $\mathcal{Q}$ are

given explicitly by

$$
\begin{aligned}
\mathcal{Q}\,\mathcal{A}_a &= \psi_a \\
\mathcal{Q}\,\psi_a &= 0 \\
\mathcal{Q}\,\overline{\mathcal{A}}_a &= 0 \\
\mathcal{Q}\,\chi_{ab} &= -\overline{\mathcal{F}}_{ab} \\
\mathcal{Q}\,\eta &= d \\
\mathcal{Q}\,d &= 0
\end{aligned}
\tag{4.10}
$$

Performing the $\mathcal{Q}$-variation on the action and integrating out the auxiliary field $d$ yields

$$
S = \frac{1}{g^2} \int \operatorname{Tr}\ \left( -\overline{\mathcal{F}}_{ab}\mathcal{F}_{ab} + \frac{1}{2}[\overline{\mathcal{D}}_a, \mathcal{D}_a]^2 - \chi_{ab}\mathcal{D}_{[a}\psi_{b]} - \eta\overline{\mathcal{D}}_a\psi_a \right)\ .
\tag{4.11}
$$

The prescription for discretization is somewhat natural. The complexified gauge fields are represented as complexified Wilson gauge fields

$$
\mathcal{A}_a(x) \rightarrow \mathcal{U}_a(\mathbf{n})\ ,
\tag{4.12}
$$

living on links of a lattice, which for the moment can be thought of as hypercubic, with integer-valued basis vectors

$$
\widehat{\boldsymbol{\mu}}_1 = (1,0), \quad \widehat{\boldsymbol{\mu}}_2 = (0,1)\ .
\tag{4.13}
$$

They transform in the usual way under $U(N)$ lattice gauge transformations

$$
\mathcal{U}_a(\mathbf{n}) \rightarrow G(\mathbf{n})\mathcal{U}_a(\mathbf{n})G^\dagger(\mathbf{n}+\widehat{\boldsymbol{\mu}}_a)\ .
\tag{4.14}
$$

Supersymmetric invariance then implies that $\psi_a(\mathbf{n})$ live on the same links and transform identically. The scalar fermion $\eta(\mathbf{n})$ is clearly most naturally associated with a
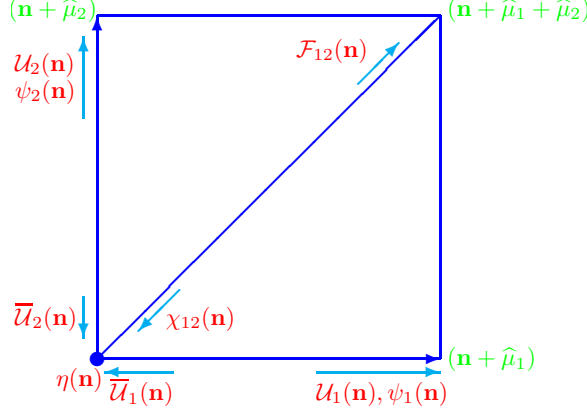
Figure 4-1: The 2d lattice for the four supercharge theory with field orientation assignments.

site and transforms accordingly

$$\eta(\mathbf{n}) \to G(\mathbf{n})\eta(\mathbf{n})G^\dagger(\mathbf{n}) . \tag{4.15}$$

The field $\chi_{ab}(\mathbf{n})$ is slightly more difficult. Naturally as a 2-form it should be associated with a plaquette. In practice we introduce diagonal links running through the center of the plaquette and choose $\chi_{ab}(\mathbf{n})$ to lie *with opposite orientation* along those diagonal links. This choice of orientation will be necessary to ensure gauge invariance. Figure 4-1 shows the resultant lattice theory.

To complete the discretization we need to describe how continuum derivatives are to be replaced by difference operators. A natural technology for accomplishing this in the case of adjoint fields was developed many years ago and yields expressions for the derivative operator applied to arbitrary lattice p-forms [122]. In the case discussed here we need just two derivatives given by the expressions

$$\mathcal{D}_a^{(+)} f_b(\mathbf{n}) = \mathcal{U}_a(\mathbf{n}) f_b(\mathbf{n} + \widehat{\boldsymbol{\mu}}_a) - f_b(\mathbf{n})\mathcal{U}_a(\mathbf{n} + \widehat{\boldsymbol{\mu}}_b) , \tag{4.16}$$

$$\overline{\mathcal{D}}_a^{(-)} f_a(\mathbf{n}) = f_a(\mathbf{n})\overline{\mathcal{U}}_a(\mathbf{n}) - \overline{\mathcal{U}}_a(\mathbf{n} - \widehat{\boldsymbol{\mu}}_a) f_a(\mathbf{n} - \widehat{\boldsymbol{\mu}}_a) . \tag{4.17}$$

The lattice field strength is then given by the gauged forward difference acting on the link field: $\mathcal{F}_{ab}(\mathbf{n}) = \mathcal{D}_a^{(+)}\mathcal{U}_b(\mathbf{n})$, and is automatically antisymmetric in its indices.

Furthermore, it transforms like a lattice 2-form and yields a gauge invariant loop on the lattice when contracted with $\chi_{ab}(\mathbf{n})$. Similarly the covariant backward difference appearing in $\overline{\mathcal{D}}_a^{(-)}\mathcal{U}_a(\mathbf{n})$ transforms as a 0-form or site field and hence can be contracted with the site field $\eta(\mathbf{n})$ to yield a gauge invariant expression.

This use of forward and backward difference operators guarantees that the solutions of the lattice theory map one-to-one with the solutions of the continuum theory and hence fermion doubling problems are evaded [120]. Indeed, by introducing a lattice with half the lattice spacing one can map this Kähler–Dirac fermion action into the action for staggered fermions [123]. Notice that, unlike the case of QCD, there is no rooting problem in this supersymmetric construction since the additional fermion degeneracy is already required in the continuum theory.

As for the continuum theory the lattice action is again $\mathcal{Q}$-exact:

$$S = \sum_{\mathbf{n}} \mathrm{Tr}\ \mathcal{Q}\Big(\chi_{ab}(\mathbf{n})\mathcal{D}_a^{(+)}\mathcal{U}_b(\mathbf{n}) + \eta(\mathbf{n})\overline{\mathcal{D}}_a^{(-)}\mathcal{U}_a(\mathbf{n}) - \frac{1}{2}\eta(\mathbf{n})d(\mathbf{n})\Big)\ . \qquad (4.18)$$

Acting with the $\mathcal{Q}$ transformation on the lattice fields and integrating out the auxiliary field $d$, we obtain the gauge and $\mathcal{Q}$-invariant lattice action:

$$S = \sum_{\mathbf{n}} \mathrm{Tr}\ \Big(\mathcal{F}_{ab}^{\dagger}(\mathbf{n})\mathcal{F}_{ab}(\mathbf{n}) + \frac{1}{2}\Big(\overline{\mathcal{D}}_a^{(-)}\mathcal{U}_a(\mathbf{n})\Big)^2 - \chi_{ab}(\mathbf{n})\mathcal{D}_{[a}^{(+)}\psi_{b]}(\mathbf{n}) - \eta(\mathbf{n})\overline{\mathcal{D}}_a^{(-)}\psi_a(\mathbf{n})\Big)\ .$$
$$(4.19)$$

### 4.2.2 Four-dimensional $\mathcal{Q} = 16$ SYM on the lattice

In four dimensions the constraint that the target theory possess sixteen supercharges singles out a unique theory for which this construction can be undertaken – the $\mathcal{N} = 4$ SYM theory.

The continuum twist of $\mathcal{N} = 4$ that is the starting point of the twisted lattice construction was first written down by Marcus in 1995 [25] although it now plays an important role in the Geometric-Langlands program and is hence sometimes called the GL-twist [124]. This four-dimensional twisted theory is most compactly expressed as the dimensional reduction of a five-dimensional theory in which the ten (one gauge

field and six scalars) bosonic fields are realized as the components of a complexified five-dimensional gauge field while the 16 twisted fermions naturally span one of the two Kähler–Dirac fields needed in five dimensions. Remarkably, the action of this theory contains a $\mathcal{Q}$-exact term of precisely the same form as the two-dimensional theory given in Eq. (4.7) provided one extends the indices labeling the fields to run now from one to five. In addition, the Marcus twist of $\mathcal{N} = 4$ YM requires a new $\mathcal{Q}$-closed term which was not possible in the two-dimensional theory

$$S_{\text{closed}} = -\frac{1}{8} \int \text{Tr } \epsilon_{mnpqr} \chi_{qr} \overline{\mathcal{D}}_p \chi_{mn} \ . \tag{4.20}$$

The supersymmetric invariance of this term then relies on the Bianchi identity

$$\epsilon_{mnpqr} \overline{\mathcal{D}}_p \overline{\mathcal{F}}_{qr} = 0 \ . \tag{4.21}$$

The four-dimensional lattice that emerges from examining the moduli space of the resulting discrete theory is called the $A_4^*$-lattice and is constructed from the set of five basis vectors $\widehat{e}_a$ pointing out from the center of a four-dimensional equilateral simplex out to its vertices together with their inverses $-\widehat{e}_a$. It is the four-dimensional analog of the two-dimensional triangular lattice. Complexified Wilson gauge link variables $\mathcal{U}_a$ are placed on these links together with their $\mathcal{Q}$-superpartners $\psi_a$. Another 10 fermions are associated with the diagonal links $\widehat{e}_a + \widehat{e}_b$ with $a > b$. Finally, the exact scalar supersymmetry implies the existence of a single fermion for every lattice site. The lattice action corresponds to a discretization of the Marcus twist on this $A_4^*$-lattice and can be represented as a set of traced closed bosonic and fermionic loops. It is invariant under the exact scalar supersymmetry $\mathcal{Q}$, lattice gauge transformations and a global permutation symmetry $S^5$ and can be proven free of fermion doubling problems as discussed above. The $\mathcal{Q}$-exact part of the lattice action is again given by Eq. (5.23) where the indices $a, b$ now correspond to the indices labeling the five basis vectors of $A_4^*$.

While the supersymmetric invariance of this $\mathcal{Q}$-exact term is manifest in the lattice theory, it is not clear how to discretize the continuum $\mathcal{Q}$ closed term. Remarkably,

it is possible to discretize Eq. (5.4) in such a way that it is indeed exactly invariant under the twisted supersymmetry

$$S_{\text{closed}} = -\frac{1}{8} \sum_{\mathbf{n}} \text{Tr } \epsilon_{mnpqr} \chi_{qr}(\mathbf{n} + \widehat{\boldsymbol{\mu}}_m + \widehat{\boldsymbol{\mu}}_n + \widehat{\boldsymbol{\mu}}_p) \overline{\mathcal{D}}_p^{(-)} \chi_{mn}(\mathbf{n} + \widehat{\boldsymbol{\mu}}_p) \qquad (4.22)$$

and can be seen to be supersymmetric since the lattice field strength satisfies an exact Bianchi identity [122].

$$\epsilon_{mnpqr} \overline{\mathcal{D}}_p^{(+)} \overline{\mathcal{F}}_{qr} = 0 . \qquad (4.23)$$

The renormalization of this theory has been recently studied in perturbation theory with some remarkable conclusions [125]; namely that the classical moduli space is not lifted to all orders in the coupling, that the one loop lattice beta function vanishes and that no fine tuning of the bare lattice parameters with cut-off is required at one-loop for the theory to recover full supersymmetry as the lattice spacing is sent to zero.

## 4.3   Towards the continuum limit

### 4.3.1   Parametrizations of the gauge links

There exist two distinct parameterizations of the gauge fields on the lattice that have been proposed for these theories. The first one follows the standard Wilson prescription where the complexified gauge fields in the continuum are mapped to link fields $\mathcal{U}_a(\mathbf{n})$ living on the link between $\mathbf{n}$ and $\mathbf{n} + \widehat{\boldsymbol{\mu}}_a$ through the mapping

$$\mathcal{U}_a(\mathbf{n}) = e^{\mathcal{A}_a(\mathbf{n})} , \qquad (4.24)$$

where $\mathcal{A}_a(\mathbf{n}) = \sum_{i=1}^{N_G} \mathcal{A}_a^i T^i$ and $T^i = 1, \ldots, N_G$ are the anti-hermitian generators of $U(N)$. The resultant gauge links belong to $GL(N, C)$. We call this realization of the bosonic links the *exponential or group based parametrization*[3].

---

[3]Notice that our lattice gauge fields are dimensionless and hence contain an implicit factor of the lattice spacing $a$.

The other parametrization of the bosonic link fields that has been used, particularly in the orbifold literature, simply takes the complex gauge links as taking values in the algebra of the $U(N)$ group

$$\mathcal{U}_a(\mathbf{n}) = \mathcal{A}_a(\mathbf{n}) \ . \tag{4.25}$$

In this case to obtain the correct continuum limit one must subsequently expand the fields around a particular point in the moduli space of the theory corresponding to giving an expectation value to a component of the link field proportional to the unit matrix. This field can be identified as the trace mode of the scalar field in the untwisted theory.

$$\mathcal{U}_a(\mathbf{n}) = \mathbf{I}_N + \mathcal{A}_a(\mathbf{n}) \ . \tag{4.26}$$

Usually the use of such an algebra based or *non compact* parametrization would signal a breaking of lattice gauge invariance. It is only possible here because the bosonic fields take values in a complexified $U(N)$ theory – so that the unit matrix appearing in Eq. (4.26) can be interpreted as the expectation value of a *dynamical field* - the trace mode of the scalars. We will refer to this parametrization as the *linear or algebra based parametrization*[4].

Both parameterizations of the gauge links are equivalent at leading order in the lattice spacing, yield the same lattice action and can be considered as providing equally valid representations of the lattice theory at the classical level. The exponential parametrization was used in studies of both $\mathcal{Q} = 4$ and $\mathcal{Q} = 16$ theories in [115] while in [114] the linear parametrization was employed to perform simulations of the $\mathcal{Q} = 4$ theory. In this work we have concentrated on the linear parametrization principally because it is naturally associated with a manifestly supersymmetric measure in the path integral - the flat measure. Explicit comparison with results from the exponential parametrization can be found in [130].

---

[4]In fact, a non-compact parametrization of the gauge-fields has also been recently used to restore BRST symmetry on the lattice in Ref. [127], i.e., to evade the so-called Neuberger 0/0 problem [128] (see also Refs. [127] and [129] for the recent progress, and [130] for the relation between the Neuberger 0/0 problem and sign problem for the lattice SYM theories.).

## 4.3.2 Potential terms

As we have described in the previous section, the linear parameterization only yields the correct naïve continuum limit if the trace mode of the scalars develops a vacuum expectation value so that appropriate kinetic terms are generated in the tree level action. In addition, we require that the fluctuations of all dimensionless lattice fields vanish as the lattice spacing is sent to zero; a non-trivial issue in theories possessing flat directions associated with extended supersymmetry. Since no classical scalar potential is present in the lattice theory[5] it is crucial to add *by hand* a suitable gauge invariant potential to ensure these features[6]. Specifically we add a potential term of the following form [114]

$$S_M = \mu^2 \sum_{\mathbf{n}} \left( \frac{1}{N} \text{Tr}(\mathcal{U}_a^{\dagger}(\mathbf{n})\mathcal{U}_a(\mathbf{n})) - 1 \right)^2 , \qquad (4.27)$$

to the lattice action. Here $\mu$ is a tunable mass parameter, which can be used to control the expectation values and fluctuations of the lattice fields. Notice that such a potential obviously breaks supersymmetry – however because of the exact supersymmetry at $\mu = 0$ all supersymmetry breaking counterterms induced via quantum effects will possess couplings that vanish as $\mu \to 0$ and so can be removed by sending $\mu \to 0$ at the end of the calculation.

To understand the effect of this term let us consider the full set of vacuum equations for the lattice theory. These are given by setting the bosonic action to zero

$$\mathcal{F}_{ab}(\mathbf{n}) = 0 , \qquad (4.28)$$

$$\overline{\mathcal{D}}_a^{(-)}\mathcal{U}_a(\mathbf{n}) = 0 , \qquad (4.29)$$

$$\frac{1}{N}\text{Tr}\left(\mathcal{U}_a^{\dagger}(\mathbf{n})\mathcal{U}_a(\mathbf{n})\right) - 1 = 0 . \qquad (4.30)$$

The first two equations imply that the moduli space consists of constant complex

---

[5]Lattice theories based on supersymmetric mass deformations have also been proposed in two dimensions [111, 114]

[6]It was precisely this requirement that led to a truncation of the $U(N)$ symmetry to $SU(N)$ in the original simulations of these theories. One can think of this truncation as corresponding to the use of a delta function potential for the $U(1)$ part of the field [115].

matrices taking values in the $N$-dimensional Cartan subalgebra of $U(N)$.

Assuming that the matrix valued complexified link fields $\mathcal{U}_a(\mathbf{n})$ are nonsingular[7], we can decompose them in the following way

$$\mathcal{U}_a(\mathbf{n}) = P_a(\mathbf{n})U_a(\mathbf{n}) \ , \tag{4.31}$$

where $P_a(\mathbf{n})$ is a positive semidefinite hermitian matrix and $U_a(\mathbf{n})$ a unitary matrix. The form of the mass term clearly does not depend on the unitary piece and clearly is minimized by setting $P_a(\mathbf{n}) = \mathbf{I}_N$. Expanding about this configuration gives the following expression for the complex link matrices

$$\mathcal{U}_a(\mathbf{n}) = P_a(\mathbf{n})U_a(\mathbf{n}) = \Big(\mathbf{I}_N + p_a(\mathbf{n})\Big)U_a(\mathbf{n}) \ , \tag{4.32}$$

where $p_a(\mathbf{n})$ is a hermitian matrix. Minimizing the mass term leads to

$$
\begin{aligned}
0 &= \frac{1}{N}\mathrm{Tr}\Big(\mathcal{U}_a^\dagger(\mathbf{n})\mathcal{U}_a(\mathbf{n})\Big) - 1 \ , \\
&= \frac{1}{N}\mathrm{Tr}\Big[U_a^\dagger(\mathbf{n})\Big(\mathbf{I}_N + p_a(\mathbf{n})\Big)\Big]\Big[\Big(\mathbf{I}_N + p_a(\mathbf{n})\Big)U_a(\mathbf{n})\Big] - 1 \ , \\
&= \frac{1}{N}\mathrm{Tr}\Big[\mathbf{I}_N + 2p_a(\mathbf{n}) + p_a^2(\mathbf{n})\Big] - 1 \ , \\
&= \frac{1}{N}\Big[\frac{2}{\sqrt{N}}p_a^0(\mathbf{n}) + \sum_{A=1}^{N}(p_a^A(\mathbf{n}))^2\Big] \ .
\end{aligned}
\tag{4.33}
$$

where we have adopted a basis in which $T^0$ is proportional to the unit matrix and all other (Cartan) generators are traceless. Analyzing the gauge transformation properties of the complexified link fields,

$$\mathcal{U}_a(\mathbf{n}) \rightarrow G(\mathbf{n})\mathcal{U}_a(\mathbf{n})G^\dagger(\mathbf{n} + \widehat{\boldsymbol{\mu}}_a) \ , \tag{4.34}$$

we see that the unitary piece $U_a(\mathbf{n})$ transforms like a link field

$$U_a(\mathbf{n}) \rightarrow G(\mathbf{n})U_a(\mathbf{n})G^\dagger(\mathbf{n} + \widehat{\boldsymbol{\mu}}_a) \tag{4.35}$$

---

[7]Having zero eigenvalues for the matrices $\mathcal{U}_a(\mathbf{n})$ would not cause a problem for us, as we are interested in expanding these fields around the point $\mathbf{I}_N$ instead of the origin of the moduli space.

while the hermitian matrix $p_a(\mathbf{n})$ transforms like a scalar field

$$p_a(\mathbf{n}) \to G(\mathbf{n})p_a(\mathbf{n})G^\dagger(\mathbf{n}). \tag{4.36}$$

Thus in this language we can identify the $p_a(\mathbf{n})$ with the scalar field fluctuations $B_a(\mathbf{n})$. The mass term then becomes

$$S_M = \mu^2 \sum_{\mathbf{n}} \frac{1}{N^2} \Big[ \frac{2}{\sqrt{N}} B_a^0(\mathbf{n}) + \sum_{A=1}^{N} (B_a^A(\mathbf{n}))^2 \Big]^2. \tag{4.37}$$

From this expression it is straightforward to see that the fluctuations of the scalar trace mode are governed by a quadratic potential while the traceless scalar field fluctuations feel only a quartic potential. Thus, if we keep $\mu \equiv \mu a$ fixed as $a \to 0$ the trace mode will acquire an infinite mass in the continuum limit and hence fluctuations of the trace more around its vacuum expectation value will be completely suppressed in that limit. In the same limit the presence of the quartic potential for the traceless Cartan generators is sufficient to regulate possible infrared problems associated with the flat directions of the $SU(N)$ sector. Finally, once the continuum limit is attained, we can restore supersymmetry by taking the final limit $\mu \to 0$.

Notice that the fact that this potential term selects out preferentially the trace mode of the scalars is trivially obvious if we adopt the exponential parametrization of the complexified gauge links since in that case we can identify $I + p_a$ with $e^{iB_a}$.

## 4.4   Simulation Results

As noted previously, we have rescaled all lattice fields by powers of the lattice spacing to make them dimensionless. This leads to an overall dimensionless coupling parameter of the form $N/(2\lambda a^2)$, where $a = \beta/T$ is the lattice spacing, $\beta$ is the physical extent of the lattice in the Euclidean time direction and $T$ is the number of lattice

sites in the time-direction. Thus, the lattice coupling is

$$\kappa = \frac{NL^2}{2\lambda\beta^2} \ ,$$

(4.38)

for the symmetric two-dimensional lattice where the spatial length $L = T$[8]. Note that $\lambda\beta^2$ is the dimensionless physical 't Hooft coupling in units of the area. In our simulations[9], the continuum limit can be approached by fixing $\lambda\beta^2$ and $N$ and increasing the number of lattice points $L \to \infty$. In practice we fix the value of $\beta = 1$ and vary $\lambda$. We have taken three different values for this coupling $\lambda = 0.5, 1.0, 2.0$ and lattice sizes ranging from $L = 2, \cdots, 16$. Systems with $U(N)$ gauge groups with $N = 2, 3$ and 4 have been examined.

The simulations are performed using anti-periodic (thermal) boundary conditions for the fermions[10]. An RHMC algorithm was used for the simulations as described in [126]. The use of a GPU accelerated solver [131] allowed us to reach larger lattices than have thus far been studied.

### 4.4.1  $\mathcal{Q} = 4$ Supersymmetries

In figure 4-2. we show results for the absolute value of the (sine of) the Pfaffian phase $|\sin\alpha|$ as a function of lattice size $L = 1/a$ for the $\mathcal{Q} = 4$ model with gauge group $U(2)$. The data corresponds to $\lambda = 1$ but similar results are obtained for $\lambda = 0.5, 2.0$ and larger numbers of colors. Three values of $\mu$ are shown corresponding to $\mu = 0.1$, $\mu = 1.0$ and $\mu = 10.0$. While modest phase fluctuations are seen for small lattices for the smallest value of $\mu$, we see that they disappear as the continuum limit is taken. As a practical matter, these results make it clear that no re-weighting of observables is needed over much of the parameter space. This point is reinforced when we plot a histogram of the phase angle in figure 4-3. Clearly the angle fluctuations contract towards the origin as the continuum limit is approached.

---

[8]Notice that this coupling multiples *all* terms in the bosonic action including those associated with the scalar potential.

[9]See [126] for the details of the code we used to simulate these theories.

[10]This forbids exact zero modes that are otherwise present in the fermionic sector.
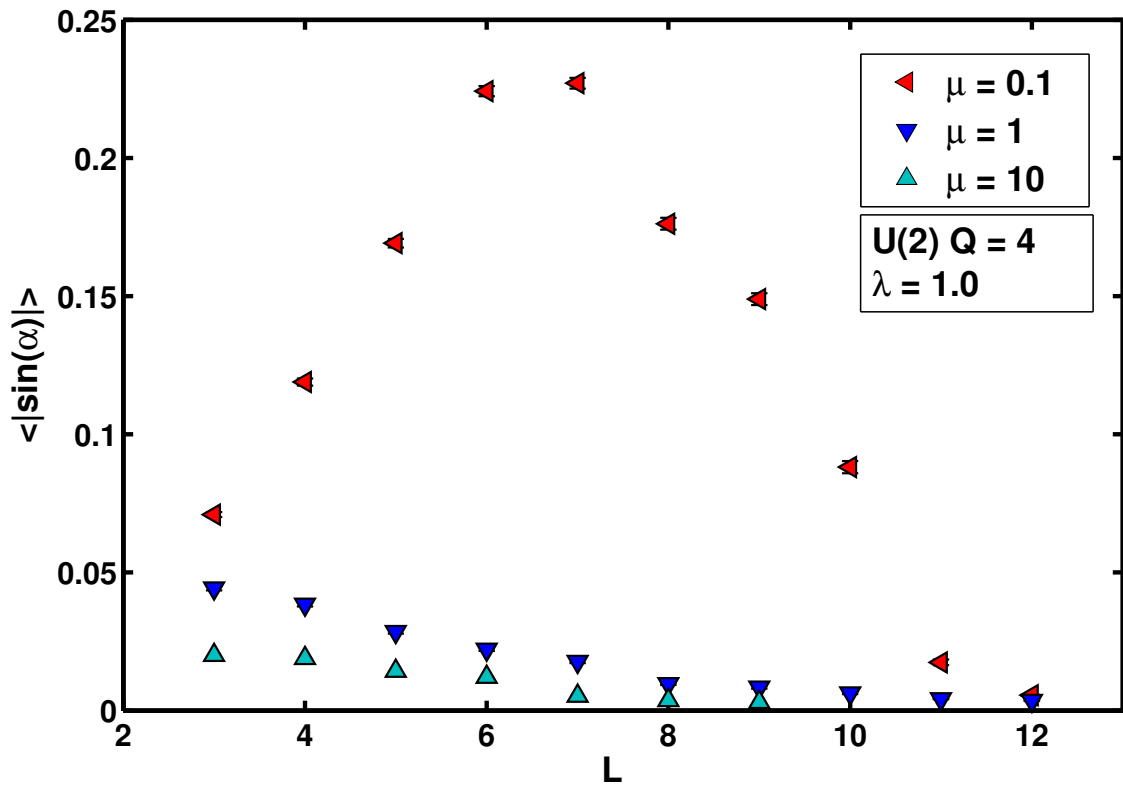
Figure 4-2: $< |\sin \alpha| >$ for $\mathcal{Q} = 4$, U(2) with $\mu = 0.1, 1, 10$
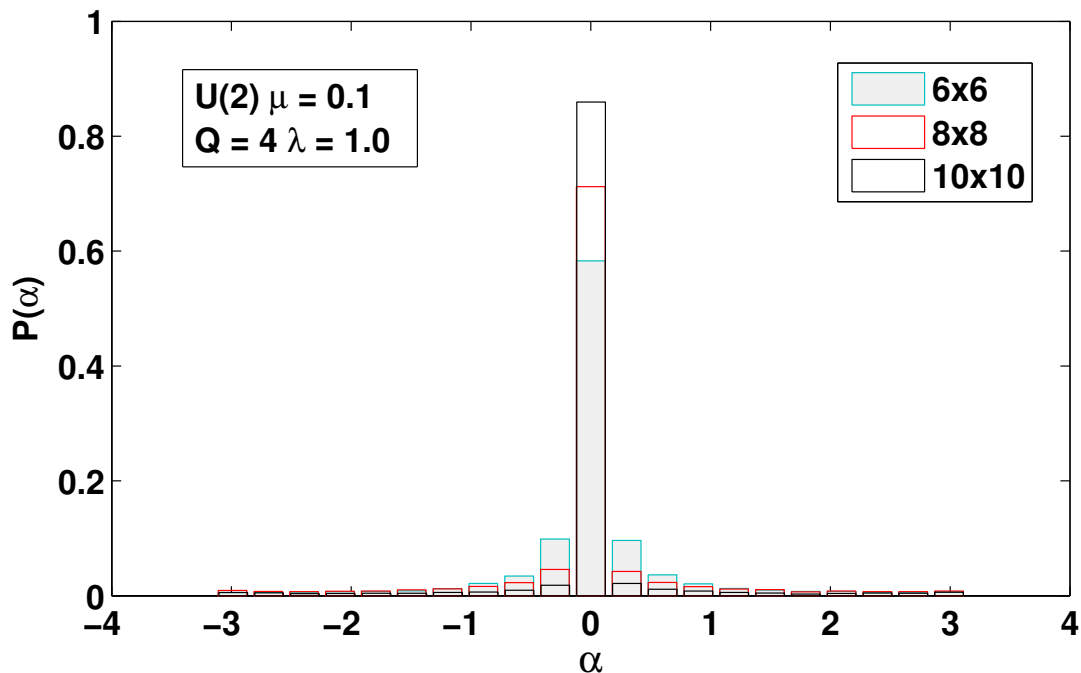
Figure 4-3: Histogram for $\alpha$, with $\mathcal{Q} = 4$, U(2), $\mu = 0.1$ and volumes of 6x6, 8x8 and 10x10.

To check for the restoration of supersymmetry in the continuum limit and as the scalar potential is sent to zero, we show in figure 4-4. a plot of the bosonic action density vs lattice size $L$. While the curves plateau for large $L$ indicating a well defined continuum limit it is clear that in general supersymmetry is broken there. Indeed, the exact value of the bosonic action which is shown by the dotted line in the plot can be computed using a simple $\mathcal{Q}$ Ward identity and yields [115]

$$< \frac{1}{L^2} \kappa S_B >= \frac{3}{2} N_G \tag{4.39}$$

It should be clear from the plot that the measured action indeed approaches this supersymmetric value if the subsequent limit $\mu \to 0$ is taken[11]. Thus the regulating procedure we have described does indeed provide a well defined procedure for studying the supersymmetric lattice theory.

Finally, to reassure ourselves that $L \to \infty$ indeed corresponds to a continuum

---

[11]Actually strictly we only expect this as $\beta \equiv \lambda \to \infty$ and thermal effects are suppressed. These appear to be already small for $\lambda = 1$ in this theory
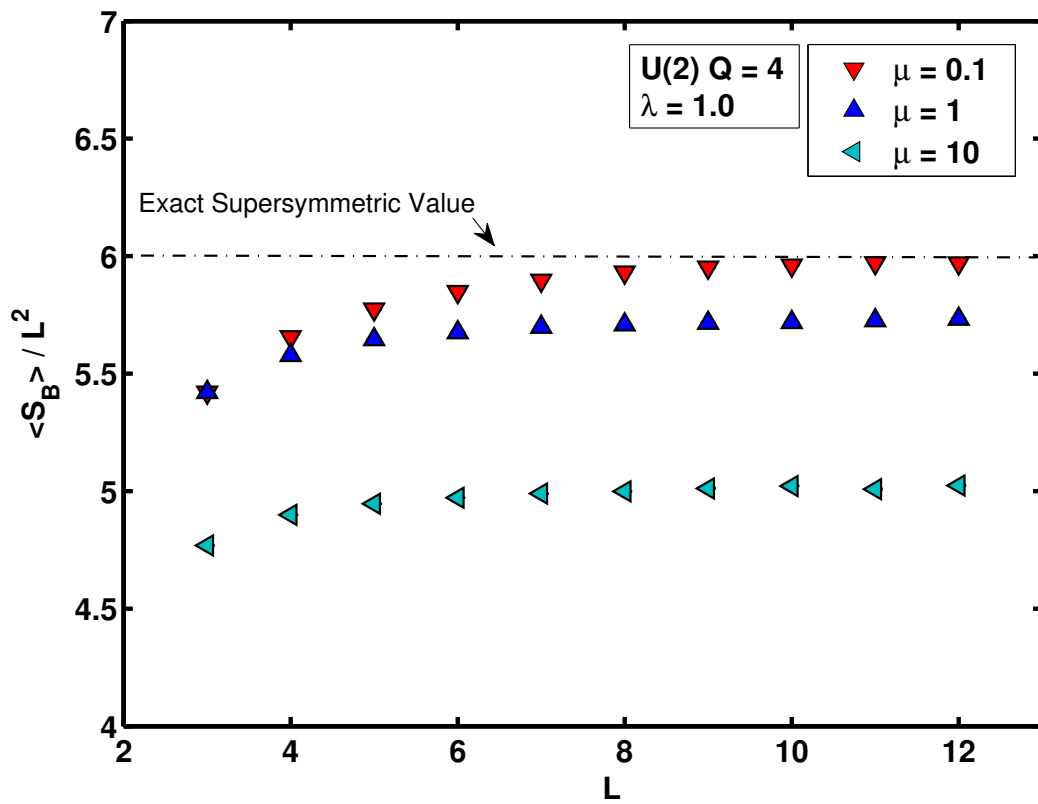
Figure 4-4: $< \kappa S_B >$ for $\mathcal{Q} = 4$, U(2) and $\mu = 0.1, 1, 10$
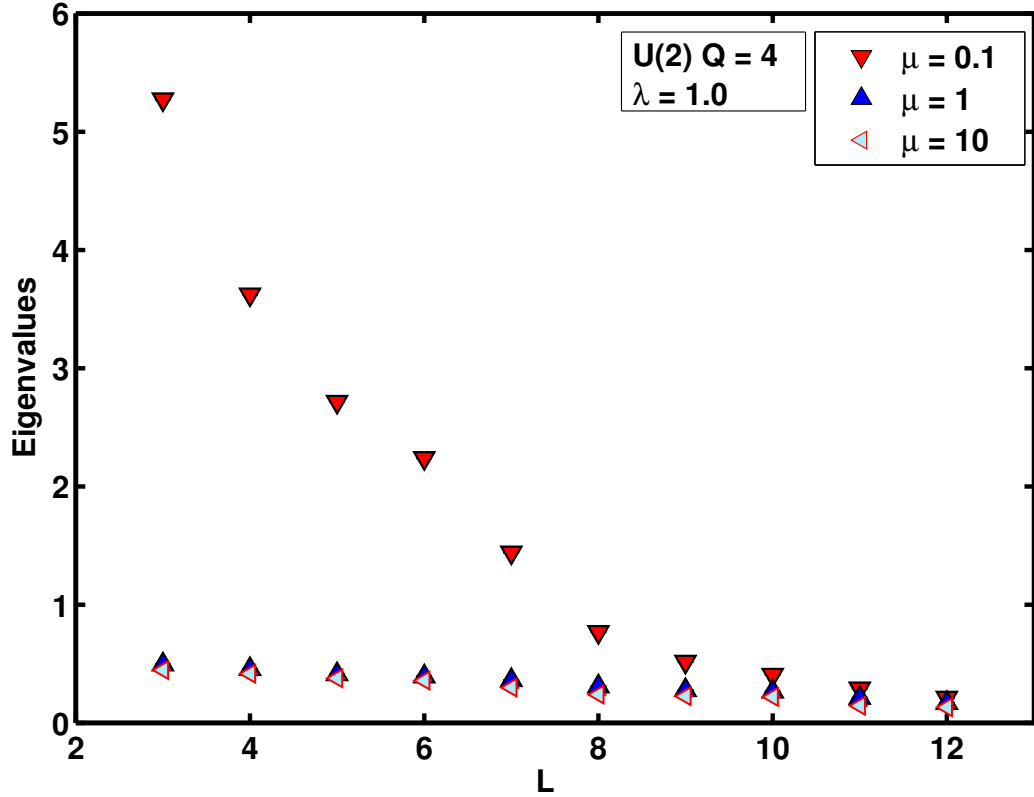
Figure 4-5: Ensemble average for the eigenvalues of the $(\mathcal{U}_a^\dagger \mathcal{U}_a - 1)$ operator for $\mathcal{Q} = 4$, U(2) and $\mu = 0.1, 1, 10$

limit, figure 4-5. shows a plot of the expectation value of the maximal eigenvalue of the operator $(\mathcal{U}_a^\dagger \mathcal{U}_a - 1)$ averaged over the lattice as a function of $L$ for $\lambda = 1$. To leading order, this expression yields the largest scalar field eigenvalue in units of the lattice spacing. Reassuringly we see that the eigenvalue indeed approaches zero as $L \to \infty$ corresponding to a vanishing lattice spacing.

### 4.4.2 $\mathcal{Q} = 16$ Supersymmetries

The results for the absolute value of the (sine of) the Pfaffian phase for the $\mathcal{Q} = 16$ supercharge model with U(2) gauge group in two dimensions are shown in figure. 4-6. As for the $\mathcal{Q} = 4$ case, we see that the average Pfaffian phase is small and decreases with $L$. Indeed, the magnitude of these angular fluctuations are $O(10^{-4})$ for all $L$ and $\mu$ - *much* smaller than that observed for $\mathcal{Q} = 4$. Thus, even on the coarsest lattice and
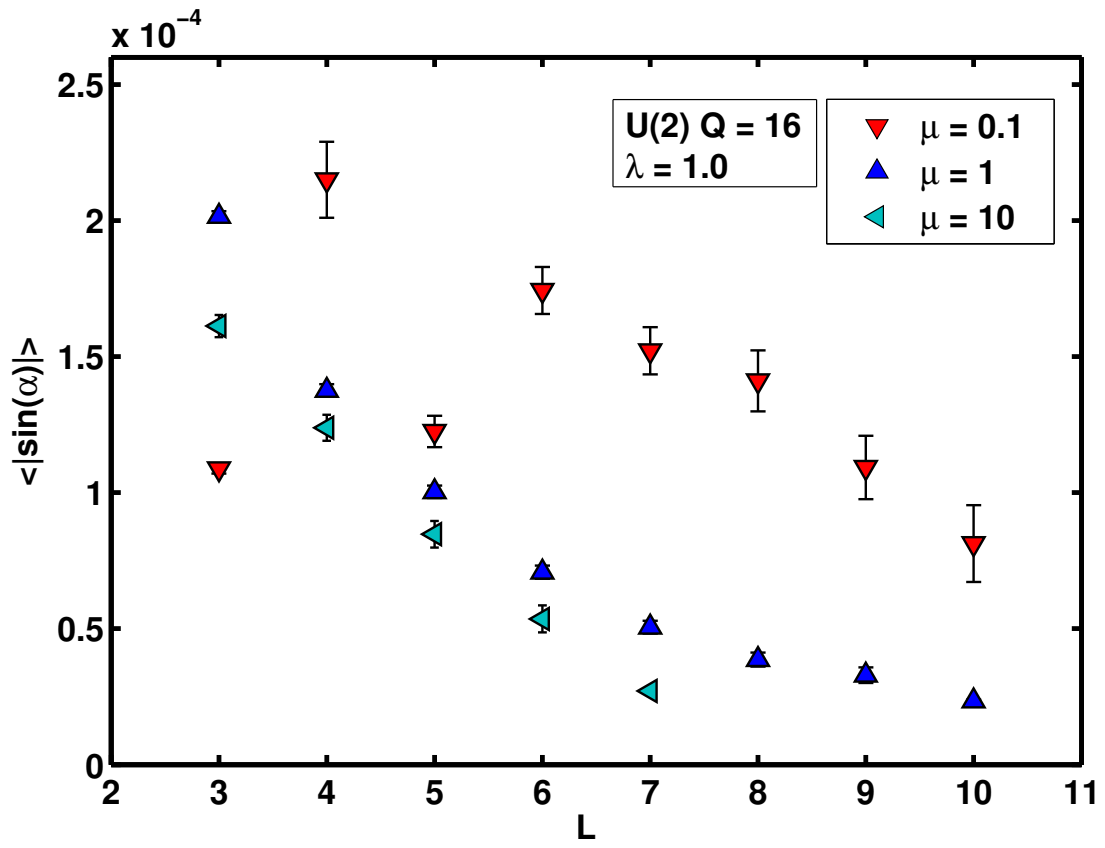
Figure 4-6: $< |\sin \alpha| >$ for $\mathcal{Q} = 16$, U(2) and $\mu = 0.1, 1, 10$
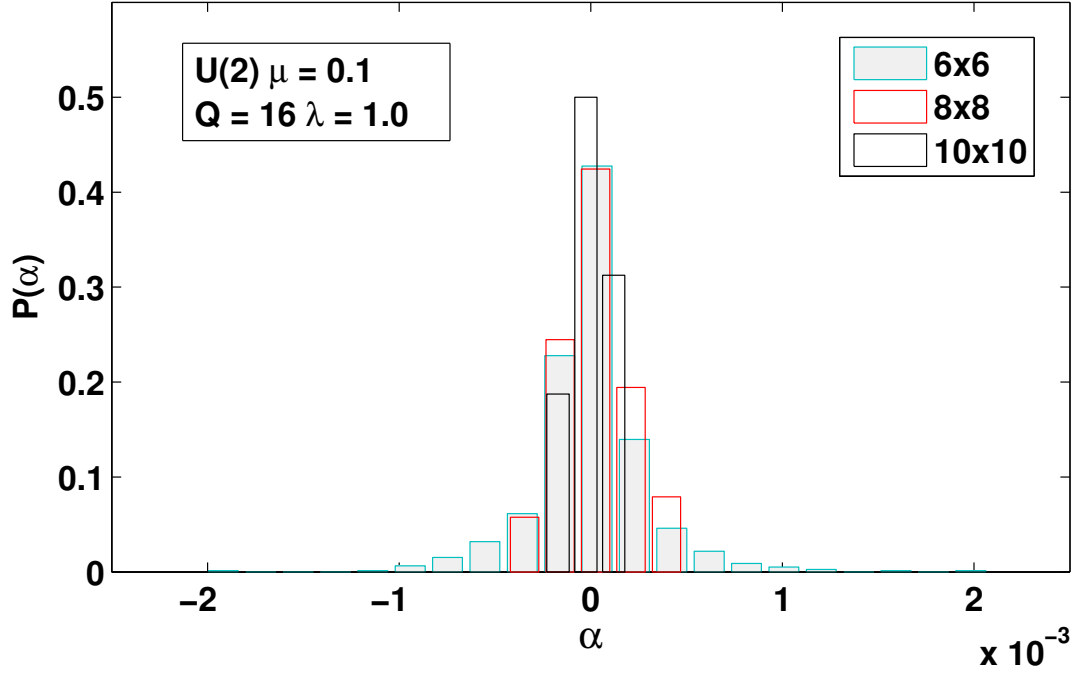
Figure 4-7: Histogram for $\alpha$, with $\mathcal{Q} = 16$, U(2), $\mu = 0.1$ for volumes of 6x6, 8x8, and 10x10.

smallest $\mu$, there is clearly no practical sign problem and certainly no sign problem in the continuum limit. Again, this picture is reinforced by looking at a histogram of the phase angle $\alpha$ as seen in figure 4-7.

The corresponding plot of the expectation value of the bosonic action vs lattice size $L$ is shown in figure 4-8. In the case of the $\mathcal{Q} = 16$ model the exact expression for the bosonic action is given by

$$< \frac{1}{L^2} \kappa S_B > = \frac{9}{2} N_G \qquad (4.40)$$

The data shown in this plot allow us to conclude that a well defined continuum limit exists for non-zero $\mu$ and furthermore, $\mathcal{Q}$-supersymmetry can be restored by subsequently sending the parameter $\mu \to 0$. As a final cross check that the limit $L \to \infty$ indeed corresponds to a true continuum limit, we have again examined the the behavior of the maximal eigenvalue of $\mathcal{U}_a^\dagger \mathcal{U} - I$ as $L \to \infty$. The result is shown in figure 4-9. and is consistent with a vanishing lattice spacing in this limit.
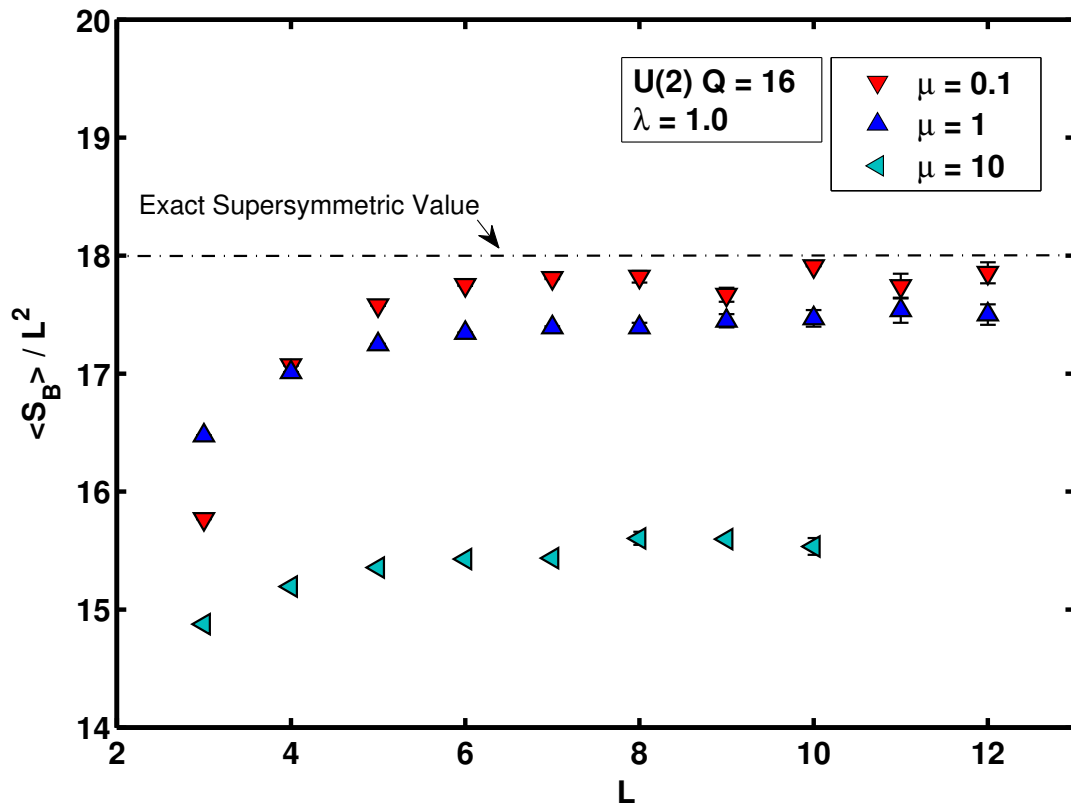
Figure 4-8: $< S_B >$ for $\mathcal{Q} = 16$, U(2) and $\mu = 0.1, 1, 10$
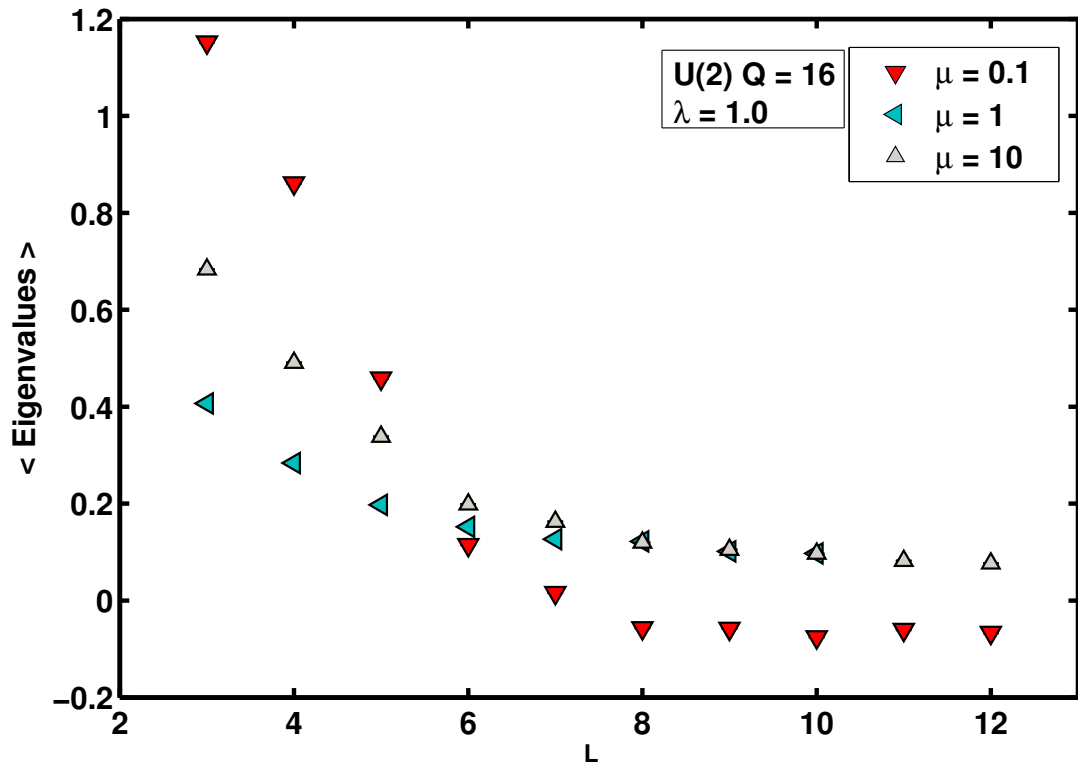
Figure 4-9: Ensemble averaged eigenvalues for the $(\mathcal{U}_a^\dagger \mathcal{U}_a - 1)$ operator for $\mathcal{Q} = 16$ with U(2) and $\mu = 0.1, 1, 10$
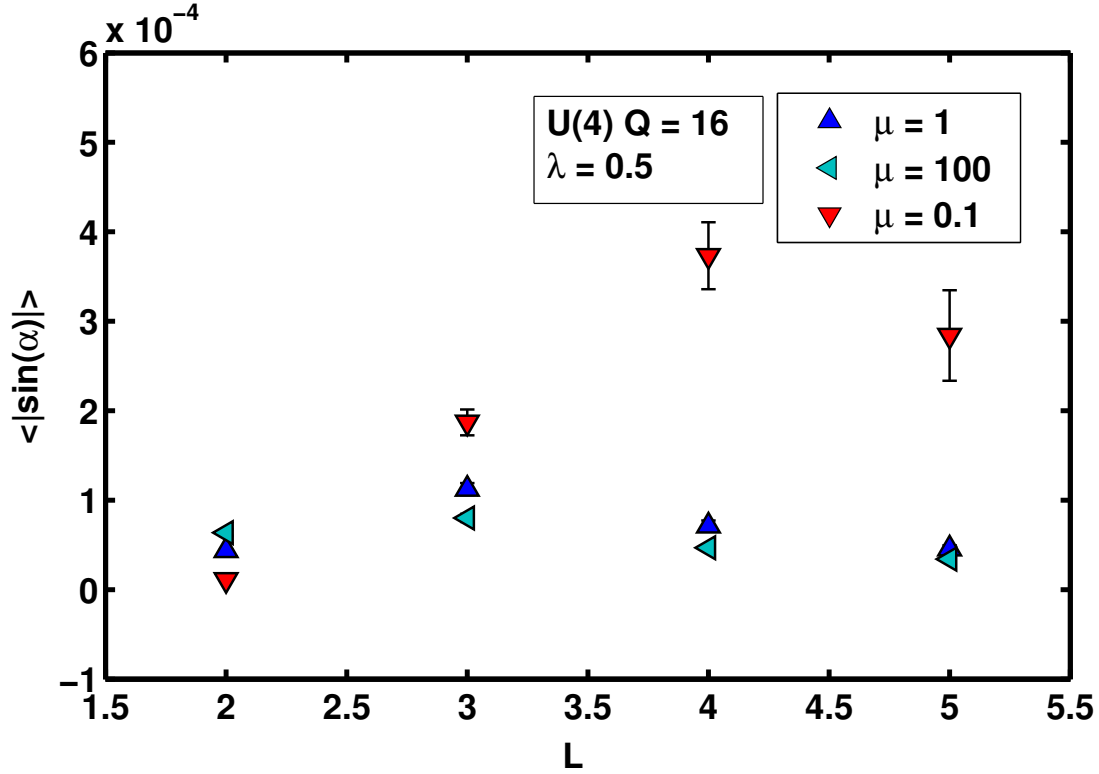
Figure 4-10: $< |\sin\alpha| >$ for $\mathcal{Q} = 16$, U(4) and $\mu = 0.1, 1, 100$

These results generalize to large numbers of colors as can be seen in figure 4-10. where we plot the expectation value of the absolute value of the sine of the Pfaffian phase for the case of the U(4) group. Notice that the Pfaffian can be proven real in the limit that the $\mathcal{Q} = 16$ theory is reduced to zero dimensions for two and three colors so that it is necessary to examine the $U(4)$ case to be sure of seeing truly generic behavior.

Nevertheless we see that U(4) looks qualitatively the same as for U(2). In fact the fluctuations in the phase angle that we observe are even *smaller* than those seen for the U(2) theory. This again indicates that this theory exhibits no sign problem even on small lattices and certainly in the continuum limit.

The plot of the bosonic action for U(4) is shown in figure 4-11. While the largest lattice we have been able to simulate thus far is rather too small to get a good continuum limit the measured bosonic action is nevertheless within a percent or so of the exact value expected on the basis of $\mathcal{Q}$-supersymmetry. The scalar field fluctuations
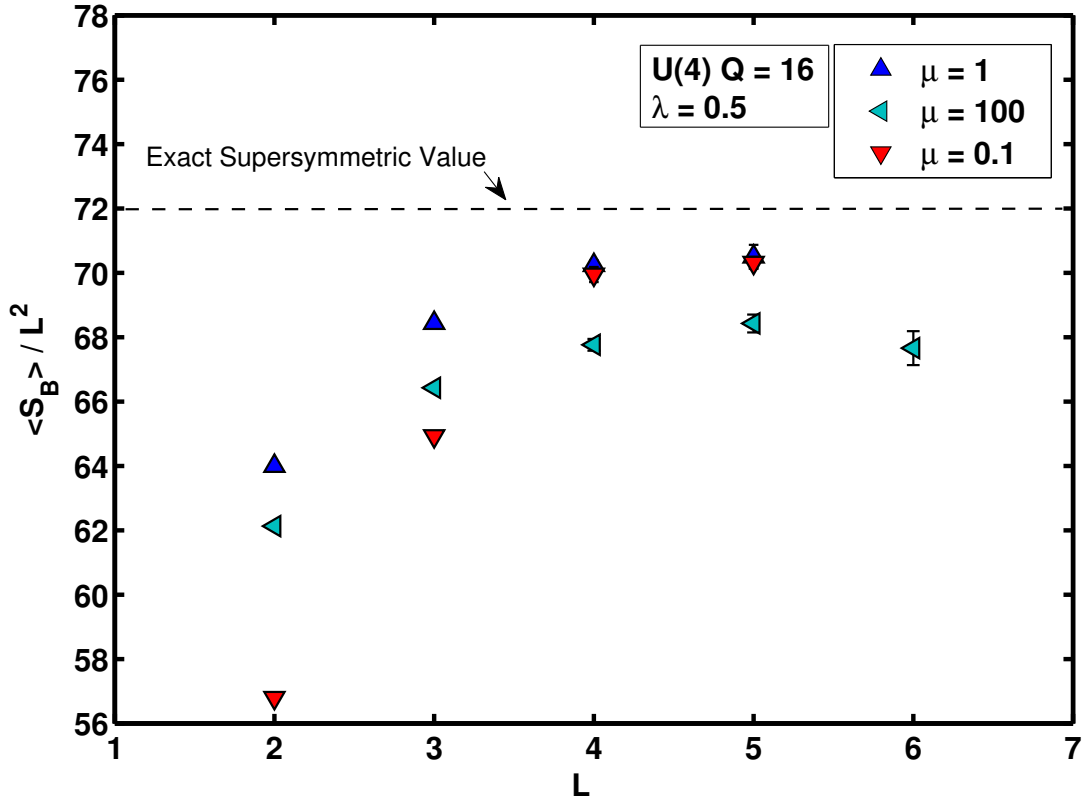
Figure 4-11: $< S_B > /L^2$ for $\mathcal{Q} = 16$, U(4) and $\mu = 0.1, 1, 100$

also decrease toward zero as the number of lattice points increase as shown in figure 4-12.

It is at first sight rather remarkable that the observed Pfaffian phase fluctuations are small in the $\mathcal{Q} = 16$ theory given that the Pfaffian is certainly complex when evaluated on a generic set of background scalar and gauge fields. It appears to be a consequence of very specific dynamics in the theory which ensure that only certain special regions of field space are important in the path integral. Of course the continuum theory does possess very special dynamics; for example the twisted supersymmetry ensures that the torus partition function $Z$ is a topological invariant. One immediate consequence of this is that $Z$ may be computed exactly at one loop where Marcus has argued that it simply reduces to an unsigned sum over isolated points in the moduli space of flat complexified connections up to complex gauge transformations [25]. Furthermore, much of this structure survives in the *lattice*
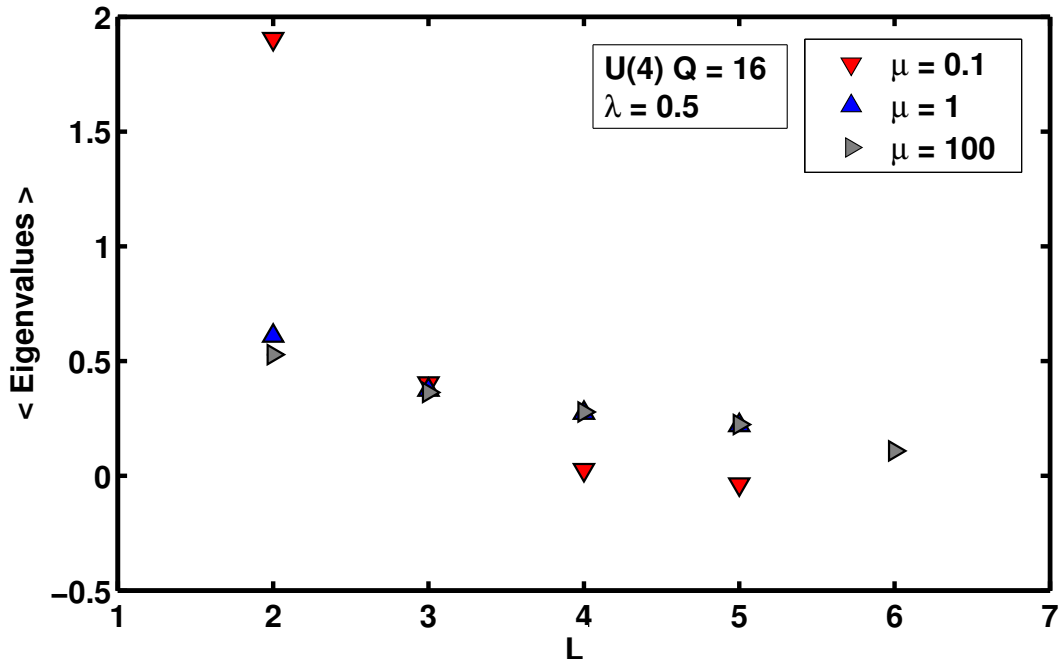
Figure 4-12: Ensemble averaged eigenvalues for the $(\mathcal{U}_a^\dagger \mathcal{U}_a - 1)$ operator for $\mathcal{Q} = 16$, U(4) and $\mu = 0.1, 1, 100$

theory; the full partition function *including* any Pfaffian phase may be calculated exactly at one loop. As in the continuum theory there is a perfect cancellation of contributions from fermions and bosons and the final result is real [125]. Of course this does not mean that simulations at finite gauge coupling should not suffer from sign problems but certainly makes it less likely. More prosaically, it is easy to see that the Pfaffian is real positive if the lattice scalar fields are set to zero - and this is what effectively happens in the continuum limit as a result of the scalar potential that we use to control the vacuum expectation value and fluctuations of the trace mode.

## 4.5 Conclusions

Numerical simulations were performed of the four and sixteen supercharge lattice SYM theories in two dimensions to investigate the occurrence of a sign problem in these theories. In contrast to the usual situation in lattice gauge theory, we utilize a non compact parameterization of the gauge fields in which the lattice fields are

expanded on the algebra of the group. While such a scheme would ordinarily break lattice gauge invariance it is shown that in the case of these twisted supersymmetric models this preserves gauge symmetry since the models in question are formulated in terms of a complexified gauge field valued in $U(N)$. The correct continuum limit is then ensured by adding an appropriate gauge invariant potential term which picks out a non-zero vacuum expectation value for the trace mode of the scalar fields in the continuum limit. It is argued that the effects of this potential on the remaining traceless modes can be subsequently removed by sending the potential to zero *after* the continuum limit is taken.

Both supersymmetric theories have been examined for several values of the dimensionless 't Hooft coupling $\lambda \beta^2$ and for gauge groups $U(2)$, $U(3)$ and $U(4)$. A careful continuum limit was taken by simulating the theories over a range of lattice size $L = 2 - 14$. In both cases it is shown that the average Pfaffian phase goes to zero for a fixed gauge invariant potential as the continuum limit is taken. The subsequent limit in which the potential is removed is also examined and evidence is shown that supersymmetry is restored. While the absence of a sign problem is not surprising in the $\mathcal{Q} = 4$ case (where one can prove the Pfaffian reduces to a real positive definite determinant in the continuum limit) it is much more non trivial matter in the $\mathcal{Q} = 16$ supercharge case. In that case the Pfaffian evaluated on a generic background is complex even in the continuum limit. Nevertheless, we observe that the Pfaffian phase is small and decreases to zero as the continuum limit is taken. Indeed, in practice it is sufficiently small even on coarse lattices that there is no need to use a reweighting procedure to compute expectation values of observables. The analysis of the $\mathcal{Q} = 16$ model is complicated by the fact that the $U(2)$ and $U(3)$ theories exhibit some special properties since in the matrix model limit they are real positive definite and real respectively. Nevertheless, the pattern we observe for the $U(4)$ group is similar to that seen for the smaller groups and the trend supports the conjecture that the sign problem is absent in the continuum limit.

These results thus help to strengthen the case that there may be no sign problem for the $\mathcal{Q} = 16$ theory in four dimensions and hence no a priori barrier to numerical

studies of this theory. In the next chapter we conclude by examining the phase structure of Wilson loops in these theories.

# Chapter 5

# Phase Structure of Lattice $\mathcal{N} = 4$ Super Yang-Mills

A first study of the phase diagram of four-dimensional $\mathcal{N} = 4$ super Yang-Mills theory is presented regulated on a space-time lattice. The lattice formulation we employ is both gauge invariant and retains at all lattice spacings one exactly preserved supersymmetry charge. Our numerical results are consistent with the

## 5.1 Twisted Supersymmetric $\mathcal{N} = 4$ Yang-Mills Theory

As discussed in the Introduction, it is possible to discretize a class of continuum supersymmetric Yang-Mills theories using ideas based on topological twisting[1]. Though the basic idea of twisting goes back to Witten in his seminal paper on topological field theory [23], it had actually been anticipated in earlier work on staggered fermions on the lattice [119]. In our context, the idea of twisting is to decompose the fields of a Euclidean supersymmetric Yang-Mills theory in $D$ space-time dimensions in representations not of the original (Euclidean) rotational symmetry $SO_{\mathrm{rot}}(D)$, but a twisted rotational symmetry, which is the diagonal subgroup of this symmetry and

---

[1]Note that the lattice actions constructed using the orbifolding and twisted methods are equivalent [116–118,132]. Indeed the original orbifold construction of this theory constitutes an independent UV complete construction of the Marcus/GL twist of $\mathcal{N} = 4$ Yang-Mills

an $SO_R(D)$ subgroup of the R-symmetry of the theory, that is,

$$SO(D)' = \text{diag}(SO_{\text{Lorentz}}(D) \times SO_R(D)) \ . \tag{5.1}$$

The continuum twist of $\mathcal{N} = 4$ that is the starting point of the twisted lattice construction was first written down by Marcus in 1995 [25]. It now plays an important role in the Geometric Langlands program and is hence sometimes called the GL-twist [124]. In the case of $\mathcal{N} = 4$ super Yang-Mills this amounts to treating the original four Majorana fermions as a $4 \times 4$ matrix and subsequently expanding this matrix on products of Dirac gamma matrices

$$\Psi = \eta I + \psi_\mu \gamma_\mu + \chi_{\mu\nu} \gamma_\mu \gamma_\nu + \overline{\psi}_\mu \gamma_5 \gamma_\mu + \overline{\eta} \gamma_5 \tag{5.2}$$

The sixteen component fields $(\eta, \psi_\mu, \chi_{\mu\nu}, \overline{\psi}_\mu, \overline{\eta})$ ($\chi_{\mu\nu}$ is antisymmetric) are the twisted fermions. In a similar fashion, four of the scalars which originally transformed as a vector under the $SO(4)$ flavor subgroup become vectors $B_\mu$ under the twisted rotational symmetry and combine with the usual gauge fields $A_\mu$ to produce complexified gauge fields $\mathcal{A}_\mu = A_\mu + iB_\mu$ in the twisted theory. The remaining two scalars remain as singlets under twisted rotations.

It is actually possible to pack these twisted fields into a more compact structure by replacing the Greek index $\mu$ running from $1 \ldots 4$ with a Roman index running from $1 \ldots 5$. The sixteen twisted fermions then comprise the set $(\eta, \psi_a, \chi_{ab})$ while the bosons can be packed into five complex gauge fields $\mathcal{A}_a$. The rationale for this final change of variables is that the twisted action can then be written in the very simple form

$$S = \frac{1}{g^2} \mathcal{Q} \int \text{Tr} \ \left( \chi_{ab} \mathcal{F}_{ab} + \eta [\overline{\mathcal{D}}_a, \mathcal{D}_b] - \frac{1}{2} \eta d \right) + S_{\text{closed}} \tag{5.3}$$

where $\mathcal{Q}$ represents a supersymmetry transformation that transforms as a scalar under the twisted rotation group (its appearance in the theory parallels that of the scalar fermion $\eta$). Furthermore the original supersymmetry algebra implies that this charge will be nilpotent with $\mathcal{Q}^2 = 0$ so that the first term appearing in the action Eqn. 5.3

is trivially invariant under $\mathcal{Q}$ transformations. The second $\mathcal{Q}$-closed term takes the form

$$S_{\text{closed}} = -\frac{1}{8} \int \text{Tr } \epsilon_{mnpqr} \chi_{qr} \overline{\mathcal{D}}_p \chi_{mn} \ . \tag{5.4}$$

The supersymmetric invariance of this term then relies on the Bianchi identity

$$\epsilon_{mnpqr} \overline{\mathcal{D}}_p \overline{\mathcal{F}}_{qr} = 0 \ . \tag{5.5}$$

The nilpotent transformations associated with the scalar supersymmetry $\mathcal{Q}$ are given explicitly by

$$
\begin{aligned}
\mathcal{Q} \, \mathcal{A}_a &= \psi_a \\
\mathcal{Q} \, \psi_a &= 0 \\
\mathcal{Q} \, \overline{\mathcal{A}}_a &= 0 \\
\mathcal{Q} \, \chi_{ab} &= -\overline{\mathcal{F}}_{ab} \\
\mathcal{Q} \, \eta &= d \\
\mathcal{Q} \, d &= 0,
\end{aligned}
\tag{5.6}
$$

where the complexified field strength $F_{ab}$ is given by

$$\mathcal{F}_{ab} = [\mathcal{D}_a, \mathcal{D}_b], \quad \overline{\mathcal{F}}_{ab} = [\overline{\mathcal{D}}_a, \overline{\mathcal{D}}_b] \ , \tag{5.7}$$

and the complex covariant derivatives are given by

$$\mathcal{D}_a = \partial_a + \mathcal{A}_a, \quad \overline{\mathcal{D}}_a = \partial_a + \overline{\mathcal{A}}_a \ . \tag{5.8}$$

It is important to recognize that the five-dimensional look of the theory is nothing to be afraid of; in fact, it simply reflects the fact that this four-dimensional field theory can be viewed as the dimensional reduction of $\mathcal{N} = 1$ super Yang-Mills theory in D=10 dimensions. The five complexified gauge connections are the ten gauge fields of that theory. In the next section we will review how easily this picture translates

into the lattice formulation.

## 5.2  $\mathcal{N} = 4$ Super Yang-Mills Theory on the Lattice

The prescription for discretization is actually quite natural. The complex gauge fields are represented as Wilson gauge fields which take their values in the *algebra* of a complexified $U(N)$ gauge group [2]

$$\mathcal{A}_a(x) \to \mathcal{U}_a(\mathbf{n}) = \sum_{C=1}^{N^2} T^C \mathcal{U}_a^C(\mathbf{n}) \tag{5.9}$$

Since we need five links in four dimensions we can simply place these Wilson link fields on a hypercubic lattice with an additional body diagonal

$$
\begin{aligned}
\widehat{\boldsymbol{\mu}}_1 &= (1,0,0,0) \\
\widehat{\boldsymbol{\mu}}_2 &= (0,1,0,0) \\
\widehat{\boldsymbol{\mu}}_3 &= (0,0,1,0) \\
\widehat{\boldsymbol{\mu}}_4 &= (0,0,0,1) \\
\widehat{\boldsymbol{\mu}}_5 &= (-1,-1,-1,-1) \ .
\end{aligned}
\tag{5.10}
$$

Thus while $\mathcal{U}_a$, $a = 1 \ldots 4$ are associated with the usual unit vectors of a hypercubic lattice the field $\mathcal{U}_5$ is then placed on the body diagonal link. Notice that the basis vectors sum to zero, consistent with the use of such a linearly dependent basis. However, it should also be clear that a more symmetrical choice would be preferable in which the five basis vectors are treated in an entirely equivalent manner. A four dimensional lattice with this higher $S^5$ point group symmetry exists and is called the $A_4^*$ lattice. It is constructed from the set of five basis vectors $\widehat{\boldsymbol{e}}_a$ pointing from the center of a four-dimensional equilateral simplex out to its vertices together with their inverses $-\widehat{\boldsymbol{e}}_a$. It is the four-dimensional analog of the two-dimensional triangular lattice. A

[2]The generators are normalized as $Tr(T^A T^B) = -\delta^{AB}$

specific basis for the $A_4^*$ lattice is given in the form of five lattice vectors

$$\widehat{e}_1 \;=\; \Big(\frac{1}{\sqrt{2}}, \frac{1}{\sqrt{6}}, \frac{1}{\sqrt{12}}, \frac{1}{\sqrt{20}}\Big) \tag{5.11}$$

$$\widehat{e}_2 \;=\; \Big(-\frac{1}{\sqrt{2}}, \frac{1}{\sqrt{6}}, \frac{1}{\sqrt{12}}, \frac{1}{\sqrt{20}}\Big) \tag{5.12}$$

$$\widehat{e}_3 \;=\; \Big(0, -\frac{2}{\sqrt{6}}, \frac{1}{\sqrt{12}}, \frac{1}{\sqrt{20}}\Big) \tag{5.13}$$

$$\widehat{e}_4 \;=\; \Big(0, 0, -\frac{3}{\sqrt{12}}, \frac{1}{\sqrt{20}}\Big) \tag{5.14}$$

$$\widehat{e}_5 \;=\; \Big(0, 0, 0, -\frac{4}{\sqrt{20}}\Big) \;. \tag{5.15}$$

The basis vectors satisfy the relations

$$\sum_{m=1}^{5} \widehat{e}_m = 0; \;\; \widehat{e}_m \cdot \widehat{e}_n = \Big(\delta_{mn} - \frac{1}{5}\Big); \;\; \sum_{m=1}^{5} (\widehat{e}_m)_\mu (\widehat{e}_m)_\nu = \delta_{\mu\nu}; \;\; \mu, \nu = 1, \cdots, 4. \tag{5.16}$$

It is not hard to see that the basis vectors of $A_4^*$ are a simple deformation of the those used in the hypercubic representation and indeed a simple Gram matrix allows one to map between the coordinates of some field in hypercubic representation to the physical coordinates relative to the $A_4^*$ lattice (see [19] for details). Indeed for the action and other local quantities it is not necessary to explicitly perform this mapping; the hypercubic lattice representation furnishes a simple arena in which one can calculate the action, check gauge invariance and carry out supersymmetry variations without explicit reference to the $A_4^*$ lattice. Only when we consider questions associated with rotational invariance or space-time dependent correlation functions do we need to map the coordinates of lattice fields into their positions relative to the "physical " $A_4^*$ lattice. We stress this point because it means that simulations can be performed in a quite standard hypercubic lattice set-up, without concerns about details of the $A_4^*$ lattice.

The Wilson links transform in the usual way under ordinary *non-complexified* $U(N)$ lattice gauge transformations

$$\mathcal{U}_a(\mathbf{n}) \to G(\mathbf{n}) \mathcal{U}_a(\mathbf{n}) G^\dagger(\mathbf{n} + \widehat{\boldsymbol{\mu}}_a) \;. \tag{5.17}$$

Supersymmetric invariance then precisely implies that $\psi_a(\mathbf{n})$ live on the same links and transform identically. A local scalar fermion $\eta(\mathbf{n})$ must clearly live on a site. It transforms accordingly,

$$\eta(\mathbf{n}) \to G(\mathbf{n})\eta(\mathbf{n})G^\dagger(\mathbf{n}) . \tag{5.18}$$

In a similar fashion we place the fermionic fields $\chi_{ab}$ on new links leading from the origin out to $\widehat{\boldsymbol{\mu}}_a + \widehat{\boldsymbol{\mu}}_b$. In the hypercubic representation these would correspond to links on two and three dimensional faces associated with the hypercube. However, there is one crucial difference from the fields $\psi_a$ - the fields $\chi_{ab}$ are chosen with opposite orientation on these links as encoded from their gauge transformation property:

$$\chi_{ab}(\mathbf{n}) \to G(\mathbf{n} + \widehat{\boldsymbol{\mu}}_a + \widehat{\boldsymbol{\mu}}_b)\chi_{ab}(\mathbf{n})G^\dagger(\mathbf{n}) . \tag{5.19}$$

This shows how naturally the supersymmetric degrees of freedom can be distributed on the lattice - the sixteen fermionic degrees of freedom at a site can all be associated with the sixteen distinct links that can be drawn in the unit four dimensional hypercube located at that site.

To complete the discretization we need to describe how continuum derivatives are to be replaced by difference operators. A natural technology for accomplishing this in the case of adjoint fields was developed many years ago. It yields expressions for the derivative operator applied to arbitrary lattice p-forms [122], and is thus very naturally tied to geometry. In the case discussed here, we need just two derivatives given by the expressions

$$\mathcal{D}_a^{(+)} f_b(\mathbf{n}) = \mathcal{U}_a(\mathbf{n})f_b(\mathbf{n} + \widehat{\boldsymbol{\mu}}_a) - f_b(\mathbf{n})\mathcal{U}_a(\mathbf{n} + \widehat{\boldsymbol{\mu}}_b) , \tag{5.20}$$

$$\overline{\mathcal{D}}_a^{(-)} f_a(\mathbf{n}) = f_a(\mathbf{n})\overline{\mathcal{U}}_a(\mathbf{n}) - \overline{\mathcal{U}}_a(\mathbf{n} - \widehat{\boldsymbol{\mu}}_a)f_a(\mathbf{n} - \widehat{\boldsymbol{\mu}}_a) . \tag{5.21}$$

These difference operators appeared automatically as a result of orbifold projection in the original constructions of supersymmetric lattice Yang-Mills theories from matrix models [133–135]. A beautiful feature has appeared here: the construction of supersymmetric lattice gauge theories by means of orbifolding is in one-to-one corre-

spondence with a simple geometrical principle [136]. Indeed, using this geometrical prescription is by far the easiest way to see how this lattice theory emerges. The lattice field strength is given by the gauged forward difference acting on the link field: $\mathcal{F}_{ab}(\mathbf{n}) = \mathcal{D}_a^{(+)}\mathcal{U}_b(\mathbf{n})$. It is automatically antisymmetric in its indices. Furthermore, as hoped for it transforms like a lattice 2-form and yields a gauge invariant loop on the lattice when contracted with $\chi_{ab}(\mathbf{n})$ (this is precisely the reason that the field $\chi$ is chosen to have opposite orientation relative to $\psi_a$). Similarly, the covariant backward difference appearing in $\overline{\mathcal{D}}_a^{(-)}\mathcal{U}_a(\mathbf{n})$ transforms as a 0-form or, correspondingly, as a site field. It can hence can be contracted with the site field $\eta(\mathbf{n})$ to yield a gauge invariant combination. Thus, the twin requirements of gauge invariance and supersymmetry naturally places strong constraints on the whole construction.

Furthermore, this use of forward and backward difference operators guarantees that the solutions of the lattice theory map one-to-one with the solutions of the continuum theory and the fermion doubling problems are hence evaded [120]. Another way to understand this is to see that by introducing a lattice with half the lattice spacing one can map this Kähler–Dirac fermion action into the action for staggered fermions [123]. We emphasize that, unlike the case of two-flavor or three-flavor QCD, there is no rooting problem in this supersymmetric construction since the additional lattice fermion degeneracy is precisely as already required in the continuum theory.

Just like the continuum theory, the lattice action again contains a $\mathcal{Q}$-exact term:

$$S = \sum_{\mathbf{n}} \operatorname{Tr} \mathcal{Q}\left(\chi_{ab}(\mathbf{n})\mathcal{D}_a^{(+)}\mathcal{U}_b(\mathbf{n}) + \eta(\mathbf{n})\overline{\mathcal{D}}_a^{(-)}\mathcal{U}_a(\mathbf{n}) - \frac{1}{2}\eta(\mathbf{n})d(\mathbf{n})\right) . \qquad (5.22)$$

Acting with the $\mathcal{Q}$ transformation on the lattice fields and integrating out the auxiliary field $d$, we obtain the gauge and $\mathcal{Q}$-invariant lattice action:

$$S_0 = \sum_{\mathbf{n}} \operatorname{Tr} \left(\mathcal{F}_{ab}^{\dagger}(\mathbf{n})\mathcal{F}_{ab}(\mathbf{n}) + \frac{1}{2}\left(\overline{\mathcal{D}}_a^{(-)}\mathcal{U}_a(\mathbf{n})\right)^2 - \chi_{ab}(\mathbf{n})\mathcal{D}_{[a}^{(+)}\psi_{b]}(\mathbf{n}) - \eta(\mathbf{n})\overline{\mathcal{D}}_a^{(-)}\psi_a(\mathbf{n})\right) .$$
$$(5.23)$$

As in the continuum theory, the $\mathcal{Q}$-exact action must be augmented by an additional

piece that is only $\mathcal{Q}$-closed,

$$S_{closed} = \frac{1}{2}\epsilon_{abcde}\chi_{de}(\mathbf{n} + \widehat{\boldsymbol{\mu}}_a + \widehat{\boldsymbol{\mu}}_b + \widehat{\boldsymbol{\mu}}_c)\overline{\mathcal{D}}_c^{(-)}\chi_{ab}(\mathbf{n} + \widehat{\boldsymbol{\mu}}_c), \qquad (5.24)$$

which is the direct analog of Eqn. (5.4) in the continuum theory. Remarkably, and as shown in [117], an exact lattice analog of the Bianchi identity,

$$\epsilon_{abcde}\overline{\mathcal{D}}_c^{(-)}\overline{\mathcal{F}}_{ab}(\mathbf{n} + \widehat{\boldsymbol{\mu}}_c) = 0, \qquad (5.25)$$

guarantees that the above term is invariant under $\mathcal{Q}$-transformations on the lattice. Note, incidentally, that the coefficient in front cannot be chosen freely. Only with the specific coefficient shown will we recover the correct naive continuum limit with full supersymmetry and Lorentz invariance. It is intriguing to speculate what happens to this relative coefficient under radiative corrections.

To show that the full action correctly reproduces the continuum theory in the naive continuum limit, one must (in some suitable gauge) expand the gauge fields around the unit matrix,

$$\mathcal{U}_a(\mathbf{n}) = I + a\mathcal{A}_a(\mathbf{n}) \qquad (5.26)$$

The following interesting phenomenon occurs: Usually the unit matrix appearing here arises trivially once one expands the group element $U_\mu = e^{aA_\mu}$ in powers of the lattice spacing. However supersymmetry requires that the bosons and the fermions be treated on an equal footing. Since the fermions are expanded in the algebra this necessitates doing the same for the bosons. Usually this would be a disaster since it would make it impossible to introduce the expansion seen in Eqn. (5.26) without breaking gauge invariance. However, in the case of a complexified $U(N)$ gauge group we have another option: the unit matrix can arise from the acquired vacuum expectation value of a dynamical field in the theory – here the trace mode of the imaginary part of the connection or, equivalently, the trace mode of the scalars in the original (untwisted) theory[3]

_____

[3]A recent construction employing only $SU(N)$ gauge symmetry is discussed in [137].

This expectation value can be achieved by adding to the supersymmetric action a gauge invariant potential of the form [114]

$$S_M = \mu_L^2 \sum_{\mathbf{n}} \left( \frac{1}{N} \text{Tr}(\mathcal{U}_a^\dagger(\mathbf{n})\mathcal{U}_a(\mathbf{n})) - 1 \right)^2 . \tag{5.27}$$

Here $\mu_L$ is a tunable mass parameter, which can be used to control the fluctuations of the lattice fields. Notice that such a potential obviously breaks supersymmetry – however because of the exact supersymmetry at $\mu_L = 0$ all supersymmetry breaking counterterms induced via quantum effects will possess couplings that vanish as $\mu_L \to 0$ and so can be removed by sending $\mu_L \to 0$ at the end of the calculation. By adopting the polar parametrization $\mathcal{U}_a = e^{A_a + iB_a}$ it should be clear that the leading effect of this term is to set the expectation value of the trace mode of $B_a$ to unity as required. Furthermore, fluctuations of this trace mode are governed by the mass $\mu_L$ while all traceless scalar modes feel only a quartic potential. Thus the limit $\mu_L \equiv \mu a \to 0$ restores the usual flat directions associated with the $SU(N)$ sector as the lattice spacing $a \to 0$. A finite mass remains for the $U(1)$ mode but since this naively decouples in the continuum limit our expectation is that this should not lead to any observable effects in the $SU(N)$ sector. This is one of the key issues we wish to investigate in this paper.

The above discussion illustrates the subtle way in which the continuum limit of this theory must be reached. Without a vacuum expectation value of the scalar trace mode, even the notion of a four dimensional continuum limit with canonically propagating degrees of freedom cannot be introduced.

Once one has such a lattice action an obvious thing to do is to perform a strong-coupling expansion. Normally, such an expansion around infinitely strong bare gauge coupling reveals a phase of the theory that is non-universal, confining, chirally broken and with a mass gap that is given in terms of the strong coupling string tension. Remarkably, such a standard strong-coupling expansion is not easily implemented in this theory. It is exact supersymmetry, or rather exact $\mathcal{Q}$-symmetry that gets in the way: this theory is massless and has only *one* coupling to all fields. The (inverse)

bare coupling multiplies all terms of the lattice action. This suggests that the only consistent strong-coupling expansion will be based on expanding the full Boltzmann factor and bringing down powers of the action. However, there is then no damping term of the functional integral. The bosonic degrees of freedom have non-compact support, and the Grassmann integrals provide the heuristic 'zero' that nevertheless could give formal meaning to such an expansion. However, the precise way in which such an expansion scheme could be implemented seems, at best, to be unclear. It is tempting to view the lack of a natural strong-coupling expansion as evidence that this theory indeed may have no strong-coupling, confining, phase at all.

One further complication should be discussed: the potential sign problem in the lattice theory. To simulate the theory requires carrying out an integration over the fermions. This process generates a Pfaffian which is generically *complex*. This invalidates the usual Monte Carlo method for computing observables since the measure is no longer real and positive definite. However, in earlier numerical work it has been shown that the phase is actually very small for this theory, at least after dimensional reduction to two dimensions and contrary to the naive expectation [138–140]. To understand this result, one can compute the partition function at one loop. This was done in Ref. [125] with the result that the exact supersymmetry leads to a perfect cancelation between bosons and fermions and no phase appears in the final effective action. This is equivalent to the statement that the Pfaffian is in fact real and positive definite when evaluated on the moduli space corresponding to constant complex commuting matrices[4] Furthermore since the partition function is a topological invariant it can be calculated *exactly* at one loop – so this result holds to all orders in perturbation theory. Since the expectation value of the Pfaffian phase factor in the phase quenched ensemble is proportional to this full partition function, this argument suggests that the phase should play no role in the lattice theory. Of course, these arguments require exact $\mathcal{Q}$ supersymmetry, which is broken by the mass term we use

[4]At least in the four supercharge case, this phenomenon can be related to the so-called Neuberger 0/0 problem which presents a hurdle to constructing a BRST transformation in lattice gauge theories where the fields are defined on a finite group manifold. For a discussion of this connection see Ref. [139]

to control the fluctuations of the scalar trace mode. Since the arguments given above do not depend on this dimensional reduction, one could expect it should also be true in the full four-dimensional theory. As we will show in the next section, our numerical results for the bosonic action (related to a derivative of the partition function) back up this conclusion – it approaches the exact supersymmetric value as $\mu_L \to 0$ in the phase quenched ensemble.

One final wrinkle occurs when we contemplate doing simulations with periodic fermion boundary conditions in all four dimensions - as is natural in an exactly supersymmetric Euclidean theory. The form of the fermion action then allows for an exact zero mode of the form $(\eta^A, \psi_a^A \chi_{ab}^A) = (\delta^{0A}, 0, 0)$ on *any* background gauge field ($A$ is an adjoint index here). This zero mode can be lifted either by use of a thermal boundary condition or by the addition of a supersymmetric term

$$S_{extra} = \mu_F \mathcal{Q}[\text{Tr}\ (\eta)\text{Tr}\ (U_a U_a^\dagger)]\ . \tag{5.28}$$

Performing the $\mathcal{Q}$ variation leads to two new contributions to the action

$$\text{Tr}\ [\overline{\mathcal{D}}_a^{(-)}\mathcal{U}_a]\text{Tr}\ (\mathcal{U}_a^\dagger\mathcal{U}_a) - \text{Tr}\ (\eta)\text{Tr}\ (\psi_a U_a^\dagger)\ . \tag{5.29}$$

The second of these removes the fermion zero mode. Thus the complete action to be simulated is

$$S = S_0 + S_{closed} + S_M + S_{extra}. \tag{5.30}$$

Although $\mathcal{Q}$-exact, we should emphasize that the last piece $S_{extra}$ has no analog in the full $\mathcal{N} = 4$ super Yang-Mills theory. Thus also this term must be tuned to zero before continuum results can be extracted. In practice we have confined our study to systems with antiperiodic boundary conditions and thsi additional term $S_{extra}$ is set to zero.

As usual in Monte Carlo simulation, the fermion variables are integrated out and their effect in the simulation is represented by a set of pseudofermion fields. Notice though that the integration measure involves only the fields $(\eta, \psi_a, \chi_{ab})$ and not their

complex conjugates. Thus it is a Pfaffian rather than a determinant that is generated. Up to a phase this in turn can be produced with a pseudofermion action of the form

$$S_{PF} = \Phi^\dagger (M^\dagger M)^{-\frac{1}{4}} \Phi \,, \tag{5.31}$$

where $M$ is the antisymmetric twisted fermion bilinear in $S$. The fractional power of the matrix is approximated by a partial fraction (multimass) expansion implemented using the Rational Hybrid Monte Carlo (RHMC) algorithm.

Thus for the lattice practitioner we have a system of

- A set of bosonic variables appearing as noncompact complex gauge fields

- A set of (twisted) fermions whose effect can be encoded using the usual RHMC algorithm.

- Both sets of fields are defined over a hypercubic lattice with additional face and body links.

This is somewhat Baroque, but it is simple and it is completely manageable. It might be useful to list what can be computed at this stage:

- We can simulate with periodic or antiperiodic fermionic boundary conditions so that we can do either zero or finite temperature (supersymmetry-breaking) simulations

- We can dial in various masses ($\mu_L$, $\mu_F$) to explicitly break various symmetries. This will ultimately be useful for computing critical exponents.

- We can compute eigenvalues of the fermion (Dirac) operator.

- We can measure Wilson and Polyakov lines to extract, for example, the static quark-antiquark potential and look for confinement/deconfinement.

- We can monitor the distribution of gauge invariant scalar eigenvalues extracted from the observable $\mathcal{U}_a^\dagger \mathcal{U}_a$ which gives us a handle on possible problems associated with integration over the flat directions.

Finally, we should stress the following. To obtain physical correlation functions from this twisted theory, one must perform the appropriate un-twisting on observables. In terms of our twisted variables, physical quantities will generically appear in rather complicated combinations of the variables described here. However, the map is straightforward and can easily be implemented in measurements. And, in the cases of spectral observables, we do not need to perform the un-twisting: operators with the same sets of space-time symmetries couple to the same set of physical states; only the relative coupling coefficients will be different.

## 5.3 Simulation Results

### 5.3.1 Introduction to the simulations

We begin with a few words about lattice observables. As usual, gauge invariance implies quite strict limitations on the observables we can construct out of our lattice variables. What is new in this theory as compared to ordinary lattice gauge theory is the natural appearance of link variables that live in the algebra of the gauge group rather than in the group itself. This also implies that the integration measure naturally is over anti-Hermitian gauge variables rather than being the invariant gauge group (Haar) measure. The reason is that the measure must remain invariant under an arbitrary shift symmetry, as is clear from Eqn. 5.6. This brings to the open an important point regarding the ordinary Yang-Mills gauge symmetry of this theory: The gauge transformations of the gauge links (which live in the algebra of the gauge group) are defined by the multiplication rule (5.17). At first glance it is not obvious that the flat integration measure associated with the gauge links is invariant under these gauge transformations: the non-linear transformation begs for the left and right invariant Haar measure instead. However, since the links are complexified one must integrate over both the field and its complex conjugate and this saves the day; the Jacobians arising after a gauge transformation cancelling against each other leaving the final measure invariant as required[5]. However this argument fails for the fermion

---

[5]We thank Issaku Kanamori for pointing this out

link fields since they do not appear with their complex conjugates in the measure. Remarkably, however one does find that the ordinary flat measure *is* invariant after taking the product over all lattice points. This is not totally surprising from the point of view of the orbifolding construction, and it is instructive to see how it arises in detail.

The gauge transformation for a typical fermion link variable such as $\psi_a(\mathbf{n})$ is written in eq. (5.17),

$$\psi_a(\mathbf{n}) \to G(\mathbf{n})\psi_a(\mathbf{n})G^\dagger(\mathbf{n}+\widehat{\boldsymbol{\mu}}_a)\,, \tag{5.32}$$

where $\psi_a(\mathbf{n}) = T^A\psi_a^A(\mathbf{n})$ and we integrate over the flat measure in the variables $\psi_a^A(\mathbf{n})$.

On a finite lattice, $G^\dagger(\mathbf{n}+\widehat{\boldsymbol{\mu}}_a)$ is a function different from $G(\mathbf{n})$. It is still sufficient to check gauge invariance for infinitesimal (but different) transformations. Let us choose

$$
\begin{aligned}
G(\mathbf{n}) &= 1 + \alpha^A T^A \\
G(\mathbf{n}+\widehat{\boldsymbol{\mu}}_a) &= 1 + \beta^A T^A \,.
\end{aligned}
\tag{5.33}
$$

Expanding and collecting terms we get the same cancellations as in the continuum plus two new terms in the transformation law for $\psi_a(\mathbf{n})$:

$$T^A\psi_a^A(\mathbf{n}) \to \alpha^A T^A T^B \psi_a^A(\mathbf{n}) - \beta^A T^A T^B \psi_a^A(\mathbf{n}) \tag{5.34}$$

In the naive continuum limit, where $\alpha^A - \beta^A \sim a$, these terms can be ignored and the usual gauge invariance of the continuum is recovered. But for finite lattice spacing $a$ the new terms remain. However, on the group $U(N)$ we can always expand a product $T^A T^B$ in the generators of the group:

$$T^A T^B = \frac{i}{2}f^{ABC}T^C + d^{ABC}T^C\,, \tag{5.35}$$

where $d^{ABC}$ are the symmetric structure constants. We can now read off the additional terms in the transformation of the components $\psi_a^A$. The first new piece vanishes because of $f^{AAC} = 0$, and only the second piece remains. For the link fermion $\psi_a(\mathbf{n})$ it is of the form $(\alpha - \beta)^C d^{AAC}$, which does not vanish. However, the measure is the product $\prod d\psi_a^A$ over all links on the lattice. Link for link the leftover pieces cancel among each other because of the conjugation involved in the gauge transformation (5.17). It is interesting to see how gauge invariance is not insured for a single link, but recovered once the transformations of the neighboring links are included. From the orbifolding construction one could perhaps have guessed that such a mechanism would need to be invoked.

It should be noted here that even for conventional U(1) lattice gauge theories de-compactified gauge-fields obtained via stereographic projection of the group manifold can be used in order to construct a lattice BRST symmetry, see [141–143].

The choice of gauge group is clearly not very essential for a first set of simulations. For simplicity, we have here simulated the (phase quenched) $U(2)$ theory on lattices of size $L = 4^4, 6^4, 8^4$ for a wide range of bare 't Hooft couplings $\lambda = 0.2 - 2.6$ and values of the regulator mass in the range $\mu_L = 0.1 - 1.0$. The simulations have mostly been performed using anti-periodic (thermal) boundary conditions for the fermions. This evidently breaks supersymmetry, but it also removes an exact fermionic zero momentum mode associated the trace mode of fermions that is otherwise present. The breaking due to anti-periodic boundary conditions turns out to be tiny, and will of course disappear as larger volumes are being considered.

An RHMC algorithm has been used for the simulations. It has been described in detail in ref. [144]. The use of a GPU accelerated solver [131] has allowed us to reach larger lattices than have thus far been studied. It is important to recognize that the supersymmetric fermion operator defined on a lattice of size $L$ is equivalent, in terms of counting degrees of freedom, to a staggered operator on a lattice of size $2L$.

### 5.3.2  Lattice moduli stabilization

As in continuum $\mathcal{N} = 4$ super Yang-Mills theory, the lattice theory possesses flat directions corresponding to the continuum of classical vacuum states in which the bosonic fields take values in the space of constant, mutually commuting, complex matrices. This continuum of vacuum states is called the moduli space of the theory and is determined by the expectation values of the scalar fields appearing as imaginary parts of gauge fields in the twisted formulation. Potential divergences appear in the partition function of the theory when integrating over these flat directions.

In the lattice theory we stabilize these moduli by the addition of the term Eq. 5.27 to the action. This term certainly lifts the moduli space of the theory but in the lattice theory with $U(N)$ gauge symmetry it plays an even more important role by generating a gauge invariant vacuum expectation value for the complexified Wilson link field $\text{Tr}\, \mathcal{U}_a^\dagger U_a = 1$. This allows one to argue that in the limit $a \to 0$ and in a fixed gauge $\mathcal{U}_a \sim I + \mathcal{A}_a + \ldots$. This latter expansion is *required* if the naive continuum limit of the lattice theory is to target a four dimensional field theory. Furthermore, the unit matrix that appears in this expression can then be interpreted as corresponding to giving a fixed vev to the trace mode of the scalar field. However, it is not clear that this vev survives quantum corrections and in principle one needs to check this in the simulations.

Clearly the correct vacuum state is picked out uniquely as $\mu_L \to \infty$. But the supersymmetric limit lies in the opposite direction where $\mu_L \to 0$. It is important to be able to locate which regions in the bare parameter space are consistent with such a link expectation value and simultaneously possess small supersymmetry breaking. Figure. 5-1 shows a plot of the spatial link and temporal link expectation values versus $\mu_L$ at 't Hooft coupling $\lambda = 1.0$ on lattices of size $L = 4$ and $L = 6$. For small enough $\mu_L$ the link vev can become destabilized either running to zero or large values. In such regions of the bare parameter space we claim that there is no possible four dimensional continuum limit. Our data indicates that this region of instability is pushed to smaller values of $\mu_L$ for larger lattices so it is likely a finite size artifact. All of the data we show in the following sections corresponds to regions of the phase
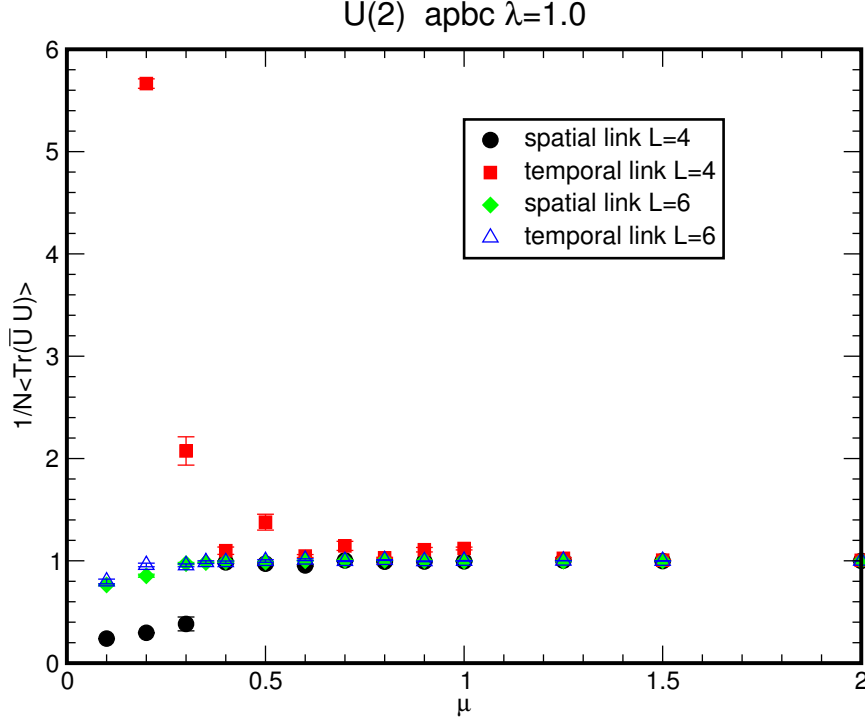
Figure 5-1: $\frac{1}{N}\text{Tr}\left(U_a^\dagger U_a\right)$ vs mass parameter $\mu_L$ at 't Hooft coupling $\lambda = 1.0$.

diagram where the link vacuum expectation value is close to unity.

Beyond leading order, the added potential term also lifts and stabilizes the regular $SU(N)$ flat directions and one might also worry that as $\mu_L \to 0$ this stabilization mechanism would also prove ineffective. To see that it does not consider the distribution of eigenvalues of $\mathcal{U}_a^\dagger \mathcal{U}_a$ for several values of $\mu_L$ on a $L = 6$ lattice. Fig. 5-2 shows the distribution of the eigenvalues of the traceless part of this quantity for several 't Hooft couplings $\lambda$ and for $\mu_L = 0.5$. For this value of $\mu_L$ the scalar eigenvalues do not wander down the flat directions but remain localized close to the origin in field space. The width of the resulting distributions does however increase as the gauge coupling is increased. Of course the most interesting issue is whether the scalar fields remain bounded as we send the supersymmetry breaking mass term to zero. The answer seems to be in the affirmative; Fig. 5-3 shows the distributions for fixed 't Hooft coupling $\lambda = 1.0$ as the mass parameter $\mu_L$ is decreased. The plots show a very weak dependence on $\mu_L$ consistent with the distributions approaching a well defined limit as $\mu_L \to 0$. However, it is important to note that this limit must be performed
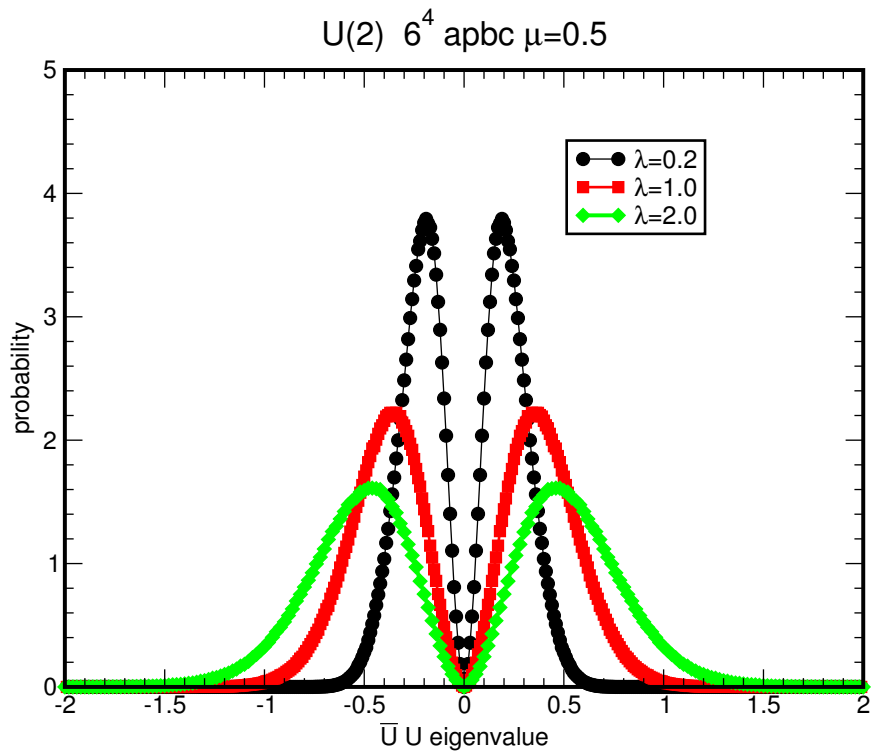
Figure 5-2: Eigenvalues of the traceless part of $\mathcal{U}_a^\dagger \mathcal{U}_a$ averaged over the Monte Carlo ensemble for $\mu_L = 0.5$ and $\lambda = 0.2, 1.0, 2.0$.

carefully; as we have seen we should send $L \to \infty$ *before* we can truly set $\mu_L$ to zero. If we don't do this we will encounter instabilities associated with the flat directions.

At first sight the apparent localization of the scalar eigenvalues close to the origin seems to indicate that the classical moduli space is in fact lifted by quantum corrections. Such a conclusion would disagree with the perturbative calculation carried out in [125] which shows that the single exact supersymmetry is sufficient to ensure that the effective potential *in the lattice theory* vanishes to all orders in perturbation theory in a fashion analogous to the continuum.

We thus do not believe that this is the correct interpretation of the results but instead that the observed localization is connected to the treatment of the zero modes in the theory. First notice that the Pfaffian vanishes on the flat directions since in the presence of a constant commuting bosonic background there appear exact fermion zero modes. In the full path integral these would formally cancel against the corresponding bosonic zero modes corresponding to fluctuations in the flat directions. However the supersymmetry breaking breaking potential we have added lifts these bosonic zero modes. The net effect is that the configurations corresponding to the exact flat directions *do not contribute* to the lattice path integral. Furthermore, since the valleys corresponding to the flat directions possess increasingly steep sides as we move away from the origin in field space we expect that the contribution of field configurations corresponding to fluctuations away from the flat directions will yield a distribution in the scalar eigenvalues that has a peak close to the origin - as we observe. These effects have been observed before by Staudacher at al [145] in the context of supersymmetric matrix models. We think that this is the correct interpretation of our eigenvalue distributions too - the zero mode sector of $\mathcal{N} = 4$ on a finite lattice corresponding to the corresponding supersymmetric matrix model.

### 5.3.3 Bosonic Action and Polyakov lines

In this initial study we have focused on understanding of the phase diagram of the lattice theory. First let us examine the bosonic action. This quantity is related to $\frac{\partial \ln Z}{\partial \lambda}$, which vanishes on account of the topological character of the partition function
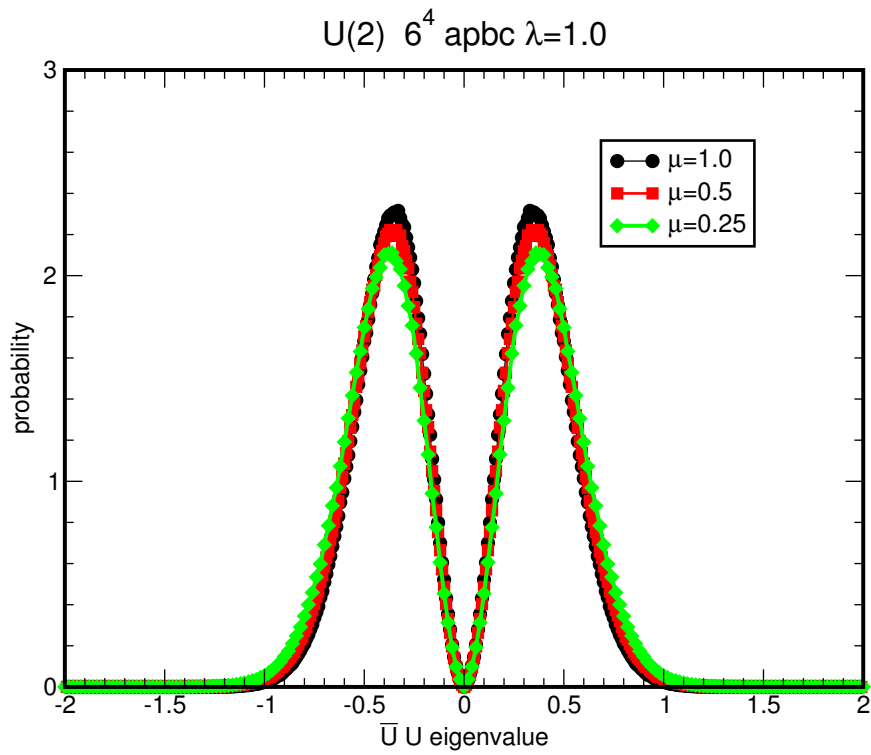
Figure 5-3: Eigenvalues of the traceless part of $\mathcal{U}_a^\dagger \mathcal{U}_a$ averaged over the Monte Carlo ensemble for $\lambda = 1.0$ and $\mu_L = 0.25, 0.5, 1.0$.
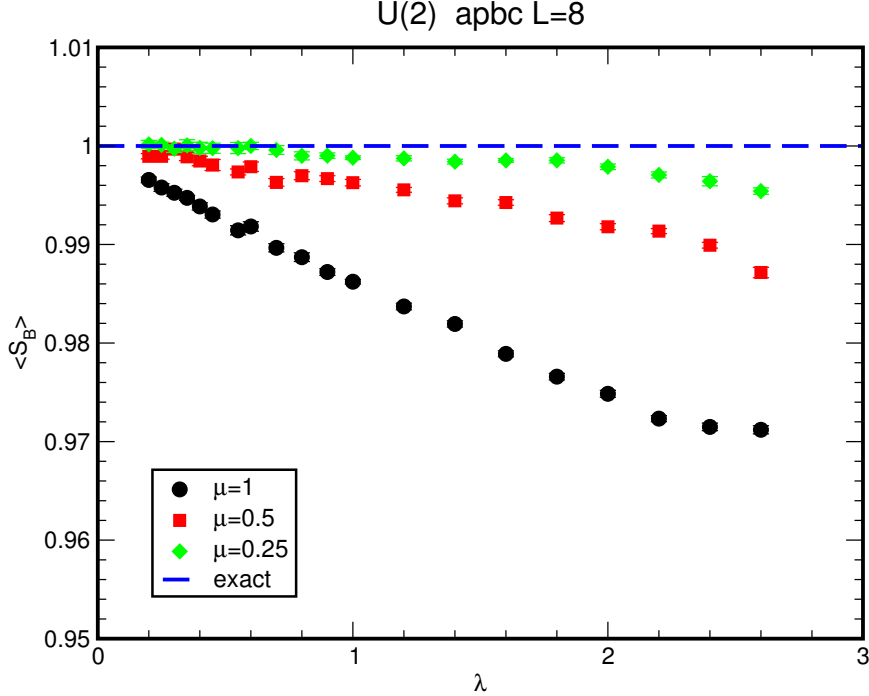
Figure 5-4: Expectation value of the bosonic action vs 't Hooft coupling $\lambda$ for $\mu_L = 0.25, 0.5, 1.0$. The data is normalized so that the supersymmetric result is unity.

in the supersymmetric limit[6]. We see in fig. 5-4 that the measured value for $<S_B>$ is indeed approximately $\lambda$-independent for small $\mu_L$ and agrees very well with the exact value $S_B/(9L^4 N^2/2) = 1$. Notice that this result is both consistent with exact supersymmetry in the lattice theory and additionally lends strength to the claim that a genuine sign problem is absent in this theory, and that the phase quenched ensemble hence is adequate for studying the theory.

We now turn to the Polyakov lines. Since $\mathcal{Q}\mathcal{U}_a = 0$ we expect that the Polyakov line is both gauge invariant and supersymmetric. Indeed as for the bosonic action the latter would guarantee that the Polyakov line would take a value which was independent of $\lambda$ in the limit $\mu_L \to 0$. Figure 5-5 shows the (absolute value of the) temporal Polyakov line versus bare coupling for $L = 8$ and $\mu_L = 0.5, 1.0$. The spatial line agrees with the temporal line within statistical errors. Unlike the bosonic action we see a dependence on the coupling $\lambda$ and little indication that taking $\mu_L$ to zero

---

[6]The fermions appear quadratically in the action and hence their expectation value can be computed via a simple scaling argument
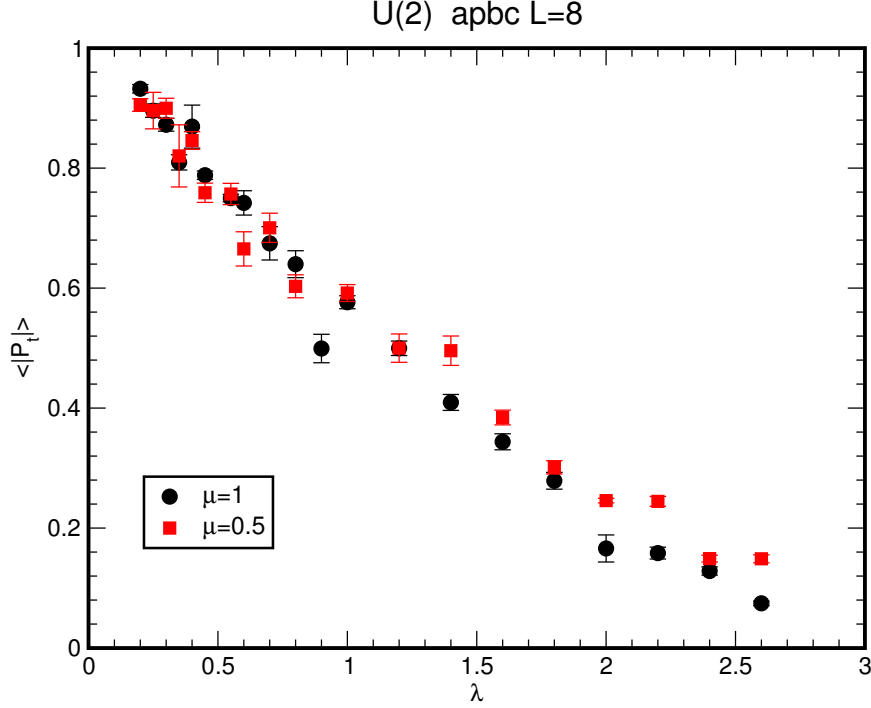
Figure 5-5: Absolute value of the temporal Polyakov line vs $\lambda$ for $\mu_L = 1.0, 0.5$ on a lattice of size $L = 8$.

will regain the supersymmetric result.

Insight into this problem can be gained by plotting a related quantity; the Polyakov line projected to the traceless $SU(2)$ sector. This is easily accomplished by taking the traceless part of $\mathcal{U}_a(x)$ and exponentiating the result to achieve a matrix in $SL(2, C)$. The corresponding temporal Polyakov line computed from this link is shown in fig. 5-6.

In this case the value of the line is approximately independent of coupling $\lambda$ as one would expect for an observable invariant under the exact supersymmetry. We deduce that the supersymmetry breaking we are seeing is associated with the U(1) sector. Perhaps one should not be too surprised by this; after all the potential term we add to stabilize the moduli space gives an explicit mass to the U(1) scalars and hence supplies a strong source of supersymmetry breaking in this sector. Intriguingly we have also computed the Polyakov line from the unitary projection of $\mathcal{U}_a$ and find a behavior similar to that in fig. 5-5. This is evidence that the breaking is actually
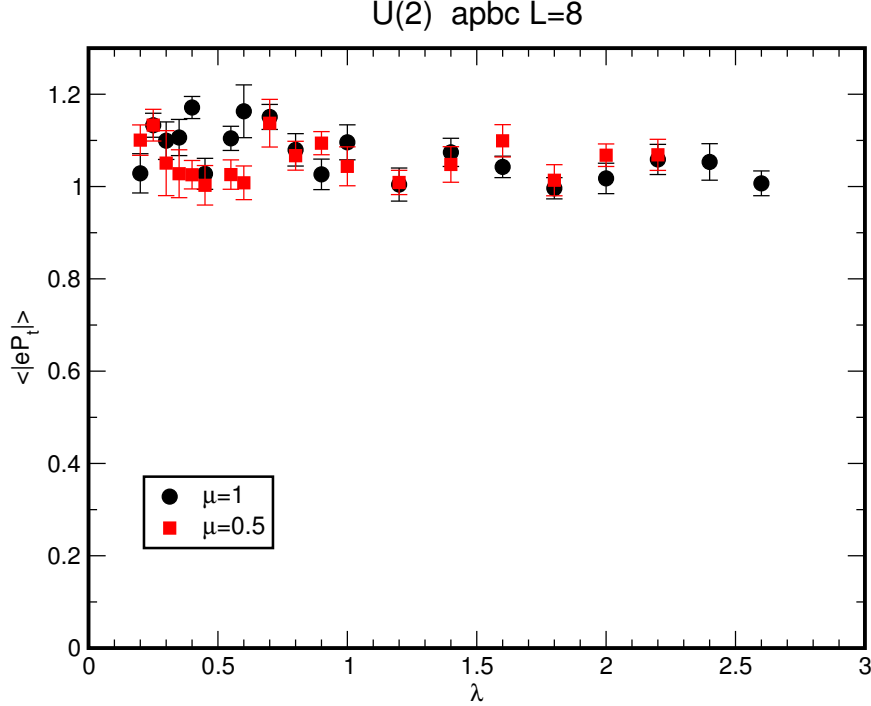
Figure 5-6: Absolute value of the traceless part of the temporal Polyakov line vs $\lambda$ for $\mu_L = 1.0, 0.5$ on a lattice of size $L = 8$.

associated not with the trace mode of the scalars but the additional massless U(1) gauge field that appears in the theory.

Let us make a final comment. Both the bosonic action and Polyakov lines show only smooth behavior as we scan in the 't Hooft coupling even as $\mu_L \to 0$. Over the entire range we have explored, $\lambda \leq 2.6$, there are no hints of phase transitions in the system associated with a two phase structure as one might have naively expected. We will present additional evidence in favor of a single lattice phase in the next section.

### 5.3.4 Wilson loops and the static potential

Finally we turn to the static potential which we compute using the "supersymmetric" Wilson loops $W(L, M)$ which include the six scalars. Denoting such Wilson loops by $W(r, t)$ where the second index indicates that we align the loop along the temporal
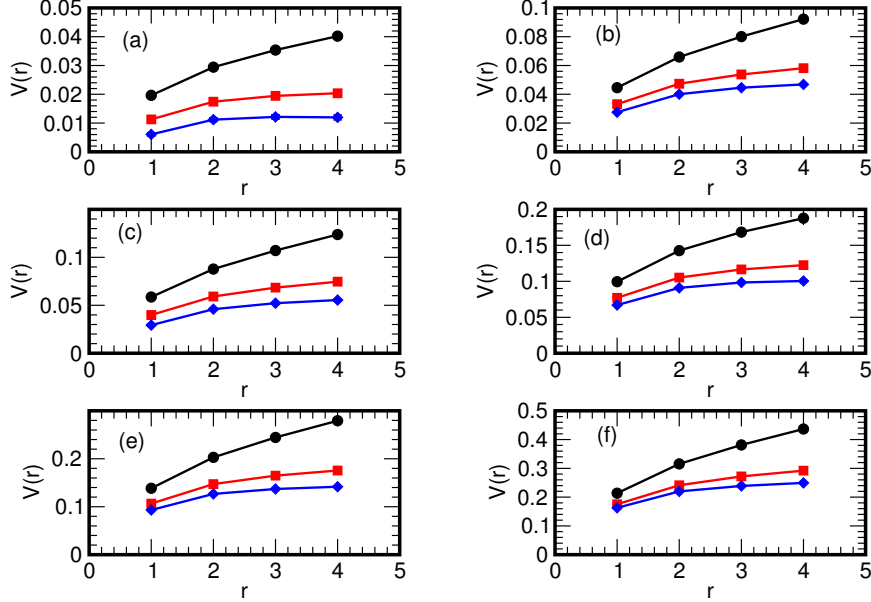
Figure 5-7: Potentials from Wilson loops, from $8^4$ $\mu_L = 1$ simulations. Octagons label potentials from $t = 1 - 2$, squares from $t = 2 - 3$ and diamonds from $t = 3 - 4$. (a) $\lambda = 0.25$; (b) $\lambda = 0.45$; (c) $\lambda = 0.6$; (d) $\lambda = 0.9$; (e) $\lambda = 1.2$; (f) $\lambda = 1.6$.

direction, we can define the potential $V(r)$ to be

$$W(r,t) = \exp(-V(r)t) \tag{5.36}$$

or, equivalently, we make an "effective mass" determination of the potential from

$$V(r) = -\log \frac{W(r, t+1)}{W(r, t)}. \tag{5.37}$$

This is a standard technique from the point of lattice QCD simulations. Examples of this analysis from our $8^4$ data sets are shown in Fig. 5-7. The fact that the data from different $t$ values are not coincident is a sign that $t$ is not large enough that Eq. 5.36 is obtained; higher-energy excitations of the Wilson loop still contribute to $W(r,t)$. Nevertheless, the figures already indicate that the potential flattens to a constant at large $r$.

We can make this statement a bit more quantitative by taking the largest-$t$ data (Wilson loops at $t = 3$ and 4), extracting the potential by fitting Eq. 5.37, and

Figure 5-8: String tension from fits to from Wilson loops with $t = 3$ and 4 from $8^4$ data sets. Circles are $\mu_L = 1.0$; diamonds, $\mu_L = 0.5$.

performing a fit to

$$V(r) = -\frac{C}{r} + A + \sigma r. \qquad (5.38)$$

For our data sets, with four values of $r$, we have one degree of freedom. We observe that $\sigma \simeq 0$ and that the fits uniformly have a $\chi^2/DoF$ smaller than unity. Of course, the quantities in the fit are highly correlated since they come from the same underlying configurations. Therefore, we fold the whole fit into a jackknife. The extracted string tension $\sigma$ is shown in Fig. 5-8. Again, it is clearly consistent with zero. Observing zero string tension raises the possibility that $V(r)$ is, in fact, Coulombic. We thus repeat the fit, but this time with $V(r) = A + C/r$. Again over the observed range of couplings we have good fits with $\chi^2/DoF$ again less than unity, now for two degrees of freedom. Fig. 5-9 shows the coefficient of the Coulomb term as a function of the 't Hooft coupling. It is remarkably linear. The naive expectation of perturbation theory (one gauge boson exchange) is
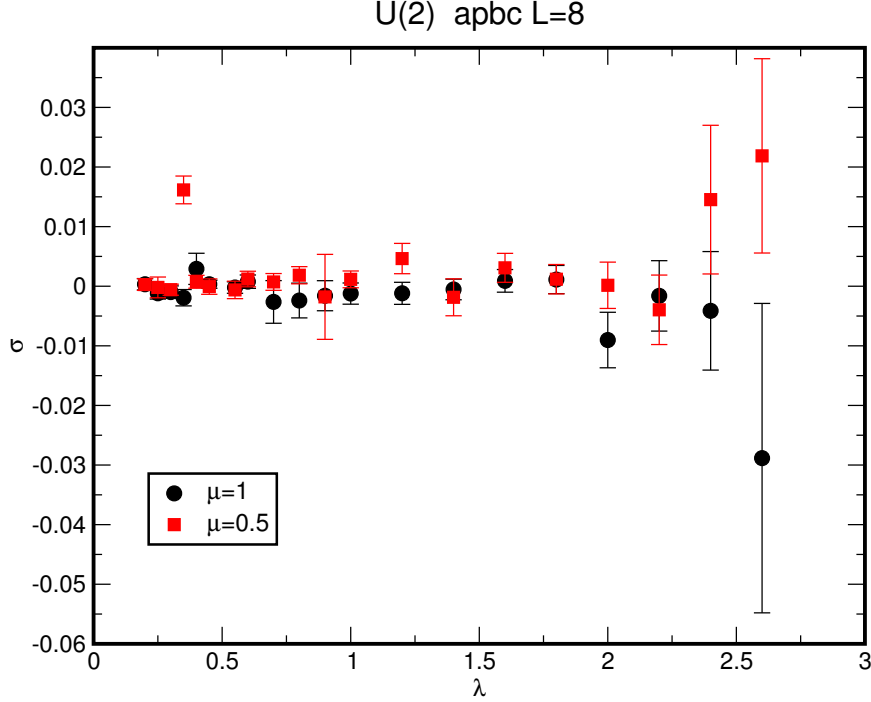
$$C = \frac{g^2 N}{4\pi} \quad . \qquad (5.39)$$

115
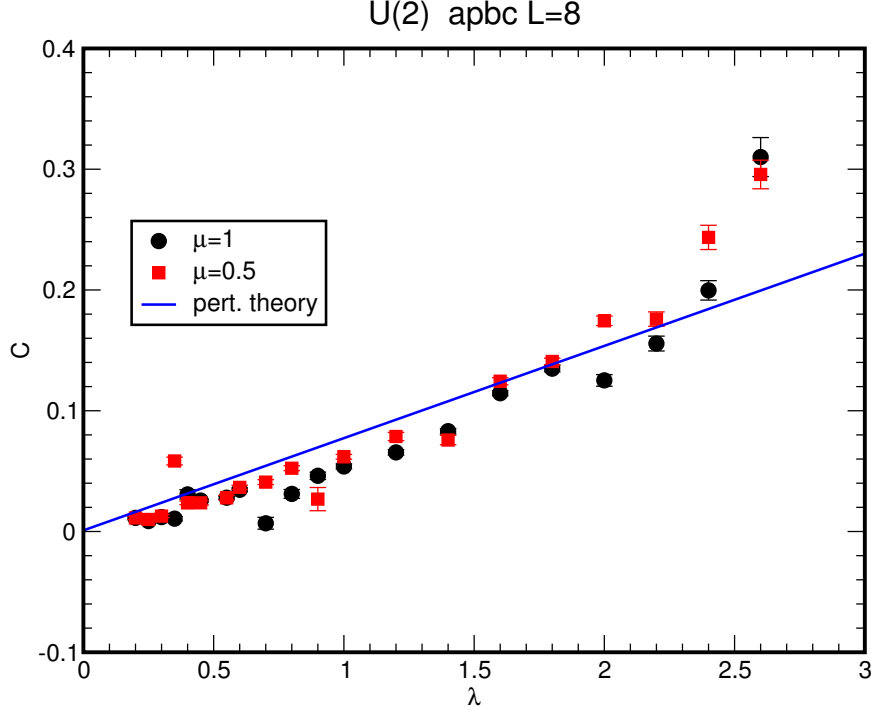
Figure 5-9: Coulomb coefficient from Wilson loops with $t = 3$ and 4 from $8^4$ data sets. Circles are $\mu_L = 1.0$; diamonds, $\mu_L = 0.5$.

This seems to describe the data well, and suggests that the strong coupling regime is above $\lambda \geq 2.5$.

Thus the Wilson loop analysis lends support to the hypothesis of a single phase structure with vanishing string tension for all bare couplings $\lambda$.

## 5.3.5   Fermion eigenvalues and chiral symmetry breaking

If the system is really conformal for all gauge couplings then it should not support a chiral condensate. To understand this better we have studied the spectrum of the twisted fermion operator on a small lattice. Fig. 5-10 shows a scatter plot of the fermion eigenvalues coming from a run with $\lambda = 0.8$ and $\mu_L = 1$ on a small $L = 3$ lattice. The most obvious feature is that *no* eigenvalues are found close to the origin. This is a robust statement; at all couplings $\lambda$ a gap appears in the spectrum independent of $\mu_L$. This, by virtue of the Banks-Casher theorem, means that chiral symmetry is not spontaneously broken in this lattice theory.
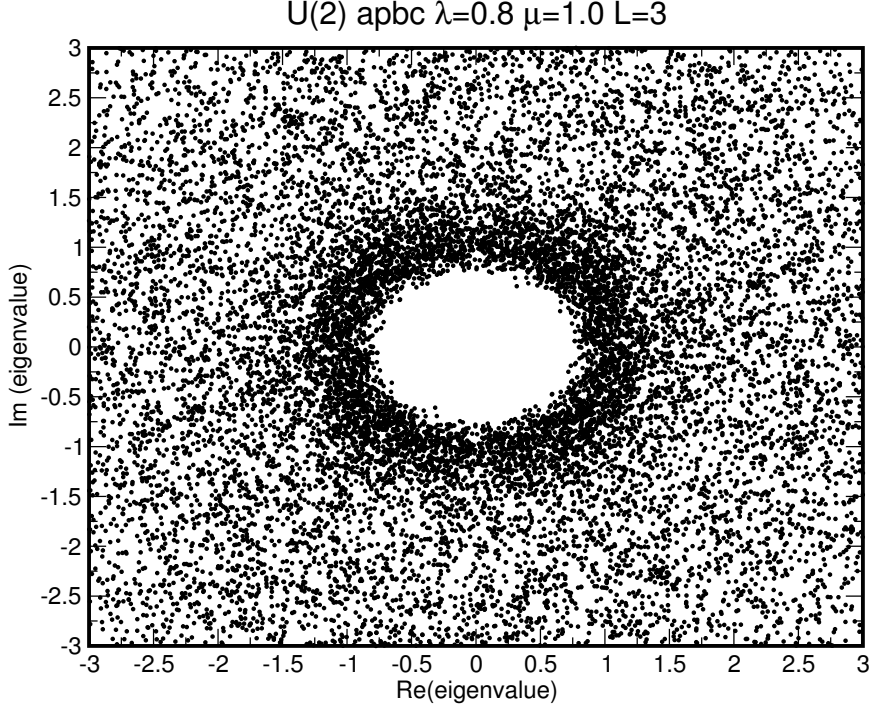
Figure 5-10: Fermion eigenvalues obtained from a Monte Carlo ensemble at $\lambda = 0.8$, $\mu_L = 1$ and $L = 3$.

We have also measured the Pfaffian on this small lattice as an explicit check that of possible sign problems. Fig. 5-11 shows the expectation value of both the cosine and sine of the Pfaffian phase as a function of $\lambda$. Rather reassuringly we see that the fluctuations in $\alpha$ are relatively small which provides a concrete numerical justification of the use the phase quenched approximation in our calculations independent of the measurement of the bosonic action or analytic arguments based on the topological character of the lattice partition function.

## 5.3.6    The continuum limit

Finally, we should address the issue of a continuum limit. If indeed this theory is conformal at all values of the bare coupling, the beta function vanishes to all orders in lattice perturbation theory, just as in the continuum[7]. If correct, this means that the notion of a "bare" gauge coupling takes on a new meaning: a renormalization

---

[7]In [125] this is shown to be true at one loop
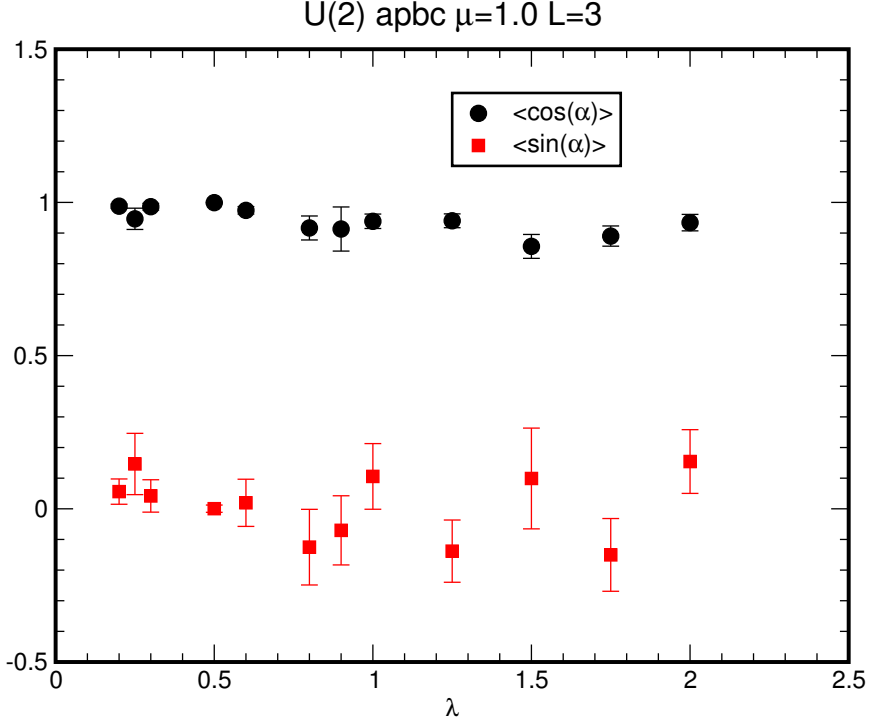
Figure 5-11:  $\cos\alpha$ and $\sin\alpha$ vs $\lambda$ for $\mu_L = 1, L = 3$.

group flow is not induced by changing the lattice spacing. Instead, the continuum limit can be reached anywhere on the real positive bare $g^2$-axis. What about lattice spacing artifacts? The simple way to eliminate these ultraviolet effects is to go to large distances (volume). In this sense, detailed simulations of this theory will be highly unusual, much like the classical solution of differential equations by means of finite differences. This of course will not mean that the theory is free: there will be anomalous dimensions and logarithmic behavior beyond classical scaling.

Perhaps it is useful to contrast this situation with ones which are more familiar to the lattice practitioner. Begin with a pure non-Abelian gauge theory, defined with an ultraviolet cutoff, the lattice spacing $a$. It possesses a Gaussian fixed point at $g^2 = 0$ which is marginally relevant or unstable under flows towards the infrared. To take the continuum limit, one must tune the bare coupling to zero. In that limit, correlation lengths $\xi$ (inverse masses of bound states) become large compared to $a$. These theories are confining, have a mass gap, and correlation functions always decay exponentially with distance. One can observe the approach to the continuum limit

in the value of dimensionless ratios of dimensionful quantities (such as mass ratios). Any lattice discretization of such a system will possess additional irrelevant operators. They will affect the spectrum, and hence the mass ratios. However, these additional irrelevant operators automatically cease to affect observables as the bare coupling is taken arbitrarily close to the Gaussian fixed point. Because these theories have a mass gap, a finite simulation volume (length $L$) typically affects observables by an amount proportional to $\exp(-mL)$ where $m$ is some characteristic mass.

Next, consider theories of fermions and gauge bosons "inside the conformal window", where the gauge coupling flows to an infrared fixed point under blocking transformations which remove ultraviolet degrees of freedom. For such theories, the fermion mass is a relevant perturbation and it must be tuned to zero by hand in order that the system approach this fixed point. In the massless limit, and in infinite volume, all correlation functions are power-law and the interesting physical parameters are the critical exponents. The distance of the gauge coupling $g$ from its fixed point value $g_c$ is an irrelevant coupling and the difference $|g - g_c|$ governs power law corrections to scaling, whose size is not universal. These effects – as well as those of all irrelevant operators – die away as the correlation length $\xi$ becomes much greater than the cutoff $a$. Besides the mass, a finite system size (technically, $1/L$) is also a relevant parameter because it converts the power-law fall-off of correlation functions into an exponential fall-off. A combination of simulations done at small but non-zero values of the relevant parameter (here the fermion mass) and finite simulation volume (finite size scaling) can, in principle, elucidate the properties of the system.

A theory with a totally vanishing beta function for all bare couplings is one step further. Let us assume that this is the case for the theory under study here. This means that when all relevant couplings in the lattice model – presumably a subset of them are $\mu_L$ and $1/L$ – are tuned to their fixed point values, the system will again exhibit algebraic decay of correlation functions at large distance. This time, the appropriate exponents will be functions of the bare 't Hooft coupling $\lambda$.

119

## 5.4 Conclusions

Numerical simulations of the phase-quenched $\mathcal{N} = 4$ supersymmetric Yang-Mills theory in four dimensions were performed. In particular, we have examined standard physical observables such as Wilson loops, Polyakov lines and the bosonic action. We have found no evidence for phase transitions as the bare gauge coupling is varied. Furthermore, the effective string tension is consistent with zero for all bare couplings at the largest distances probed. Indeed we see evidence for Coulomb-like behavior in the static quark potential and a gap opens up in the spectrum of the fermion operator indicating the absence of chiral symmetry breaking. Furthermore, the expectation value of the bosonic action appears to be independent of the gauge coupling as the regulator mass $\mu_L$ is sent to zero and it equals the value expected on the basis of exact supersymmetry. This gives indirect evidence that the sign problem is indeed absent in this lattice theory, and that for all practical purposes the phase of the Pfaffian can be ignored in actual simulations.

With this first study we have provided ample evidence that it is feasible to study this supersymmetric lattice gauge theory by numerical means. The effects of phase quenching, a bosonic mass term to stabilize the flat directions, and anti-periodic boundary conditions for the fermions, can all be carefully monitored by means of supersymmetric Ward Identities that are exact in the lattice-regularized theory. The apparent existence of a single deconfined phase with vanishing string tension at all bare couplings indicates that this theory is conformal at any coupling, as is the continuum theory with all the remaining supercharges being conserved. Apparently the exact conservation of one supersymmetric charge is extremely powerful; in particular, it ensures a perfect match between bosonic and fermionic degrees of freedom in the multiplet. We hope this work may stimulate renewed numerical efforts in the same direction: the lattice offers direct access to the computation of observables in the most interesting supersymmetric gauge theory in four dimensions. It can probe both weak and strong coupling, and comparisons can be made to predictions from the continuum based on gauge-gravity duality.

Our results presented here are of course only a beginning and should be confirmed by future studies on bigger systems and at stronger coupling. The evaluation of non-trivial correlation functions should be initiated. A study of the broken Ward Identities associated with supercharges that are not exactly conserved on the lattice should made. This will give direct evidence for how full supersymmetry is recovered in the continuum limit. There is obviously much exciting work ahead.

# Bibliography

[1] A. H. Guth, "The Inflationary Universe: A Possible Solution to the Horizon and Flatness Problems," Phys. Rev. D **23**, 347 (1981).

[2] D. Baumann *et al.* [CMBPol Study Team Collaboration], "CMBPol Mission Concept Study: Probing Inflation with CMB Polarization," AIP Conf. Proc. **1141**, 10 (2009) [arXiv:0811.3919 [astro-ph]].

[3] R. Easther, R. Galvez, O. Ozsoy and S. Watson, "Supersymmetry, Nonthermal Dark Matter and Precision Cosmology," arXiv:1307.2453 [hep-ph].

[4] L. Kofman, A. D. Linde and A. A. Starobinsky, "Towards the theory of reheating after inflation," Phys. Rev. D **56**, 3258 (1997) [hep-ph/9704452].

[5] M. Dine, L. Randall and S. D. Thomas, "Baryogenesis from flat directions of the supersymmetric standard model," Nucl. Phys. B **458**, 291 (1996) [hep-ph/9507453].

[6] S. Mollerach, "Isocurvature Baryon Perturbations and Inflation," Phys. Rev. D **42**, 313 (1990).

[7] S. R. Coleman, "Q Balls," Nucl. Phys. B **262**, 263 (1985) [Erratum-ibid. B **269**, 744 (1986)].

[8] E. J. Chun and S. Scopel, "Quintessential Kination and Leptogenesis," JCAP **0710**, 011 (2007) [arXiv:0707.1544 [astro-ph]].

[9] C. P. Burgess, "Lectures on Cosmic Inflation and its Potential Stringy Realizations," Class. Quant. Grav. **24**, S795 (2007) [PoS P **2GC**, 008 (2006)] [PoS CARGESE **2007**, 003 (2007)] [arXiv:0708.2865 [hep-th]].

[10] D. H. Lyth and E. D. Stewart, "Thermal inflation and the moduli problem," Phys. Rev. D **53**, 1784 (1996) [hep-ph/9510204].

[11] A. L. Erickcek and K. Sigurdson, "Reheating Effects in the Matter Power Spectrum and Implications for Substructure," Phys. Rev. D **84**, 083503 (2011) [arXiv:1106.0536 [astro-ph.CO]].

[12] M. Lemoine, J. Martin and J. 'i. Yokoyama, "Constraints on moduli cosmology from the production of dark matter and baryon isocurvature fluctuations," Phys. Rev. D **80**, 123514 (2009) [arXiv:0904.0126 [astro-ph.CO]].

[13] A. RLiddle and S. MLeach, "How long before the end of inflation were observable perturbations produced?," Phys. Rev. D **68**, 103503 (2003) [astro-ph/0305263].

[14] S. Dodelson and L. Hui, "A Horizon ratio bound for inflationary fluctuations," Phys. Rev. Lett. **91**, 131301 (2003) [astro-ph/0305113].

[15] L. Alabidi and D. H. Lyth, "Inflation models and observation," JCAP **0605**, 016 (2006) [astro-ph/0510441].

[16] P. Adshead, R. Easther, J. Pritchard and A. Loeb, "Inflation and the Scale Dependent Spectral Index: Prospects and Strategies," JCAP **1102**, 021 (2011) [arXiv:1007.3748 [astro-ph.CO]].

[17] P. Binetruy, "Supersymmetry: Theory, experiment and cosmology," Oxford, UK: Oxford Univ. Pr. (2006) 520 p

[18] I. L. Buchbinder and S. M. Kuzenko, "Ideas and methods of supersymmetry and supergravity: Or a walk through superspace," *Bristol, UK: IOP (1998) 656 p*

[19] S. Catterall, D. B. Kaplan, M. Unsal, "Exact lattice supersymmetry," Phys. Rept. **484**, 71-130 (2009). [arXiv:0903.4881 [hep-lat]].

[20] J. M. Maldacena, "The large N limit of superconformal field theories and supergravity," Adv. Theor. Math. Phys. **2**, 231 (1998) [Int. J. Theor. Phys. **38**, 1113 (1999)] [arXiv:hep-th/9711200].

[21] S. R. Coleman and J. Mandula, "ALL POSSIBLE SYMMETRIES OF THE S MATRIX," Phys. Rev. **159**, 1251 (1967).

[22] R. Haag, J. T. Lopuszanski and M. Sohnius, "All Possible Generators Of Supersymmetries Of The S Matrix," Nucl. Phys. B **88**, 257 (1975).

[23] E. Witten, "Topological Quantum Field Theory," Commun. Math. Phys. **117**, 353 (1988).

[24] S. Catterall, "A geometrical approach to N = 2 super Yang-Mills theory on the two dimensional lattice," JHEP **0411**, 006 (2004) [arXiv:hep-lat/0410052].

[25] N. Marcus, "The Other topological twisting of N=4 Yang-Mills," Nucl. Phys. B **452**, 331 (1995) [arXiv:hep-th/9506002].

[26] D. Baumann and L. McAllister, "Inflation and String Theory," arXiv:1404.2601 [hep-th].

[27] S. Kachru, R. Kallosh, A. D. Linde and S. P. Trivedi, "De Sitter vacua in string theory," Phys. Rev. D **68**, 046005 (2003) [hep-th/0301240].

[28] B. Dutta and K. Sinha, "Holomorphic Bisectional Curvatures, Supersymmetry Breaking, and Affleck-Dine Baryogenesis," Phys. Rev. D **86**, 103517 (2012) [arXiv:1205.6267 [hep-th]].

[29] L. Covi, M. Gomez-Reino, C. Gross, J. Louis, G. A. Palma and C. A. Scrucca, "Constraints on modular inflation in supergravity and string theory," JHEP **0808**, 055 (2008) [arXiv:0805.3290 [hep-th]].

[30] C. P. Burgess, J. M. Cline, H. Stoica and F. Quevedo, "Inflation in realistic D-brane models," JHEP **0409**, 033 (2004) [hep-th/0403119].

[31] J. P. Conlon, "Moduli Stabilisation and Applications in IIB String Theory," Fortsch. Phys. **55**, 287 (2007) [hep-th/0611039].

[32] S. Kachru, R. Kallosh, A. D. Linde, J. M. Maldacena, L. P. McAllister and S. P. Trivedi, "Towards inflation in string theory," JCAP **0310**, 013 (2003) [hep-th/0308055].

[33] R. Kallosh, A. Linde and T. Rube, "General inflaton potentials in supergravity," Phys. Rev. D **83**, 043507 (2011) [arXiv:1011.5945 [hep-th]].

[34] C. Long, L. McAllister and P. McGuirk, "Heavy Tails in Calabi-Yau Moduli Spaces," JHEP **1410**, 187 (2014) [arXiv:1407.0709 [hep-th]].

[35] M. Kreuzer and H. Skarke, "Complete classification of reflexive polyhedra in four-dimensions," Adv. Theor. Math. Phys. **4**, 1209 (2002) [hep-th/0002240].

[36] K. Becker, M. Becker, M. Haack and J. Louis, "Supersymmetry breaking and alpha-prime corrections to flux induced potentials," JHEP **0206**, 060 (2002) [hep-th/0204254].

[37] M. J. Mortonson, H. V. Peiris and R. Easther, "Bayesian Analysis of Inflation: Parameter Estimation for Single Field Models," Phys. Rev. D **83**, 043505 (2011) [arXiv:1007.4205 [astro-ph.CO]].

[38] R. Easther and H. V. Peiris, "Bayesian Analysis of Inflation II: Model Selection and Constraints on Reheating," Phys. Rev. D **85**, 103533 (2012) [arXiv:1112.0326 [astro-ph.CO]].

[39] J. Norena, C. Wagner, L. Verde, H. V. Peiris and R. Easther, "Bayesian Analysis of Inflation III: Slow Roll Reconstruction Using Model Selection," Phys. Rev. D **86**, 023505 (2012) [arXiv:1202.0304 [astro-ph.CO]].

[40] William H. Kinney and Antonio Riotto. Theoretical uncertainties in inflationary predictions. *JCAP*, 0603:011, 2006.

[41] Hiranya V. Peiris and Richard Easther. Primordial Black Holes, Eternal Inflation, and the Inflationary Parameter Space after WMAP5. *JCAP*, 0807:024, 2008.

[42] Jerome Martin and Christophe Ringeval. First CMB Constraints on the Inflationary Reheating Temperature. *Phys.Rev.*, D82:023511, 2010.

[43] Jerome Martin and Christophe Ringeval. Inflation after WMAP3: Confronting the Slow-Roll and Exact Power Spectra to CMB Data. *JCAP*, 0608:009, 2006.

[44] Gianfranco Bertone, Dan Hooper, and Joseph Silk. Particle dark matter: Evidence, candidates and constraints. *Phys.Rept.*, 405:279–390, 2005.

[45] Daniel J.H. Chung, Edward W. Kolb, and Antonio Riotto. Production of massive particles during reheating. *Phys.Rev.*, D60:063504, 1999.

[46] N. Fornengo, A. Riotto, and S. Scopel. Supersymmetric dark matter and the reheating temperature of the universe. *Phys.Rev.*, D67:023514, 2003.

[47] C. Pallis. Massive particle decay and cold dark matter abundance. *Astropart.Phys.*, 21:689–702, 2004.

[48] Graciela B. Gelmini and Paolo Gondolo. Neutralino with the right cold dark matter abundance in (almost) any supersymmetric model. *Phys.Rev.*, D74:023510, 2006.

[49] Graciela Gelmini, Paolo Gondolo, Adrian Soldatenko, and Carlos E. Yaguna. The Effect of a late decaying scalar on the neutralino relic density. *Phys.Rev.*, D74:083514, 2006.

[50] Scott Watson. Reevaluating the Cosmological Origin of Dark Matter. In Gordon L Kane, editor, *Perspectives on supersymmetry II*, pages 305–324. World Scientific, Singapore, 2009.

[51] Rouzbeh Allahverdi, Bhaskar Dutta, Rabindra N. Mohapatra, and Kuver Sinha. A Supersymmetric Model for Dark Matter and Baryogenesis Motivated by the Recent CDMS Result. 2013.

[52] C. Kelso, S. Profumo and F. S. Queiroz, "Non-thermal WIMPs as "Dark Radiation" in Light of ATACAMA, SPT, WMAP9 and Planck," Phys. Rev. D **88**, 023511 (2013) arXiv:1304.5243 [hep-ph].

[53] D. Hooper, F. S. Queiroz and N. Y. Gnedin, "Non-Thermal Dark Matter Mimicking An Additional Neutrino Species In The Early Universe," Phys. Rev. D **85**, 063513 (2012) arXiv:1111.6599 [astro-ph.CO].

[54] Graciela B. Gelmini and Paolo Gondolo. Ultra-cold WIMPs: relics of non-standard pre-BBN cosmologies. *JCAP*, 0810:002, 2008.

[55] Phill Grajek, Gordon Kane, Dan Phalen, Aaron Pierce, and Scott Watson. Is the PAMELA Positron Excess Winos? *Phys.Rev.*, D79:043506, 2009.

[56] Phill Grajek, Gordon Kane, Daniel J. Phalen, Aaron Pierce, and Scott Watson. Neutralino Dark Matter from Indirect Detection Revisited. 2008.

[57] Bhaskar Dutta, Louis Leblond, and Kuver Sinha. Mirage in the Sky: Non-thermal Dark Matter, Gravitino Problem, and Cosmic Ray Anomalies. *Phys.Rev.*, D80:035014, 2009.

[58] Gordon Kane, Ran Lu, and Scott Watson. PAMELA Satellite Data as a Signal of Non-Thermal Wino LSP Dark Matter. *Phys.Lett.*, B681:151–160, 2009.

[59] Pearl Sandick and Scott Watson. Constraints on a Non-thermal History from Galactic Dark Matter Spikes. *Phys.Rev.*, D84:023507, 2011.

[60] Jonathan L. Feng, Philipp Kant, Stefano Profumo, and David Sanford. 3-Loop Corrections to the Higgs Boson Mass and Implications for Supersymmetry at the LHC. 2013.

[61] Michael R. Douglas. The String landscape and low energy supersymmetry. 2012.

[62] Nima Arkani-Hamed, Arpit Gupta, David E. Kaplan, Neal Weiner, and Tom Zorawski. Simply Unnatural Supersymmetry. 2012.

[63] Takeo Moroi and Lisa Randall. Wino cold dark matter from anomaly mediated SUSY breaking. *Nucl.Phys.*, B570:455–472, 2000.

[64] Bobby Samir Acharya, Gordon Kane, Scott Watson, and Piyush Kumar. A Non-thermal WIMP Miracle. *Phys.Rev.*, D80:083529, 2009.

[65] B. Acharya, P. Kumar, K. Bobkov, G. Kane, J. Shao, and S. Watson. Non-thermal Dark Matter and the Moduli Problem in String Frameworks. *JHEP*, 0806:064, 2008.

[66] Emilian Dudas, Andrei Linde, Yann Mambrini, Azar Mustafayev, and Keith A. Olive. Strong moduli stabilization and phenomenology. 2012.

[67] Jason L. Evans, Masahiro Ibe, Keith A. Olive, and Tsutomu T. Yanagida. Universality in Pure Gravity Mediation. 2013.

[68] Mark B. Hoffman and Michael S. Turner. Kinematic constraints to the key inflationary observables. *Phys.Rev.*, D64:023506, 2001.

[69] Dominik J. Schwarz, Cesar A. Terrero-Escalante, and Alberto A. Garcia. Higher order corrections to primordial spectra from cosmological inflation. *Phys.Lett.*, B517:243–249, 2001.

[70] William H. Kinney. Inflation: Flow, fixed points and observables to arbitrary order in slow roll. *Phys.Rev.*, D66:083508, 2002.

[71] P.A.R. Ade et al. Planck 2013 results. XXII. Constraints on inflation. 2013.

[72] Edward W. Kolb and Michael S. Turner. The Early universe. *Front.Phys.*, 69:1–547, 1990.

[73] J. Beringer et al. Review of Particle Physics (RPP). *Phys.Rev.*, D86:010001, 2012.

[74] Howard Baer, Vernon Barger, and Azar Mustafayev. Implications of a 125 GeV Higgs scalar for LHC SUSY and neutralino dark matter searches. *Phys.Rev.*, D85:075010, 2012.

[75] G.D. Coughlan, W. Fischler, Edward W. Kolb, S. Raby, and Graham G. Ross. Cosmological Problems for the Polonyi Potential. *Phys.Lett.*, B131:59, 1983.

[76] B. de Carlos, J.A. Casas, F. Quevedo, and E. Roulet. Model independent properties and cosmological implications of the dilaton and moduli sectors of 4-d strings. *Phys.Lett.*, B318:447–456, 1993.

[77] Tom Banks, David B. Kaplan, and Ann E. Nelson. Cosmological implications of dynamical supersymmetry breaking. *Phys.Rev.*, D49:779–787, 1994.

[78] Michael S. Turner. Coherent Scalar Field Oscillations in an Expanding Universe. *Phys.Rev.*, D28:1243, 1983.

[79] Steen Hannestad. What is the lowest possible reheating temperature? *Phys.Rev.*, D70:043506, 2004.

[80] M. Kawasaki, Kazunori Kohri, and Naoshi Sugiyama. MeV scale reheating temperature and thermalization of neutrino background. *Phys.Rev.*, D62:023506, 2000.

[81] M. Kawasaki, Kazunori Kohri, and Naoshi Sugiyama. Cosmological constraints on late time entropy production. *Phys.Rev.Lett.*, 82:4168, 1999.

[82] Francesco De Bernardis, Luca Pagano, and Alessandro Melchiorri. New constraints on the reheating temperature of the universe after WMAP-5. *Astropart.Phys.*, 30:192–195, 2008.

[83] Oscar Loaiza-Brito, Johannes Martin, Hans Peter Nilles, and Michael Ratz. Log(M(Pl) / m(3/2)). *AIP Conf.Proc.*, 805:198–204, 2006.

[84] Gerard Jungman, Marc Kamionkowski, and Kim Griest. Supersymmetric dark matter. *Phys.Rept.*, 267:195–373, 1996.

[85] M. Ackermann et al. Constraining Dark Matter Models from a Combined Analysis of Milky Way Satellites with the Fermi Large Area Telescope. *Phys.Rev.Lett.*, 107:241302, 2011.

[86] DarkSUSY Team. DarkSUSY: Computing supersymmetric dark matter properties numerically. *JCAP*, 0407:008, 2004.

[87] N. Arkani-Hamed, A. Delgado, and G.F. Giudice. The Well-tempered neutralino. *Nucl.Phys.*, B741:108–130, 2006.

[88] Takeo Moroi, Minoru Nagai, and Masahiro Takimoto. Non-Thermal Production of Wino Dark Matter via the Decay of Long-Lived Particles. 2013.

[89] Gordon Kane, Ran Lu, and Scott Watson. PAMELA satellite data as a signal of non-thermal wino LSP dark matter. *Nucl.Instrum.Meth.*, A630:82–86, 2011.

[90] Daniel Feldman and Pearl Sandick. Well-Mixed Dark Matter and the Higgs. 2013.

[91] Clifford Cheung, Lawrence J. Hall, David Pinner, and Joshua T. Ruderman. Prospects and Blind Spots for Neutralino Dark Matter. 2012.

[92] Search for direct production of charginos and neutralinos in events with three leptons and missing transverse momentum in 13.0 fb-1 of pp collisions at sqrt(s)=8 TeV with the ATLAS detector. 2012.

[93] Serguei Chatrchyan et al. Search for electroweak production of charginos and neutralinos using leptonic final states in *pp* collisions at $\sqrt{s} = 7$ TeV. *JHEP*, 1211:147, 2012.

[94] E. Aprile et al. Dark Matter Results from 225 Live Days of XENON100 Data. *Phys.Rev.Lett.*, 109:181301, 2012.

[95] Paolo Beltrame. Direct Dark Matter search with the XENON program. 2013.

[96] Dan Hooper, Chris Kelso, Pearl Sandick, and Wei Xue. Closing Supersymmetric Resonance Regions With Direct Detection Experiments. 2013.

[97] Richard Easther, Raphael Flauger, and James B. Gilmore. Delayed Reheating and the Breakdown of Coherent Oscillations. *JCAP*, 1104:027, 2011.

[98] J. Fan and M. Reece, In Wino Veritas? Indirect Searches Shed Light on Neutralino Dark Matter. arXiv:1307.4400 [hep-ph].

[99] A. Abramowski et al. Search for a Dark Matter annihilation signal from the Galactic Center halo with H.E.S.S. *Phys.Rev.Lett.*, 106:161301, 2011.

[100] D. B. Kaplan, "Recent developments in lattice supersymmetry," Nucl. Phys. Proc. Suppl. **129**, 109 (2004) [arXiv:hep-lat/0309099].

[101] J. Giedt, "Deconstruction and other approaches to supersymmetric lattice field theories," Int. J. Mod. Phys. A **21**, 3039 (2006) [arXiv:hep-lat/0602007].

[102] A. Joseph, "Supersymmetric Yang–Mills theories with exact supersymmetry on the lattice," Int. J. Mod. Phys. A **26**, 5057 (2011) arXiv:1110.5983 [hep-lat].

[103] F. Sugino, "A Lattice formulation of superYang-Mills theories with exact supersymmetry," JHEP **0401** (2004) 015. [hep-lat/0311021].

[104] F. Sugino, "SuperYang-Mills theories on the two-dimensional lattice with exact supersymmetry," JHEP **0403** (2004) 067. [hep-lat/0401017].

[105] A. D'Adda, I. Kanamori, N. Kawamoto and K. Nagata, "Exact extended supersymmetry on a lattice: Twisted N=2 super Yang-Mills in two dimensions," Phys. Lett. B **633**, 645 (2006) [hep-lat/0507029].

[106] A. D'Adda, I. Kanamori, N. Kawamoto and K. Nagata, "Exact Extended Supersymmetry on a Lattice: Twisted N=4 Super Yang-Mills in Three Dimensions," Nucl. Phys. B **798**, 168 (2008) [arXiv:0707.3533 [hep-lat]].

[107] I. Kanamori, H. Suzuki, "Restoration of supersymmetry on the lattice: Two-dimensional N = (2,2) supersymmetric Yang-Mills theory," Nucl. Phys. **B811** (2009) 420-437. [arXiv:0809.2856 [hep-lat]].

[108] M. Hanada, I. Kanamori, "Lattice study of two-dimensional N=(2,2) super Yang-Mills at large-N," Phys. Rev. **D80** (2009) 065014. [arXiv:0907.4966 [hep-lat]].

[109] M. Hanada, S. Matsuura, F. Sugino, "Two-dimensional lattice for four-dimensional N=4 supersymmetric Yang-Mills," [arXiv:1004.5513 [hep-lat]].

[110] M. Hanada, "A proposal of a fine tuning free formulation of 4d N = 4 super Yang-Mills," JHEP **1011** (2010) 112. [arXiv:1009.0901 [hep-lat]].

[111] M. Hanada, S. Matsuura, F. Sugino, "Non-perturbative construction of 2D and 4D supersymmetric Yang-Mills theories with 8 supercharges," [arXiv:1109.6807 [hep-lat]].

[112] J.E. Hirsch, "Two-dimensional Hubbard model: Numerical simulation study," Phys. Rev. **B31**, 4403 (1985).

[113] J. Giedt, "Nonpositive fermion determinants in lattice supersymmetry," Nucl. Phys. **B668**, 138-150 (2003). [hep-lat/0304006].

[114] M. Hanada, I. Kanamori, "Absence of sign problem in two-dimensional N = (2,2) super Yang–Mills on lattice," JHEP **1101**, 058 (2011). arXiv:1010.2948 [hep-lat].

[115] S. Catterall, "First results from simulations of supersymmetric lattices," JHEP **0901**, 040 (2009) [arXiv:0811.1203 [hep-lat]].

[116] M. Unsal, "Twisted supersymmetric gauge theories and orbifold lattices," JHEP **0610**, 089 (2006). [hep-th/0603046].

[117] S. Catterall, "From Twisted Supersymmetry to Orbifold Lattices," JHEP **0801**, 048 (2008). [arXiv:0712.2532 [hep-th]].

[118] P. H. Damgaard and S. Matsuura, "Relations among Supersymmetric Lattice Gauge Theories via Orbifolding," JHEP **0708**, 087 (2007) [arXiv:0706.3007 [hep-lat]].

[119] S. Elitzur, E. Rabinovici, A. Schwimmer, "Supersymmetric Models On The Lattice," Phys. Lett. **B119**, 165 (1982).

[120] J. M. Rabin, "Homology Theory Of Lattice Fermion Doubling," Nucl. Phys. **B201**, 315 (1982).

[121] P. Becher, H. Joos, "The Dirac-Kahler Equation and Fermions on the Lattice," Z. Phys. **C15**, 343 (1982).

[122] H. Aratyn, M. Goto, A. H. Zimerman, "A Lattice Gauge Theory For Fields In The Adjoint Representation," Nuovo Cim. **A84**, 255 (1984).

[123] T. Banks, Y. Dothan, D. Horn, "Geometric Fermions," Phys. Lett. **B117**, 413 (1982).

[124] A. Kapustin, E. Witten, "Electric-Magnetic Duality And The Geometric Langlands Program,"

[hep-th/0604151].

[125] S. Catterall, E. Dzienkowski, J. Giedt, A. Joseph, R. Wells, "Perturbative renormalization of lattice N=4 super Yang-Mills theory," JHEP **1104**, 074 (2011). arXiv:1102.1725 [hep-th].

[126] S. Catterall, A. Joseph, "An object oriented code for simulating supersymmetric Yang–Mills theories," arXiv:1108.1503 [hep-lat].

[127] D. Mehta, "Lattice vs. Continuum: Landau Gauge Fixing and 't Hooft-Polyakov Monopoles," Ph.D. Thesis, "The University of Adelaide, Australasian Digital Theses Program, Adelaide, Australia, 2009; L. von Smekal, D. Mehta, A. Sternbeck and A. G. Williams, "Modified Lattice Landau Gauge," PoSLAT **2007** (2007) 382 [arXiv:0710.2410 [hep-lat]]; L. von Smekal, A. Jorkowski, D. Mehta and A. Sternbeck, "Lattice Landau gauge via Stereographic Projection," PoSCONFINEMENT **8** (2008) 048 [arXiv:0812.2992 [hep-th]].

[128] H. Neuberger, "Nonperturbative Brs Invariance," Phys. Lett. B **175** (1986) 69; H. Neuberger, "Nonperturbative Brs Invariance And The Gribov Problem," Phys. Lett. B **183** (1987) 337.

[129] D. Mehta, A. Sternbeck, L. von Smekal and A. G. Williams, "Lattice Landau Gauge and Algebraic Geometry," PoSQCD **-TNT09** (2009) 025 [arXiv:0912.0450 [hep-lat]]; D. Mehta and M. Kastner, "Stationary point analysis of the one-dimensional lattice Landau gauge fixing functional, aka random phase XY Hamiltonian," Annals Phys. **326** (2011) 1425 [arXiv:1010.5335 [cond-mat.stat-mech]]; L. von Smekal, "Landau Gauge QCD: Functional Methods versus Lattice Simulations," arXiv:0812.0654 [hep-th].

[130] D. Mehta, S. Catterall, R. Galvez, A. Joseph, "Investigating the sign problem for two-dimensional $\mathcal{N} = (2, 2)$ and $\mathcal{N} = (8, 8)$ lattice super Yang–Mills theories,"

Talk presented at Lattice 2011; D. Mehta, S. Catterall, R. Galvez, A. Joseph, To appear.

[131] R. Galvez and G. van Anders, "Accelerating the solution of families of shifted linear systems with CUDA," arXiv:1102.2143 [hep-lat].

[132] T. Takimi, "Relationship between various supersymmetric lattice models," JHEP **0707**, 010 (2007) [arXiv:0705.3831 [hep-lat]].

[133] A. G. Cohen, D. B. Kaplan, E. Katz and M. Unsal, "Supersymmetry on a Euclidean space-time lattice. 1. A Target theory with four supercharges," JHEP **0308**, 024 (2003) [hep-lat/0302017].

[134] A. G. Cohen, D. B. Kaplan, E. Katz and M. Unsal, "Supersymmetry on a Euclidean space-time lattice. 2. Target theories with eight supercharges," JHEP **0312**, 031 (2003) [hep-lat/0307012].

[135] D. B. Kaplan and M. Unsal, "A Euclidean lattice construction of supersymmetric Yang-Mills theories with sixteen supercharges," JHEP **0509**, 042 (2005) [hep-lat/0503039].

[136] P. H. Damgaard and S. Matsuura, "Geometry of Orbifolded Supersymmetric Lattice Gauge Theories," Phys. Lett. B **661** (2008) 52 [arXiv:0801.2936 [hep-th]].
P. Becher, H. Joos, "The Dirac-Kahler Equation and Fermions on the Lattice," Z. Phys. **C15**, 343 (1982).

[137] I. Kanamori, "Lattice formulation of two-dimensional N=(2,2) super Yang-Mills with SU(N) gauge group," JHEP **1207**, 021 (2012) [arXiv:1202.2101 [hep-lat]].

[138] S. Catterall, R. Galvez, A. Joseph and D. Mehta, "On the sign problem in 2D lattice super Yang-Mills," JHEP **1201**, 108 (2012) [arXiv:1112.3588 [hep-lat]].

[139] D. Mehta, S. Catterall, R. Galvez and A. Joseph, "Supersymmetric gauge theories on the lattice: Pfaffian phases and the Neuberger 0/0 problem," PoS LATTICE **2011**, 078 (2011) [arXiv:1112.5413 [hep-lat]].

[140] R. Galvez, S. Catterall, A. Joseph and D. Mehta, "Investigating the sign problem for two-dimensional $\mathcal{N} = (2,2)$ and $\mathcal{N} = (8,8)$ lattice super Yang–Mills theories," PoS LATTICE **2011**, 064 (2011) [arXiv:1201.1924 [hep-lat]].

[141] Dhagash Mehta, "Lattice vs. Continuum: Landau Gauge Fixing and 't Hooft-Polyakov Monopoles," Ph.D. Thesis 2009, The Uni. of Adelaide, Australasian Digital Theses Program.

[142] L. von Smekal, A. Jorkowski, D. Mehta and A. Sternbeck, "Lattice Landau gauge via Stereographic Projection," PoS CONFINEMENT **8**, 048 (2008) [arXiv:0812.2992 [hep-th]].

[143] L. von Smekal, D. Mehta, A. Sternbeck and A. G. Williams, "Modified Lattice Landau Gauge," PoS LAT **2007**, 382 (2007) [arXiv:0710.2410 [hep-lat]].

[144] S. Catterall and A. Joseph, "An Object oriented code for simulating supersymmetric Yang-Mills theories," Comput. Phys. Commun. **183**, 1336 (2012) [arXiv:1108.1503 [hep-lat]].

[145] W. Krauth and M. Staudacher, "Eigenvalue distributions in Yang-Mills integrals," Phys. Lett. B **453**, 253 (1999) [hep-th/9902113].

# Curriculum Vitae: Richard A. Galvez

EDUCATION

Ph.D. Physics, Syracuse University

- Thesis Title: "Topics in Supersymmetry: Implications for Cosmology and Non-Perturbative Studies on a Spacetime Lattice"
- Adviser: Professor Scott Watson
- Area of Study: Physics

M.S. Physics, Florida International University, May 2009

- Thesis Topic: Large-$N$ Quantum Field theory
- Adviser: Professor Rajamani Nayaranan
- Area of Study: Physics

B.S. Physics, Florida International University, June 2007

| HONORS | | |
|---|---|---|
| Harvard Society of Fellows, nominee | | 2015-2017 |
| Data Incubator Data Science Fellowship, finalist | | 2015 |
| Levinstein Fellowship Syracuse University, | | 2014-2015 |
| East Asia and Pacific Summer Institutes, National Science Foundation Fellowship Auckland, NZ | | May 2013- September 20134 |
| Ford Foundation Dissertation Year Fellowship, Alternate/Honorable Mention Syracuse University, | | 2014-2015 |
| AGEP/STEM Graduate Fellowship Syracuse University | | 2009 - 2011, 2013 - 2015 |
| Outstanding Academic Achievement Award Florida International University | | April 2009 |
| Physics Undergraduate Fellowship Florida International University | | 2005-2007 |

CONTRIBUTED TALKS

*"Flexing Our Cosmological Muscles: What are the Bicep Results Telling Us?"*
SACNAS National Conference, Los Angeles, CA                    October 2014

*"Calabi-Yau Inflation in Type IIB String Theory: Insights from the Holomorphic Sectional Curvature."*
DESY Hamburg, Germany                    September 2014
Syracuse University                    August 2014

*"Supersymmetry, Non-Thermal Dark Matter and Precision Cosmology"*

| | |
|---|---|
| CP3-Origins Institute, Denmark | June 2014 |
| Pennsylvania State University, US | March 2014 |

*"Spontaneous Symmetry Breaking of Lorentz Symmetry"*

University of Auckland, NZ — August 2013

*"The Recent Results of the Planck Satellite"*

Onondaga Community College, Syracuse, NY — May 2013

*"Beyond the Standard Model of Particle Physics and Cosmology"*

Florida International University, Miami, FL — August 2012

*"Violating the Null Energy Condition via Symmetry Breaking of a Ghost Condensate in Dilaton Gravity"*

East Coast Gravity Meeting, Syracuse University, NY — May 2012

*"The Twisted Formulation of $\mathcal{N} = 4$ Supersymmetric Gauge Theories."*

George Washington University, Washington, DC — March 2012

*"The Fermionic Sign Problem in 2D and 4D Supersymmetric Gauge Theory."*

High Energy Physics Seminar, Syracuse University, NY — January 2012

*"The Sign Problem in $\mathcal{N} = 2$ and $\mathcal{N} = 4$ Supersymmetric Gauge Theories."*

The XXIX International Symposium on Lattice Field Theory, Lake Tahoe, California — July 2011

*"Center Symmetric Large-N Gauge Theory with Adjoint Fermions."*

The XXVIII International Symposium on Lattice Field Theory. Sardinia, Italy — July 2010

*"Two Dimensional Large N QCD at Finite Density."*

South Eastern Section of APS (SESAPS). Raleigh, North Carolina. — October 2008

| | | |
|---|---|---|
| SUMMER SCHOOLS | Prospects in Theoretical Physics: String Theory | |
| | Institute for Advanced Study, Princeton | 2014 |
| OUTREACH | Panelist for Minority PhD Student Orientation | |
| | Syracuse University | 2012, 2013, 2014 |
| | Science volunteer work | |
| | at Jamesville-Dewitt Junior Highschool | 2013 |
| | at Corcoran High School | 2013 |
| | at Onondaga Community College | 2013 |

UNDERGRADUATE RESEARCH    Large Hadron Collider (LHC) at the European Organization
                          for Nuclear Research (CERN), Geneva, Switzerland          May-July 2007

SELECTED
PUBLICATIONS

1. R. Easther, R. Galvez, O. Ozsoy and S. Watson,
   "Supersymmetry, Nonthermal Dark Matter and Precision Cosmology,"
   Phys. Rev. D **89**, 023522 (2014) [arXiv:1307.2453 [hep-ph]].

2. S. Catterall, P. H. Damgaard, T. Degrand, R. Galvez and D. Mehta,
   "Phase Structure of Lattice N=4 Super Yang-Mills,"
   JHEP **1211**, 072 (2012) [arXiv:1209.5285 [hep-lat]].

3. R. Galvez, S. Catterall, A. Joseph and D. Mehta,
   "Investigating the sign problem for two-dimensional $\mathcal{N} = (2,2)$ and $\mathcal{N} = (8,8)$ lattice super Yang–Mills
   theories," PoS LATTICE **2011**, 064 (2011) [arXiv:1201.1924 [hep-lat]].

4. D. Mehta, S. Catterall, R. Galvez and A. Joseph,
   "Supersymmetric gauge theories on the lattice: Pfaffian phases and the Neuberger 0/0 problem,"
   PoS LATTICE **2011**, 078 (2011) [arXiv:1112.5413 [hep-lat]].

5. S. Catterall, R. Galvez, A. Joseph and D. Mehta,
   "On the sign problem in 2D lattice super Yang-Mills,"
   JHEP **1201**, 108 (2012) [arXiv:1112.3588 [hep-lat]].

6. S. Catterall, R. Galvez, J. Hubisz, D. Mehta and A. Veernala,
   "Non-abelian gauged NJL models on the lattice,"
   Phys. Rev. D **86**, 034502 (2012) [arXiv:1112.1855 [hep-lat]].

7. R. Galvez and S. Catterall,
   "Center symmetry restoration with 2 flavor large N Yang-Mills in the adjoint representation,"
   PoS LATTICE **2010**, 050 (2010).

8. R. Galvez and G. van Anders,
   "Accelerating the solution of families of shifted linear systems with CUDA,"
   arXiv:1102.2143 [hep-lat].

9. S. Catterall, R. Galvez and M. Unsal,
   "Realization of Center Symmetry in Two Adjoint Flavor Large-N Yang-Mills,"
   JHEP **1008**, 010 (2010) [arXiv:1006.2469 [hep-lat]].

10. R. Galvez, A. Hietanen and R. Narayanan,
    "Large N QCD in two dimensions with a baryonic chemical potential,"
    Phys. Lett. B **672**, 376 (2009) [arXiv:0812.3449 [hep-lat]].

TEACHING EXPERIENCE    Syracuse University
                       Graduate Course Instructor                      June 2011, June 2012
                       Undergraduate Physics Teaching Assistant              2011, 2012, 2014